FINAL TECHNICAL REPORT

"Optimal Control of a Surge-Mode WEC in Random Waves"

Principal Investigator:
Allan Chertok
Senior Engineer
Resolute Marine Energy, Inc.
3 Post Office Square – 3rd floor
Boston, MA 02109
achertok@resolutemarine.com

Submitted to:
U.S. Department of Energy
Golden Field Office
1617 Cole Blvd.
Golden, CO 80401

Project Team Members:
University of Michigan – Dr. Jeffrey Scruggs
Re Vision Consulting – Mr. Mirko Previsic
University of Minnesota – Dr. James Van de Ven

Acknowledgement: This report is based upon work supported by the U.S. Department of Energy under Award No. DE-EE0006402.

Introduction

Resolute Marine Energy (RME) has developed a marine hydrokinetic (MHK) device for capturing energy from ocean waves which employs a hinged flap attached to the ocean floor which is driven landward and seaward principally by wave surge force. Integrated with the flap hinges are rotary vane hydraulic pumps which deliver pressurized working fluid[1] via a closed circuit pipeline system to a hydraulic motor which in turn drives a variable speed generator connected to the grid via a power converter.

In the operation of this device a key design consideration is how best to control the reaction torque presented to the flap by the vane pumps so as to achieve maximum energy capture (aka "capture efficiency").[2] For testing sub-scale 2m wide flaps in both tank [3] and ocean trials [4] as well as ocean testing a larger 5m wide device [5], RME employed a control policy known as "Coulomb damping" wherein the flap load is controlled in quasi-real-time by slowly adjusting the hydraulic system pressure according to observations of sea conditions indicated by measurement and computation of significant wave height (Hs) and peak power period (Tp). Values of Hs and Tp updated every 5 to 15 minutes were used to index a table of optimum system pressures pre-determined by RME's numerical model of the system.

While Coulomb damping control has been demonstrated by RME and others [1,2] to be a viable method, RME anticipated that one or more advanced methods of controlling flap load in real-time could significantly improve flap capture efficiency. The challenge was to determine if the economic value of the increased flap productivity would more than offset added costs associated with reduced availability and added capital and operational costs (CAPEX and OPEX) to implement advanced control.

To answer this question RME and its sub-contract controls experts…

- Professor Jeff Scruggs at the University of Michigan and PhD student assistant;
- Professor Jim Van de Ven at the University of Minnesota; and
- Mirko Previsic and his team at Re-Vision Consulting LLC.

…undertook an investigation of eight real-time flap load control policies with the salient objective of assessing the potential improvement of annual average capture efficiency at a reference site. Four methods investigated by Re-Vision employed predicted advance information from sensors seaward of the flap device using model predictive control (MPC) techniques which are of a non-causal class. Prof. Scruggs and his assistant explored four causal methods that leverage after-the-fact information provided by operational sensors and require no deployment of seaward sensors.

[1] As will be described below the working fluid is filtered seawater
[2] Analogous to the determination of an electrical load impedance to extract maximum power from a source

Introduction - continued

All advanced methods retained baseline Coulomb damping control to set short-term average conditions while real-time adjustment of flap load was superimposed by modulating the effective displacement of the flap pumps.

Coulomb damping control is readily implemented with near commercial off-the-shelf (COTS) hydraulic components[3] since quasi-real-time control of flap load can be achieved by slowly adjusting the speed of the hydraulic motor by power electronic control of the driven generator speed. However, while causal and non-causal solutions for real-time flap loadings are achievable with available and affordable computer hardware, a remaining challenge is how to translate computed commands into flap load adjustments in real-time. After consideration of several concepts RME decided to pursue the possibility of applying state-of-the-art valve switching techniques for modulating the effective displacement of the mechanically fixed displacement flap pumps. So-called switch-mode hydraulics employs concepts paralleling those well-established in the field of power electronics to achieve high efficiency, high bandwidth control of pumps and motors. RME engaged the assistance of Prof. James Van de Ven at the University of Minnesota—an expert in the field of switch-mode hydraulics—to investigate the feasibility of achieving real-time control of flap load by modulating the effective displacement of the flap pumps and to estimate the cost of high bandwidth switching valves and related components.

Objectives

The objective of this project was to develop one or more real-time feedback and feed-forward (MPC) control algorithms for an Oscillating Surge Wave Converter (OSWC) developed by RME called SurgeWEC™ that leverages recent innovations in wave energy converter (WEC) control theory to maximize power production in random wave environments. The control algorithms synthesized innovations in dynamic programming and nonlinear wave dynamics using anticipatory wave sensors and localized sensor measurements; e.g. position and velocity of the WEC Power Take Off (PTO), with predictive wave forecasting data. The result was an advanced control system that uses feedback or feed-forward data from an array of sensor channels comprised of both localized and deployed sensors fused into a single decision process that optimally compensates for uncertainties in the system dynamics, wave forecasts, and sensor measurement errors.

Summary of Results

The best performance in terms of increase in WEC efficiency was achieved by configuration #8 (MPC, continuous, bi-directional). Comparisons between the project objectives achieved using configuration 8 and the project's initial objectives are provided in Table 1.

[3] For sub-scale tank and ocean trials RME successfully used COTS rotary vane hydraulic actuators with conventional hydraulic fluid as flap pumps. Preliminary designs of purpose-built larger pumps capable of operation with filtered sea water are underway. Hydraulic motors operable with filtered sea water used in sea water reverse osmosis plants are readily available COTS components. Piping, accumulators, valves and other components suitable for operation with filtered sea water are also available as COTS components.

- In most cases, the project outcomes exceeded project initial expectations i.e.: (1) an increase in power rating by 80% vs. 56% as was expected; and (2) an increase in average flap capture efficiency of 67% vs. 63% as was expected.
- The objective of achieving an increase in availability could not be realized because the definition of availability changed during the project. Initially, availability was defined (by RME) as the % of time the WEC can operate in a given wave energy environment. RME's initial availability estimate was therefore defined as a wave energy domain between 10 and 60 kW/m in Yakutat, AK. During the project, we changed our LCOE methodology to comply with the DOE's recommended approach wherein availability was a limiting factor applied once the "theoretical power captured" was calculated, while still factoring our "operating domain" limit in the calculation of the theoretical power. We therefore applied a double knock-down of performance which we believe to be very conservative. Furthermore, we assumed an 81% availability factor, which we believe to be conservative (we believe we could reasonably achieve 90%). Finally, as availability was now defined as an arbitrary factor applied once the theoretical power capture was calculated, any improvement in WEC performance could not have impacted the system availability as defined by DOE.
- Regarding LCOE, our best solution achieved a 17% improvement. This is less than the 41% expected but we attribute this discrepancy to: (1) the change in methodology; and (2) the limitation imposed on the size of our WEC which limited our ability to capture the benefits of the advanced control solutions. Still, because LCOE is a measure that factors both the increase in Annual Energy Production (AEP) and the associated increase in CAPEX and OPEX, we consider a 17% improvement to be a very positive outcome.

Table 1 – Statement Of Project Objectives (SOPO)

	P1 SOPO			P2 SOPO			FINAL SOPO			
Parameter	**Baseline**	**Advanced**	**Benefits**	**Baseline**	**Advanced**	**Benefits**	**Baseline**	**Advanced**	**Benefits**	**Notes**
Rated plant power (kW)	720	1,123	56%	315	405	29%	73,200	131,760	80%	**[1], [2]**
Average flap capture eff (%)	35	57	63%	26	36	38%	24%	40%	67%	**[3]**
Plant capacity factor (%)	26	28	8%	42	54	29%	40%	38%	5%	**[3], [4]**
SPA#1: Power density (W/kg)	0.37	0.62	67%	0.29	0.37	29%	0.50	0.89	79%	**[5], [6]**
SPA#2: Availability (%)	61%	70%	15%				81%	81%	0%	**[7]**
LCOE ($/kWh)	0.44	0.26	41%				0.44	0.36	17%	**[8]**

[1] For P1 and P2, rated plant power was calculated using RME's methodology (e.g. Yakutat Cannon Beach conditions; 18-WEC plant); For FINAL, rated power was calculated using DOE's required methodology and plant sizing requirements [4].
[2] For FINAL, results showed for configuration #8 (highest performance); Baseline system optimized at 30 kW/WEC power rating; advanced system optimized at 55 kW/WEC to be able to capture benefits of advanced control solutions. Costs of equipment were assumed to increase linearly with power rating.
[3] P1, P2 using sea conditions at Yakutat Cannon Beach; FINAL using sea conditions at Humboldt Bay (DOE's requirement); P2 and FINAL reflect latest model performance estimated by RME (more realistic findings are associated with substantially improved analysis tools since time of P1 SOPO)
[4] FINAL: The marginal increase in power rating (kW/WEC) leads to the plant operating at full capacity less frequently, thus the decrease in capacity factor.
[5] Changes from P1, P2 and FINAL mostly due to better characterization of components and improvements in analytical tools since time of P1 SOPO. For FINAL, improvements are principally related to increased power rating.
[6] Revised weight does not include dominant and site-dependent foundation mass. Advanced control configurations add little mass.
[7] P1: Availability defined, according to RME's model, as %/time wave energy is sufficient to operate system (i.e. between 10 and 60 kW/m); In FINAL, availability defined according to DOE's requirements[1], as probability that the system will work as required during the period where waves are sufficient to operate the system. Advanced control solutions have no impact on availability as defined in DOE's methodology. RME conservatively used 81% availability instead of 90% recommended by DOE.
[8] P1: LCOE calculated using RME's methodology at Yakutat Cannon Beach and at 100% availability; FINAL: LCOE calculated using DOE's methodology at Humboldt Bay; at 81% availability; and using latest RME's analysis tools and latest (more realistic) cost assumptions.

[4] [1] "Standardized Cost and Performance Reporting for Marine and Hydrokinetic Technologies", DOE, 2015
[2] "DE-FOA-1418 Cost and Performance Reporting Template Instructions", DOE, October 2015

System Impact

This project initially included series of tasks associated with implementing the developed advanced control systems in "real-world" conditions, i.e. in hardware-in-the-loop experiments designed to provide important information. The series of tasks were designed to:

1) Verify that the eight developed control strategies are computationally efficient enough to operate in real time;
2) Identify components capable of executing the control commands;
3) Confirm the costs of selected components;
4) Test the durability of selected components;
5) Compare observed results with initial performance improvement estimates and further-refine LCOE calculations.

At the conclusion of Budget Period 1, the Department of Energy declined to fund RME's proposed hardware-in-the-loop experiments and thus the tasks listed above will be conducted under a different R&D program. That said, key questions surrounding real-world implementation challenges were compiled by RME and project partner Dr. James. van de Ven at the University of Minnesota and are ready to be investigated. Therefore, the initially encouraging outcomes of this project will remain in the theoretical realm until further work is completed.

Background

Oscillating Wave Surge Converters (OWSCs) have shown great promise as a cost-effective means of harnessing the power of ocean waves. OWSCs are designed to operate near shore in relatively shallow water where, as depth increases, surface waves are transformed into surge waves wherein water particle motion is largely horizontal. The energy content of surge waves may vary greatly depending upon the dynamic interaction of several variables including water depth, tidal range, bathymetry and geomorphology. RME's SurgeWEC™ commercialization efforts began in earnest in October, 2010 and have encompassed advanced computer modeling, engineering design and production, and a series of wave tank and ocean experiments verifying performance predictions while also identifying the potential for significant improvements in power generation using advanced control strategies and system hardware.

Improvements in the hardware capability of the SurgeWEC™ can be made to afford a much greater degree of controllability over the instantaneous power generated by the system. These improvements would allow torque T (and therefore the power generated, P_{gen}) to be controlled in real-time as a feedback function of the dynamic response of the WEC to incident waves. This is advantageous for two reasons:

- The control algorithm described above constitutes an *instantaneous* feedback algorithm for power generation control; i.e., $T(t)$ is a simple function of $\omega(t)$ at each time t. It is almost always the case, however, that power generation is optimized via a *dynamic* feedback function.

- Although the baseline Coulomb damping control algorithm described above is optimized for a given sea state, it does not exploit information about waves that are about to interact with the WEC. However, if $T(t)$ could be actively controlled, then this information could

be used in real-time to enhance energy extraction. Additionally, if forecasting information about near-future waves were available, further enhancements in performance are achievable via anticipatory use of this information.

In this project, funded under the DOE Marine and Hydrokinetic System Performance Advancement Funding Opportunity (DE-FOA-0000848), the goal was to augment the baseline SurgeWEC™ control system to include a variety of techniques for increased controllability of torque $T(t)$ over and above that provided by the baseline Coulomb damping system. RME refers to each such technique as a **control augmentation**, which varies in their level of sophistication, as well as the marginal costs associated with their implementation and maintenance.

Thus, the primary objectives of this project were to quantify the marginal increase in average power associated with each control augmentation with its feedback algorithm optimized—and equally important to estimate the impact on availability losses, CAPEX and OPEX in order to see if there is a net economic advantage to adding advanced control. Hence the project undertook an investigation of state-of-the-art switch-mode hydraulic control means to implement real-time flap load commands by modulating the effective displacement of the mechanically fixed displacement flap pumps

Figure 1 depicts the overall RME SurgeWEC™ system and its components described below:

1. Flap and flap-driven rotary vane pumps pressurize filtered sea water;
2. Flow rectifier converts oscillating pump flow into a train of uni-directional flow pulses;
3. Pulse-width modulated shunt valve and check valve modulate the effective displacement of the pump;
4. Front-end high pressure accumulator (HPA) suppresses flow and power pulsations;
5. Front-end low pressure accumulator (LPA) maintains net positive pump suction head;
6. Pressure pipe carries pressurized fluid to "back-end" shore station;
7. Suction line provides return path for the working fluid supplied by a pressurized reservoir;
8. Back-end high pressure accumulator (HPA) further suppresses twice-wave-frequency; pulsations of pump flow and suppresses pressure fluctuations due to the episodic nature of wave arrivals—i.e., tendency for waves to arrive in groups;
9. The fixed displacement hydraulic motor (FDM) powered by pressurized HPA fluid drives a variable speed generator coupled to the grid via a power converter;
10. Baseline Coulomb damping control is achieved by adjusting the speed of the generator and FDM to extract fluid from the HPA so as to adjust its pressure to meet a set point determined by a look up table indexed by observed values of Hs and Tp;
11. A flywheel energy storage unit (FW ESU) provides additional suppression of episodic wave power fluctuations to maintain a power ramp rate acceptable to the grid operator;
12. Coulomb damping control as well as other supervision, control and data acquisition (SCADA) functions are provided by a programmed logic controller (PLC).
13. Advanced real-time control is implemented by auxiliary control depicted in Figures 2 and 3.

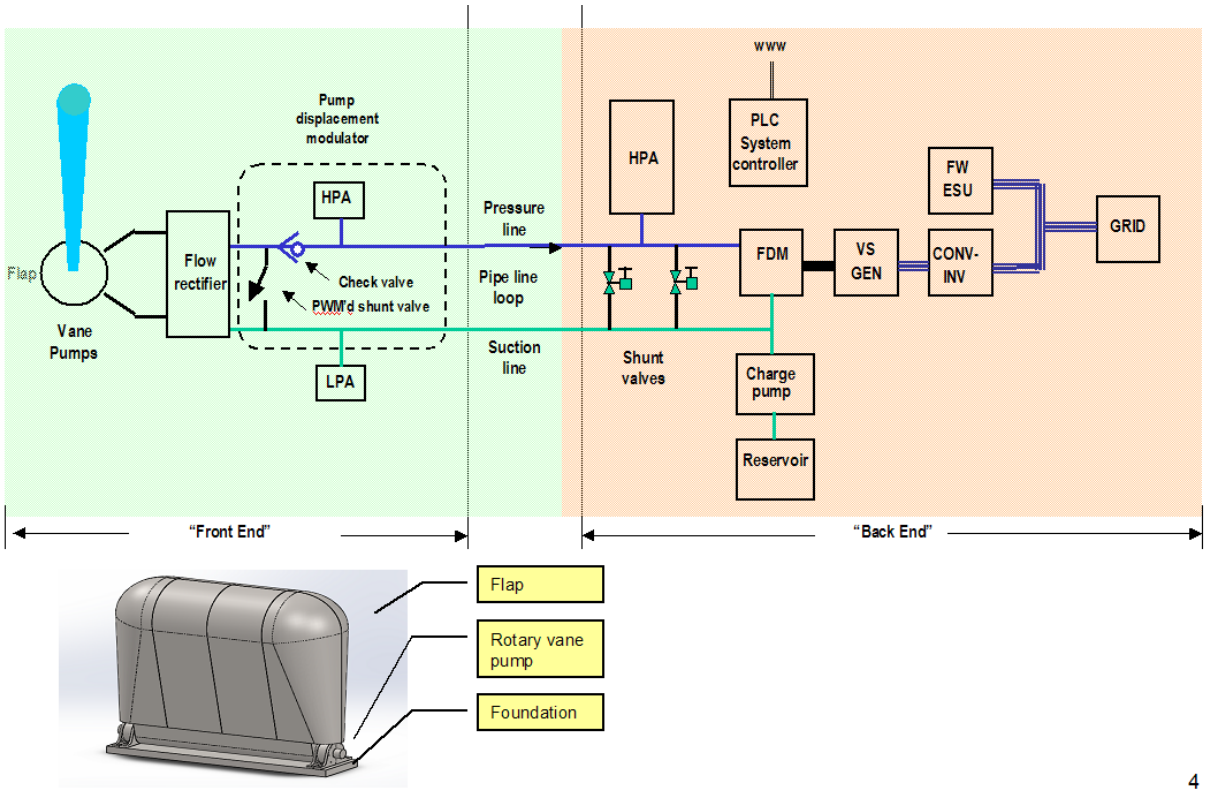

Figure 1 – Overall RME system

An overview of the advanced real-time control policies investigated is summarized by Figure 2.

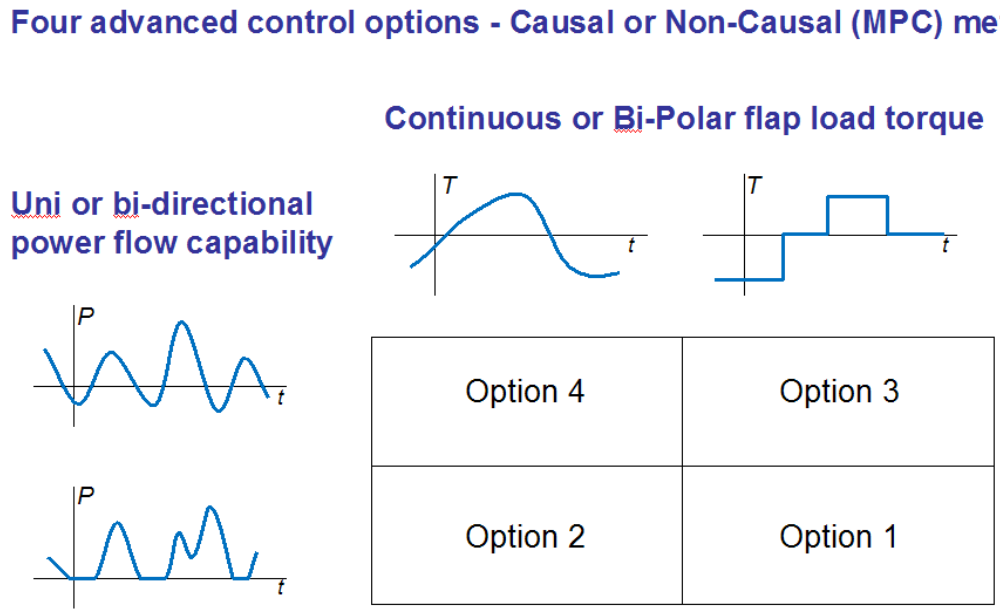

Figure 2 – Graphical summary of 8 advanced control policies investigated

Causal and non-causal (aka MPC) methods were investigated respectively by team leaders Dr. Jeff Scruggs at the University of Michigan and Mirko Previsic at Re-Vision. Each investigation considered the 4 options depicted in Figure 2 briefly summarized as follows:

- Options 4 and 2 assumed continuous control of flap load torque by pulse width modulation of flap pump shunt valves. With shunts closed effective pump displacement would be the mechanically determined fixed value. With shunts open effective displacement would be zero. For duty cycles in between various degrees of effective displacement—and reaction torque—could be achieved with nominally fixed hydraulic system pressure set by Coulomb damping control

- Options 3 and 1 assumed tri-state control of flap loading to reduce the frequency of shunt valve switching events and there by increase valve endurance

- Options 4 and 3 implemented reverse (reactive) power flow with the intent of better matching flap natural mode with the dominant site Tp

- Options 2 and 1 implemented only forward power control from flap to shore station

Figure 3 illustrates the core aspects of the flap pump switch mode displacement modular explored by Prof. James Van de Ven at the University of Minnesota.

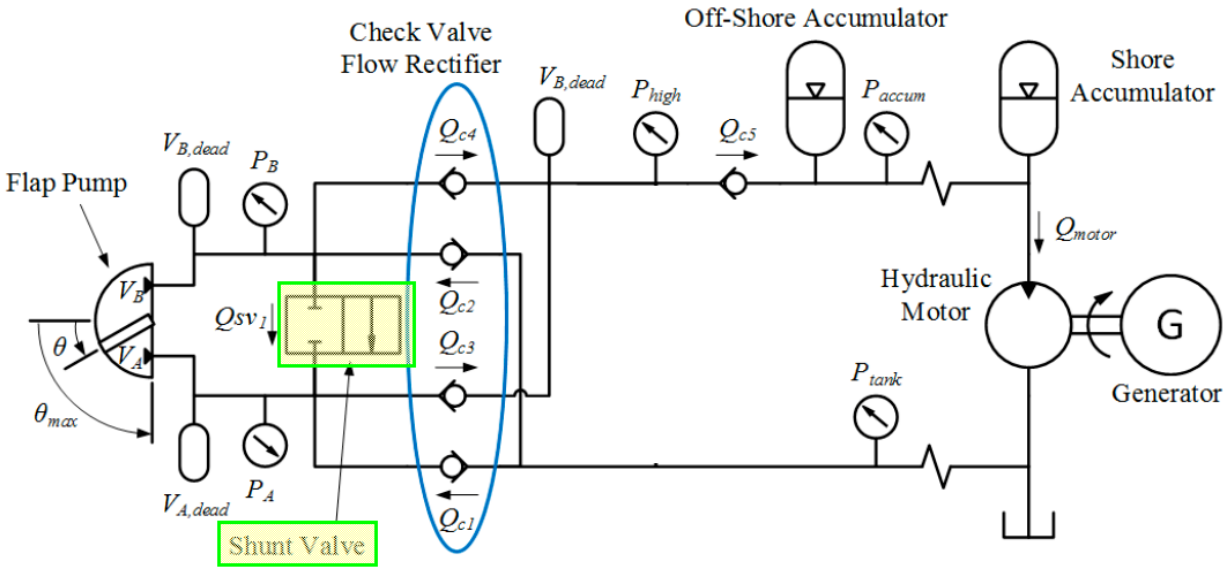

- When shunt is open pump ports are bypassed and effective displacement = 0
- Alternatively can view shunt as a pump pressure modulator
- Pump reaction torque = pressure x displacement -- so either controls flap load

Figure 3 – flap pump switch-mode displacement modulator

Note that it was determined that higher efficiency can be obtained by placing the shunt valve directly across the pump ports as shown here rather than across the output of the flow rectifier as depicted in Figure 1.

Block diagrams of the control hardware for the baseline Coulomb damping system and add-ons to implement various advanced real-time control methods are depicted below.

[REMAINDER OF PAGE PURPOSELY LEFT BLANK]

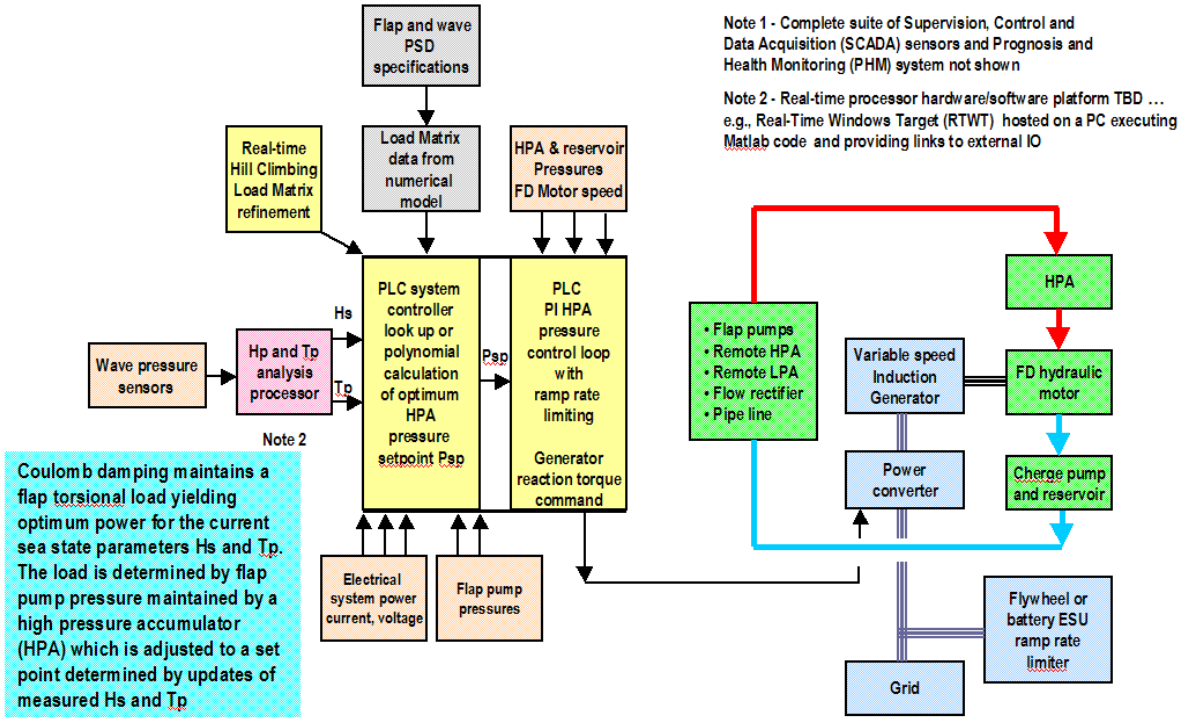

Figure 4 – Baseline Coulomb damping control system block diagram

1. Estimates of Hs and Tp are made by real-time analysis of signals from wave pressure sensors adjacent the flap

2. Hs and Tp estimates point to a look up table of hydraulic pressure required to obtain optimum flap pump reaction torque loading of the flap. Alternatively, pressure can be calculated on the fly by evaluating polynomial functions

3. The determined optimum pressure then becomes the set point for a PID pressure controller that adjusts the speed of the hydraulic motor-generator set so that fluid is extracted from the HPA at a rate to attain the set point pressure.

•

[REMAINDER OF PAGE PURPOSELY LEFT BLANK]

Figure 5 depicts the added hardware to implement causal control with unidirectional power flow.

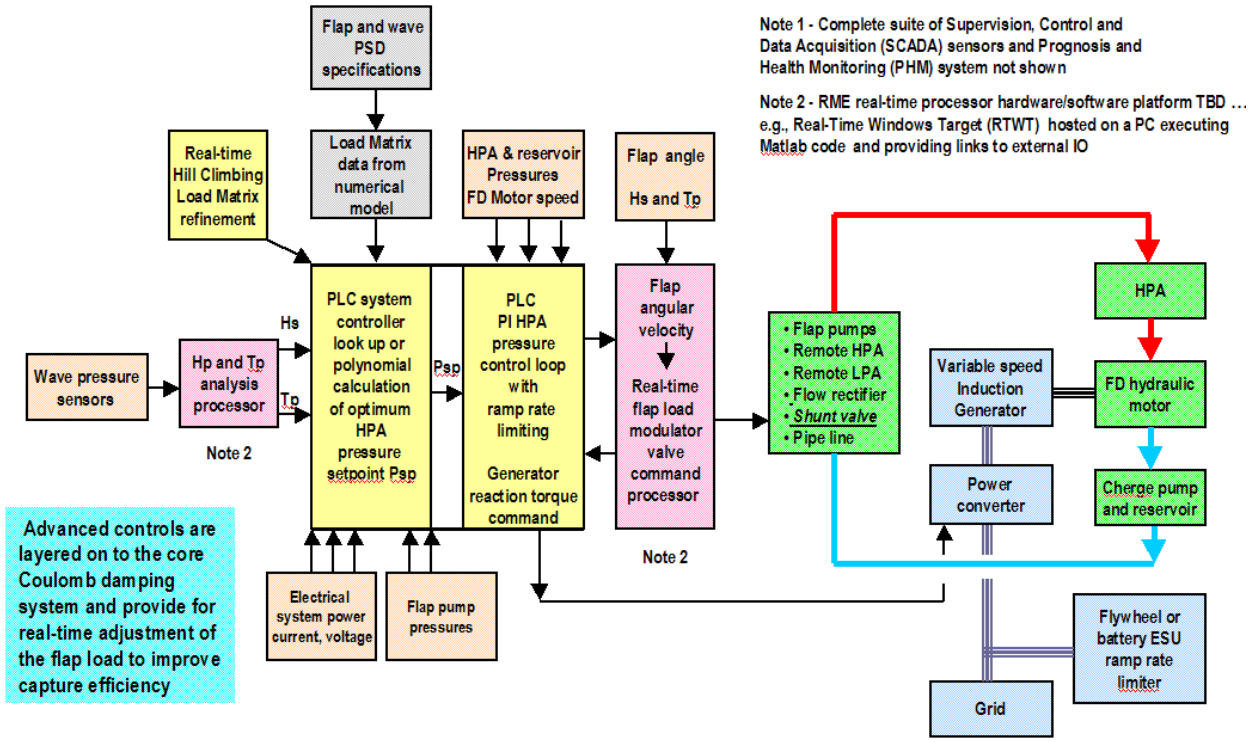

Figure 5 – Adding causal real-time control with uni-directional power flow

1. Flap angle, Hs and Tp are inputs to a real-time load controller which outputs a flap pump displacement modulator command—either PWM or tri-state—to the pump shunt valve

2. Additional real-time control could be hosted on a PC running Real Time Windows Target (RTWT) executing Matlab code.

•

[REMAINDER OF PAGE PURPOSELY LEFT BLANK]

Figure 6 depicts the added hardware to implement causal control with bi-directional power flow.

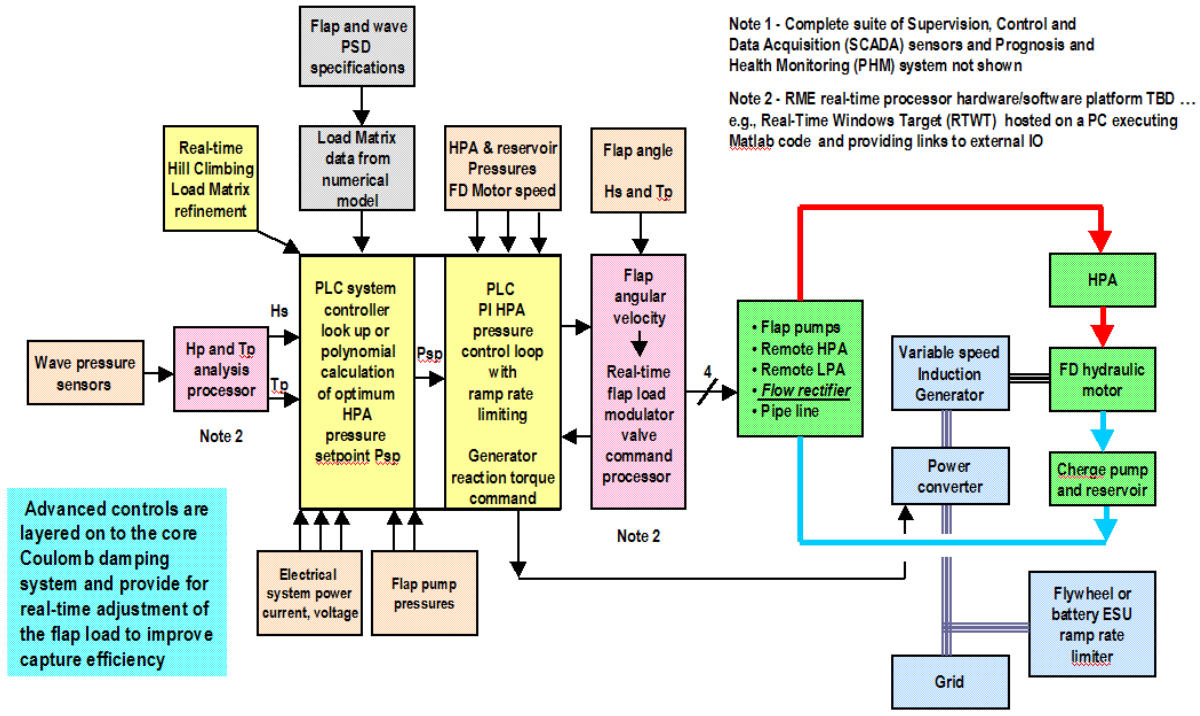

Figure 6 – Adding causal real-time control with bi-directional power flow

1. The block diagram is the same as for uni-directional power flow except that the PWM or tri-state commands are directed to each of the flow rectifier valves and the shunt modulator valve is no longer required

2. The flow rectifier valves now must be capable of active control and are considerably more costly than passive check valves used in the uni-directional power flow case.

[REMAINDER OF PAGE PURPOSELY LEFT BLANK]

Figure 7 depicts the added hardware to implement non-causal MPC control with uni-directional power flow.

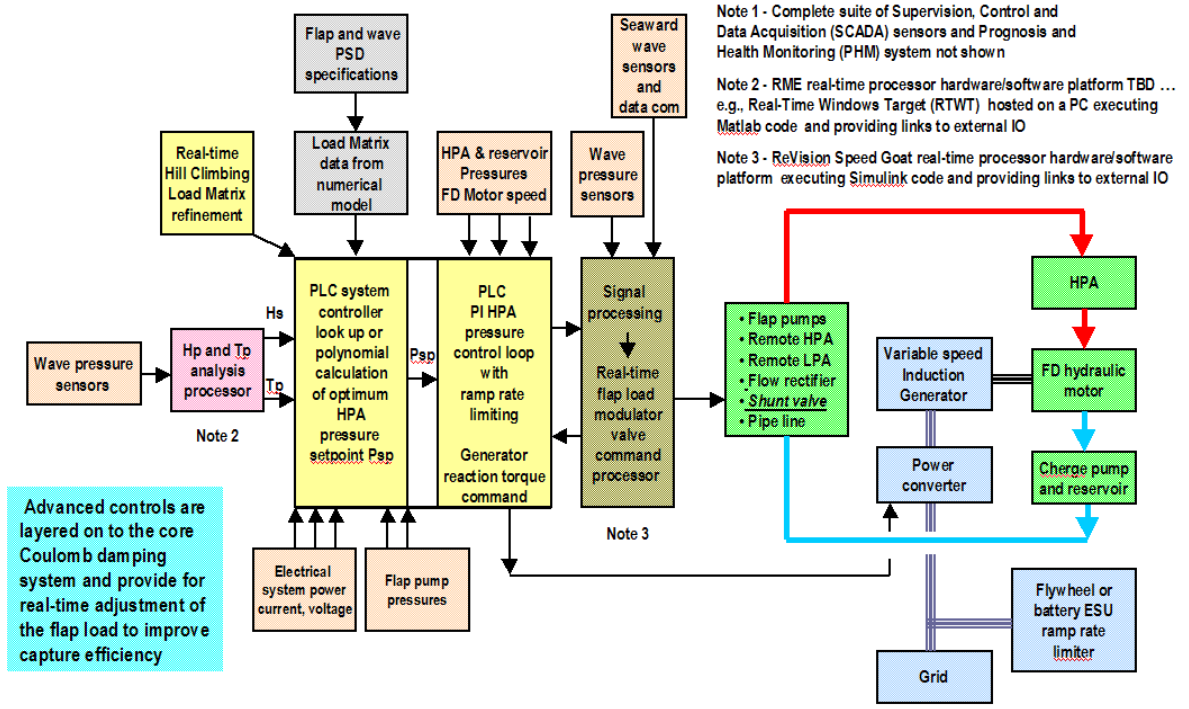

Figure 7 – Adding non-causal, MPC real-time control with uni-directional power flow

1. The block diagram is similar to the causal control case except for the addition of seaward wave sensors and a data communication link to the shore station. The real-time processor also utilizes wave sensor signals but does not compute Hs and Tp from these.

2. The MPC output provides either PWM or tri-state command signals to the flap pump shunt valve to modulate its effective displacement.

•

[REMAINDER OF PAGE PURPOSELY LEFT BLANK]

Figure 8 depicts the added hardware to implement non-causal MPC control with bi-directional power flow.

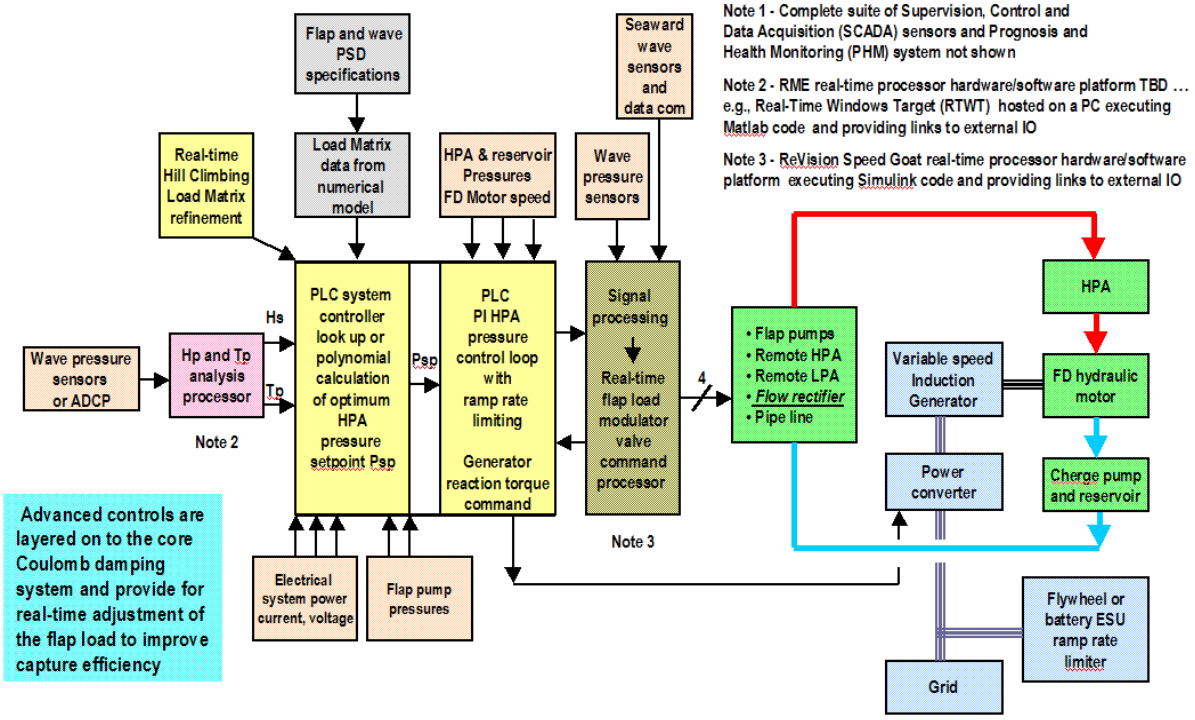

Figure 8 – Adding non-causal MPC real-time control with bi-directional power flow

1. The block diagram is the same as for uni-directional power flow except that the PWM or tri-state commands are directed to each of the flow rectifier valves and the shunt modulator valve is no longer required

2. The flow rectifier valves now must be capable of active control and are considerably more costly than passive check valves used in the uni-directional power flow case.

TASKS PERFORMED

This portion of the report describes the program tasks and milestones as defined in the Statement of Project Objectives (SOPO)

Task 1: Detailed Implementation Planning
Task Summary: A detailed implementation plan was developed establishing clear timelines and scope-of-work statements for all parties involved. All contractual arrangements were negotiated and closed and a 2-day in-person kick-off meeting was held to allow for detailed technical discussions among the team to resolve any technical issues. A program Management Plan was written and delivered. Additionally, the IP Management Plan was drafted and delivered.

Task 2: Establish Baseline Site Conditions

Task 2 Summary: Existing data-sets that were used for preliminary assessments in this study were obtained from previously conducted Electric Power Research Institute (EPRI) studies. The results from these studies were to be updated with a new SWAN (Simulating WAves Nearshore) model run to ensure accurate prediction of wave action at originally proposed Yakutat AK deployment site. A short wave measurement validation program to be conducted by the University of Alaska was to be used to collect validation data for the SWAN modeling results but was not timely completed and available for this purpose.

Well into the conduct of the research several significant changes were planned

1. Reassess the flap capture efficiency performance gains for a more recent 8m wide flap with broadly rounded contour in place of the numerical performance model of a prismatic 10m wide flap originally proposed. The reason being that RME had determined that the coefficient of damping assumed in the analysis of the 10m prismatic flap had been understated leading to an overly optimistic baseline capture efficiency. A revised design now the focus of RME's business development plan is 8m wide to better match its natural mode to Tp at sites of interest and its edges are boldly rounded to reduce drag prediction when a more realistic coefficient of drag is assumed in the numerical analysis. It was RME's intent to re-run all flap efficiency performance cases with this new flap but unfortunately program funds were depleted before this work could be undertaken.

2. Employ filtered sea water as the working fluid to substantially reduce fluid cost and eliminate environmental hazards due to leaks. This had no immediate impact on flap capture efficiency performance gains but does have impacts on LCOE—lower cost of fluid but higher cost of components capable of operation with seawater.

3. Utilize the DOE Humboldt Bay deep water reference site with prescribed adjustments for shallow water operation to make the results of the research directly comparable with those of others observing this standard reference. While the research had been largely completed using wave characteristics surmised for the Yakutat AK site the intent of the RME team was to re-run the analyses of flap capture efficiency enhancement using the Humboldt data but unfortunately program funds were depleted before this work could be undertaken

Task 2 Status

In consequence of the above changes RME's best efforts will be as follows:

1. Report the flap capture efficiency gains determined with the original 10m prismatic flap using wave data for the originally proposed Yakutat AK site

2. Assume similar capture efficiency gains would be achieved with a new 8m rounded flap

3. Conduct LCOE analysis assuming
    a. Flap efficiency capture efficiency gains determined for the 10m prismatic flap
    b. DOE Humboldt Bay deep water site conditions adjusted for a shallow water device

c. PTO system costs based on electric power rating of the 8m rounded flap (~30kWe)
d. An array of 18 units achieving a rating of 18 * 30 = 540kW

Task 3: Create and Validate Time-Domain Model

Task Summary: As part of its cost-share RME provided a flap design that leverages the extensive WAMIT®-TDM (Time-Domain Model) work previously completed. The RME numerical flap hydrodynamic model was originally developed by RME Intern Eshwan Ramadu under the direction of Prof. Yuming Liu of MIT. It was subsequently refined by the joint efforts of Dr. Matt Folley and former PhD student Darragh Clabby employed by RME. Subsequent extreme loads tank testing at Orion Laboratories in Inverness Scotland provided significant validation of the code integrity.

The 10m wide prismatic flap was developed in conjunction with the controls development work and site characterization for optimum performance in Yakutat. However—as explained above—well into the controls research it was determined that the flap model assumed an optimistically low coefficient of drag Cd.

Task 3 Status: Task 3 was completed in Budget Period 1 (BP1). The baseline capture efficiency of an improved, rounded edge 8m wide flap was found superior to the first proposed prismatic 10m wide design while allowing for a higher drag coefficient than originally assumed. Phase 1 controls analyses performed with the 10m flap characterization were to be revised to the preferred 8m wide design but program funds were depleted before this additional work could be undertaken

Task 4: Establish Techno-Economic System Values

Task Summary: Deciding on an optimal control strategy requires an understanding of the trade-offs with respect to: (1) PTO configuration, (2) Control strategy, and (3) cost of each configuration. LCOE was estimated for the baseline and 8 control concepts (4 causal and 4 non-causal). As RME has since set the goal of employing filtered sea water as the hydraulic system working fluid to avoid any environmental concerns the power range of commercially available sea water compatible components—in particular hydraulic motors—limit assessment of costs to units with maximum power rating of 30kWe. All control options to be considered will employ the baseline Coulomb damping system hydraulic apparatus and add a flap pump displacement modulator to enable real-time control of load torque. Non-causal controllers will add the cost of an array of wave elevation sensors to enable wave forecasting. Based on advise offered by Re-Vision and anticipated SurgeWEC unit spacing the cost of 3 sensor arrays were allocated in the LCOE analysis. WEC array effects which might aid or compromise performance were not considered but a knock down array performance factor prescribed in the DOE performance assessment document was observed.

Detailed availability analysis was part of the program scope. Hence LCOE estimates are reported at a presumed baseline 95% availability and knockdowns made for each advanced control system according to its complexity.

Techno-economic system values to be reported were to include power/weight ratio and LCOE established for 8 advanced PTO control methods with individual WEC units of 30kWe rating in an illustrative 18-unit array at the DOE Humboldt bay reference site.

Task 4 Status: Estimation of baseline costs and weights was largely completed during BP1 and was refined during BP2. A preliminary search for pump displacement modulator valves was started during BP1 and was continued during BP2 with the assistance of switch mode hydraulics expert Professor James Van de Ven of the University of Minnesota. A detailed LCOE analysis following DOE prescribed methods was carried out by RME CFO Olivier Ceberio with assistance of:

1. Mirko Previsic regarding costs of seaward wave sensor CAPEX and OPEX as well as control platform CAPEX;
2. Prof. James Van de Ven regarding cost and service life of switching valves;
3. Austin Engineering regarding an estimate of flap pump manufacturing cost;
4. Vendors, e.g.,
    a. Fiberspar LinePipe™ piping cost;
    b. Danfoss seawater-capable hydraulic motor;
    c. Tillotson Pearson – flap manufacturing cost;
    d. Yaskawa Electric – variable speed generator control;
    e. Marathon Electric – induction generator.

A description of the methodology and results for the baseline and 8 advanced real-time control methods is presented in Appendix A. An analysis of power/weight ratio is presented in Appendix B.

Task 5: Wave Probe Placement Optimization

Task Summary: Mirko Previsic et al of Re-Vision studied optimal wave probe placement configurations with the objective to minimize the number of wave probes required while keeping prediction errors within an acceptable range. Re-Vision leveraged RME's established WAMIT – TDM and wave-simulation models for this task and introduce virtual wave measurement buoys augmented by wave radar. The results fed into the controls optimization task undertaken in Task 7 and identified measurement buoy density.

Task 5 Status: The following Task 5 investigations were completed during BP1:

1. Establishment of a site-specific wave field simulation;
2. Evaluation of sensor placement trade-offs; and
3. Optimization of wave probe placement.

While consideration was given to use of wave radar, at this time it is anticipated that measurements would be implemented with floating surface sensors and the cost of these units and communication means have been factored into the LCOE calculations.

Task 6: Control Optimization – *Without Wave Prediction*

Task Summary: RME's partner Prof. Jeff Scruggs and his graduate assistant at the University of Michigan developed advanced control algorithms to maximize power generation using only sensor measurements localized at the SurgeWEC™. Specifically, the control algorithm will require only feedback from flap position and velocity sensors, together with Hs and Tp outputs from analysis of the wave elevation sensors located on the base of the device. Extensions were made to existing control theory to accommodate the SurgeWEC™ dynamic model, including its fundamental nonlinearities and hydraulic loss model. This extended theory, together with the

advanced time domain model from Task 3 and the site characterization from Task 2, was used to produce power matrices for the four control augmentations described below. The analysis was made sufficiently general that it can be used to examine other power conversion technologies beyond those directly relevant to this project, including direct drive power take-off systems, with minimal extra effort. Specifically, such extensions will only require new characterizations of the loss models associated with the new conversion systems

Task 6 status: The following were accomplished during BP1 Task 6 for causal control options without wave forecasting:

1. Finalized stochastic wave loading model, appropriate for use in control design;
2. Finalized results for optimal control for bi-directional power and continuous torque control;
3. Finalized results for optimal control for uni-directional power and continuous torque control;
4. Finalized results for optimal control for bi-directional power and tri-state shunt valve control;
5. Finalized results for optimal control for uni-directional power and tri-state shunt valve control.

Task 7: **Control Optimization – *With Wave Prediction***

Task Summary: RME's partner Re Vision utilized its existing controls optimization framework to develop a control system using errors in the wave-prediction established under Task 3. Parametric study of the impact that the different PTO topologies have on the power generated as well as the impact of various degrees of wave forecasting errors were evaluated. Subtasks were:

1. 7.1: Setup MPC controls framework and testing;
2. 7.2: Study optimal performance vs. wave forecasting horizon and wave prediction error;
3. 7.3: Study optimal performance given the PTO constraints given by the system configurations to be studied.

Task 7 Status: Tasks 7.1, 7.2 and 7.3 for non-causal model predictive control (MPC) of WEC flap loading assisted by wave forecasting were completed for control options 4 and 2 with continuous load torque control. Investigation of Option 3 with tri-state control was completed during BP2 along with Option 1 (tri-state control with uni-directional power flow).

Task 8: Integration of Controls Approaches

Task Summary: Task 6 and Task 7 approached the controls optimization problem from two very different angles. The results of these studies allowed the team to establish an economic evaluation of LCOE for each control strategy and corresponding PTO configuration.

During this process aspects of the two different controls approaches prompted ideas for hybrids with potential for LCOE cost reduction were considered and are briefly described herein.

RESULTS AND DISCUSSION

Generic control system model description

The generic control system model employed is depicted below in Figure 9. The 4 power train options considered for both causal and non-causal (MPC) approaches, in order of perceived complexity, were as follows:

Option 1	Uni-directional power flow, tri-state load control
Option 2	Uni-directional power flow, continuous load control
Option 3	Bi-directional power flow, tri-state load control
Option 4	Bi-directional power flow, continuous load control

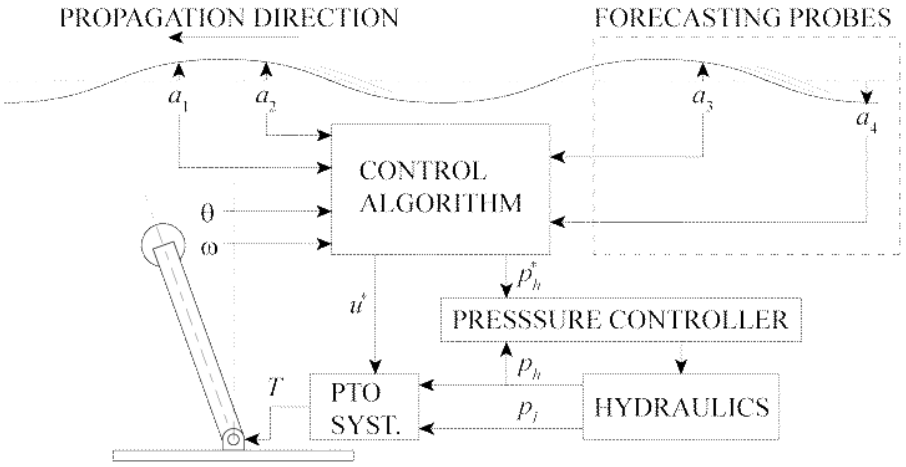

Objective is to maximize:

$$\bar{P}_{gen} = \frac{1}{T}\int_0^T \left(T(t)v(t) - P_{loss}(t)\right)dt$$

Baseline is optimal effective Coulomb damping
- **2 information options** (causal and non-causal)
- **4 power train options** (Options 1-4)

} 9 cases

Figure 9 – Generic control system model

[REMAINDER OF PAGE PURPOSELY LEFT BLANK]

RESULTS AND DISCUSSION - continued

Loss model

Figure 10 depicts the generic loss modeling approach.

Same loss model assumed throughout the analysis

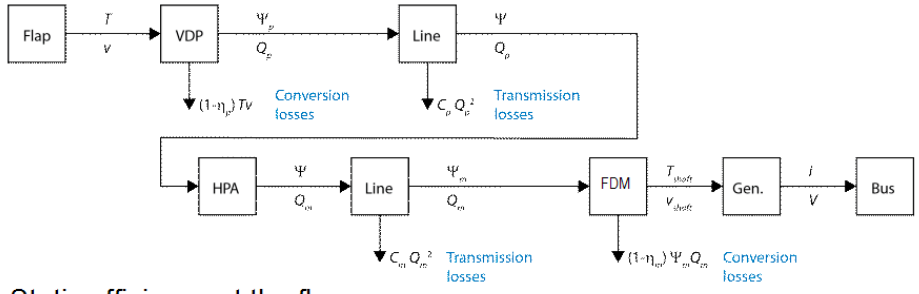

- Static efficiency at the flap pump -- η_p
  VDP is actually a fixed-displacement pump augmented by a switch-mode effective displacement modulator
- Static efficiency at the generator -- η_m
  combines variable speed FDM / generator losses
- Ideal linear viscous dissipation in transmission lines – C_p and C_m
  $\Rightarrow$ Important quantity is $P_0 = \Psi^2/(C_p+C_m)$ (has units of power)

Values assumed for the entire study:
$\eta_p = 0.75$, $\eta_m = 0.90$, $P_0 = 8\text{MW}$

Resulting loss model equation

- Define

$$P = Tv \qquad \text{Absorbed power at flap}$$

$$P_{gen} = iV \qquad \text{Generated power}$$

$$P_0 = \frac{\Psi^2}{C_p + C_m} \qquad \text{Pipe loss parameter (units of power)}$$

- Loss equation relates P to P_{gen}

$$P_{gen} = \begin{cases} \dfrac{P}{\eta_m \eta_p}\left(1 - \dfrac{1}{\eta_p}\dfrac{P}{P_0}\right) & : \quad P < 0 \\ \eta_m \eta_p P\left(1 - \eta_p \dfrac{P}{P_0}\right) & : \quad 0 \le P \le P_0/\eta_p \\ \dfrac{\eta_p P}{\eta_m}\left(1 - \eta_p \dfrac{P}{P_0}\right) & : \quad P > P_0/\eta_p \end{cases}$$

Generator (as motor) supplies power to flap

Generator power = flap power - losses
Losses < flap power
Generator power available

Generator power = flap power - losses
Losses > flap power
No generator power available

Figure 10 – loss model

RESULTS AND DISCUSSION - continued

Baseline Coulomb damping control

The baseline Coulomb damping control model is depicted in Figure 11. Numerical modeling determined that it was advantageous to employ a flap load approximately 70% of the optimal maximum energy capture value as this enables a significant reduction in the required flap pump displacement and its cost with a relative small (e.g., 3%) loss of flap capture efficiency. Moreover, operation at off-optimum load also increases average flap and pump angular velocity magnitude which enables further reduction of pump displacement and cost. After making these adjustments the nominal per-pump displacement for our 8m flap is 18L/rad.

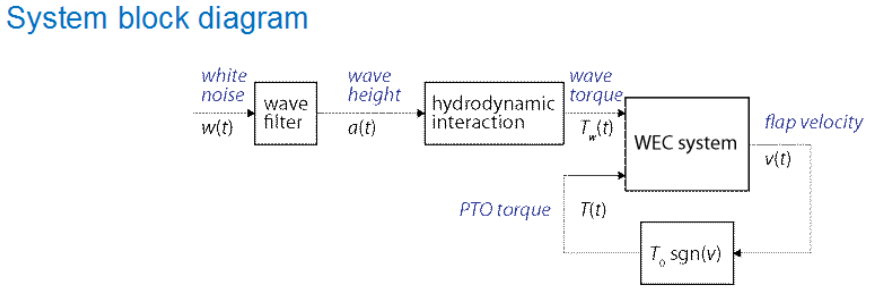

- Design variable is Coulomb torque T_0

Assumptions

- T_0 can be varied for each sea state
- Optimize T_0 for optimal or near-optimal flap capture efficiency
- Limits may be placed on T_0 in optimization to:
  - Reduce required flap pump displacement and pump cost
  - Increase flap and pump angular velocity to also reduce pump cost
  - Achieve a more favorable LCOE

Figure 11 – Coulomb damping control model

[REMAINDER OF PAGE PURPOSELY LEFT BLANK]

RESULTS AND DISCUSSION - continued

Causal control model

The model employed for causal systems is depicted below in Figure 12.

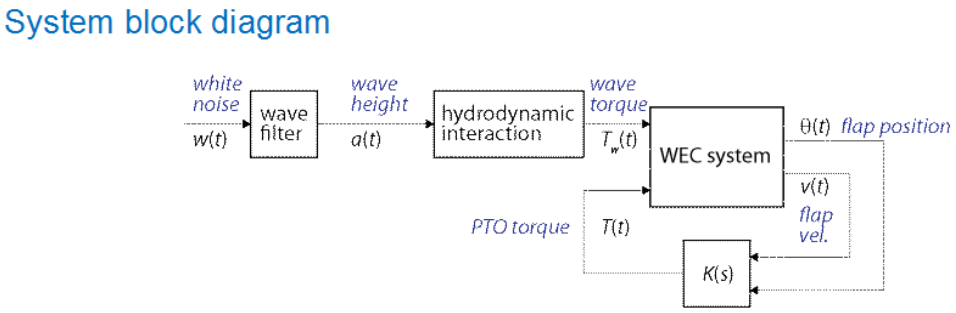

Figure 12 – Causal control model

[REMAINDER OF PAGE PURPOSELY LEFT BLANK]

RESULTS AND DISCUSSION - continued

Non-causal control model

The non-causal (MPC) model, assuming perfect wave prediction, is depicted by Figure 13.

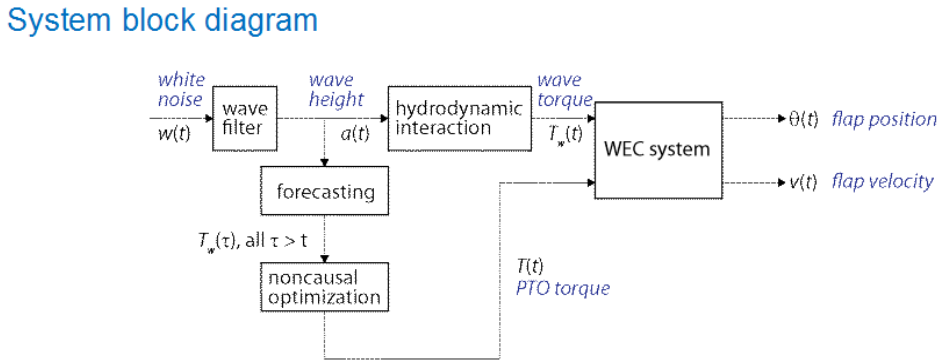

Figure 13 – Non-causal control model

[REMAINDER OF PAGE PURPOSELY LEFT BLANK]

RESULTS AND DISCUSSION - continued

Methodology for control performance assessment – power matrix

Figure 14 depicts the power matrix formulation used to assess the performance of each control system option. An illustrative power matrix is shown in Table 1.

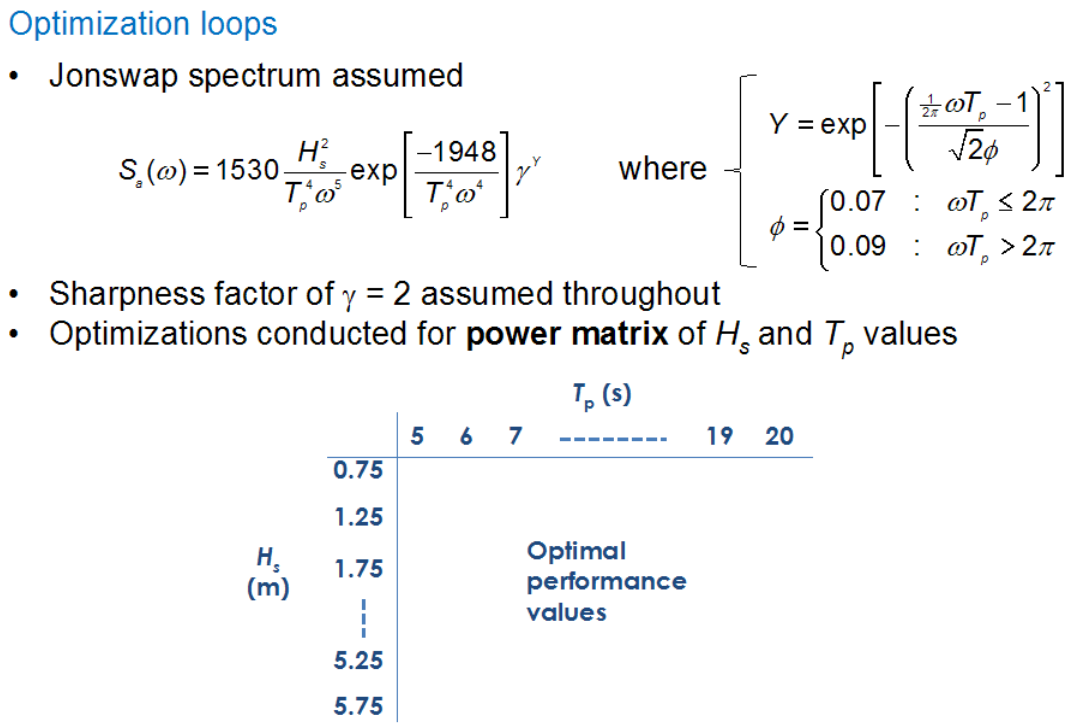

Figure 14 – Power matrix formulation for control performance assessment

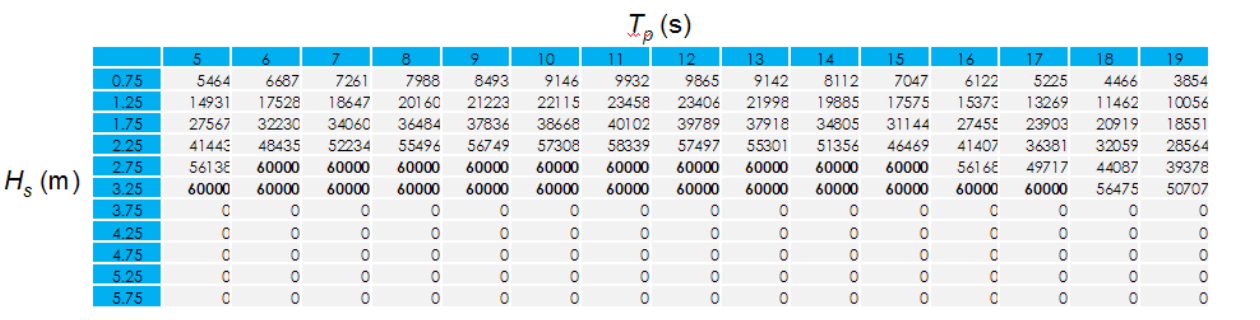

T_p (s)

H_s (m)	5	6	7	8	9	10	11	12	13	14	15	16	17	18	19
0.75	5464	6687	7261	7988	8493	9146	9932	9865	9142	8112	7047	6122	5225	4466	3854
1.25	14931	17528	18647	20160	21223	22115	23458	23406	21998	19885	17575	15373	13269	11462	10056
1.75	27567	32230	34060	36484	37836	38668	40102	39789	37918	34805	31144	27455	23903	20919	18551
2.25	41443	48435	52234	55496	56749	57308	58339	57497	55301	51356	46469	41407	36381	32059	28564
2.75	56138	60000	60000	60000	60000	60000	60000	60000	60000	60000	60000	56168	49717	44087	39378
3.25	60000	60000	60000	60000	60000	60000	60000	60000	60000	60000	60000	60000	60000	56475	50707
3.75	0	0	0	0	0	0	0	0	0	0	0	0	0	0	0
4.25	0	0	0	0	0	0	0	0	0	0	0	0	0	0	0
4.75	0	0	0	0	0	0	0	0	0	0	0	0	0	0	0
5.25	0	0	0	0	0	0	0	0	0	0	0	0	0	0	0
5.75	0	0	0	0	0	0	0	0	0	0	0	0	0	0	0

Table 1 – Illustrative power matrix

RESULTS AND DISCUSSION - continued

Methodology for control performance assessment – resource characterization

Table 2 depicts an illustrative resource scatter matrix and Table 3 incident wave power values

Resource characterization

- Yakutat scatter matrix used for all cases

T_p (s)

H_s (m)	5	6	7	8	9	10	11	12	13	14	15	16	17	18	19
0.25	0.000	0.000	0.000	0.001	0.000	0.000	0.001	0.000	0.001	0.000	0.000	0.000	0.000	0.000	0.000
0.75	0.005	0.017	0.028	0.034	0.025	0.019	0.015	0.011	0.007	0.004	0.001	0.000	0.000	0.001	0.000
1.25	0.003	0.023	0.046	0.061	0.042	0.029	0.020	0.013	0.010	0.006	0.003	0.001	0.000	0.001	0.001
1.75	0.001	0.007	0.030	0.051	0.035	0.018	0.008	0.009	0.008	0.005	0.002	0.002	0.002	0.001	0.000
2.25	0.000	0.000	0.009	0.023	0.039	0.027	0.013	0.006	0.005	0.005	0.004	0.001	0.001	0.001	0.000
2.75	0.000	0.000	0.001	0.006	0.022	0.026	0.021	0.008	0.005	0.003	0.001	0.001	0.001	0.000	0.000
3.25	0.000	0.000	0.000	0.001	0.007	0.016	0.019	0.015	0.007	0.003	0.002	0.002	0.001	0.001	0.001
3.75	0.000	0.000	0.000	0.000	0.000	0.004	0.011	0.020	0.009	0.004	0.002	0.000	0.000	0.000	0.000
4.25	0.000	0.000	0.000	0.000	0.000	0.000	0.002	0.008	0.008	0.005	0.001	0.001	0.000	0.000	0.000
4.75	0.000	0.000	0.000	0.000	0.000	0.000	0.000	0.000	0.001	0.002	0.003	0.002	0.001	0.000	0.000
5.25	0.000	0.000	0.000	0.000	0.000	0.000	0.000	0.000	0.000	0.001	0.001	0.001	0.001	0.001	0.000
5.75	0.000	0.000	0.000	0.000	0.000	0.000	0.000	0.000	0.000	0.000	0.000	0.000	0.000	0.000	0.000

Table 2 – Illustrative scatter matrix

- Incident wave power (in Watts)

T_p (s)

H_s (m)	5	6	7	8	9	10	11	12	13	14	15	16	17	18	19
0.25	1490	1840	2130	2370	2560	2720	2840	2940	3030	3090	3150	3200	3240	3280	3310
0.75	13420	16540	19190	21340	23070	24450	25570	26480	27230	27850	28370	28810	29180	29500	29770
1.25	37270	45940	53300	59280	64080	67930	71040	73570	75640	77360	78800	80020	81050	81930	82690
1.75	73040	90040	104460	116190	125590	133140	139230	144190	148260	151630	154450	156830	158850	160580	162080
2.25	120750	148840	172680	192060	207610	220090	230160	238360	245080	250660	255320	259250	262590	265460	267920
2.75	180370	222340	257950	286910	310140	328780	343820	356060	366110	374440	381410	387280	392270	396540	400230
3.25	251930	310540	360280	400720	433170	459200	480210	497310	511350	522980	532710	540910	547880	553850	559000
3.75	335410	413440	479670	533510	576710	611370	639340	662100	680790	696280	709230	720150	729430	737380	744230
4.25	430810	531040	616100	685260	740750	785270	821200	850430	874430	894330	910960	924990	936910	947120	955920
4.75	538140	663340	769600	855980	925290	980900	1025780	1062300	1092290	1117140	1137920	1155440	1170330	1183080	1194070
5.25	657390	810340	940140	1045670	1130340	1198280	1253100	1297710	1334350	1364700	1390080	1411490	1429680	1445260	1458690
5.75	788580	972040	1127750	1254330	1355900	1437390	1503160	1556670	1600610	1637020	1667470	1693150	1714970	1733650	1749760

Table 3 – Illustrative incident power matrix

[REMAINDER OF PAGE PURPOSELY LEFT BLANK]

Methodology for control performance assessment – performance metrics

Performance metrics employed for performance assessment are reported by Figure 15.

Performance metrics independent of PTO system P_{rat}

Metric	Explanation
E_{inc}	Annual incident flap energy
E_{abs}	Annual absorbed flap energy
Q	Annual flap capture efficiency = E_{abs}/E_{inc}
Q_n	Q normalized by that of the baseline

Performance metrics dependent on PTO system P_{rat}

Metric	Explanation
P_{avg}	Annually-averaged power generation (kW)
E_{avg}	Annual energy production (GWh)
C	Electric plant capacity factor
C_n	C normalized by that of the baseline

Figure 15 – Performance metrics

[REMAINDER OF PAGE PURPOSELY LEFT BLANK]

RESULTS AND DISCUSSION - continued

Capture efficiency enhancement results

Table 4 reports the percent improvement (Qn) in flap capture efficiency for each advanced real-time control method relative to the baseline Coulomb damping method. In all but the case of causal control option 1 the trend is that performance increases with control system complexity—and cost. Performance gains are independent of the PTO power rating. However, the LCOE analysis presented in Appendix A assumes that the PTO power rating is that of the baseline Coulomb damping system.

Assumptions

- Cutoff wave height H_c = 3.75m (inclusive)
- PTO rating P_{rat} varied between 25 and 200 kW
- Option 3 & 1 results reflect optimization of T_0 over all possible values

Performance metrics independent of P_{rat}

Information option	Power train option	E_{inc} (GWh)	E_{abs} (GWh)	Q	Q_n
Causal	4	1.84	0.68	0.37	145%
	2	1.84	0.64	0.35	137%
	3	1.84	0.61	0.33	131%
	1	1.84	0.62	0.34	134%
Non-causal	4	1.84	0.88	0.48	188%
	2	1.84	0.75	0.41	161%
	3	1.84	0.83	0.45	177%
	1	1.84	0.73	0.40	157%
Baseline		1.84	0.47	0.25	100%

Table 4 – Improvement of flap capture efficiency over baseline Coulomb damping

[REMAINDER OF PAGE PURPOSELY LEFT BLANK]

RESULTS AND DISCUSSION - continued

Performance gains as a function of PTO power rating

For each control method figure 16 reports annual average power vs PTO power rating. The benefit of increased power capacity (and increased PTO system cost) begins to diminish above 65 to 85kW. Figure 17 reports annual average electrical energy vs PTO power rating.

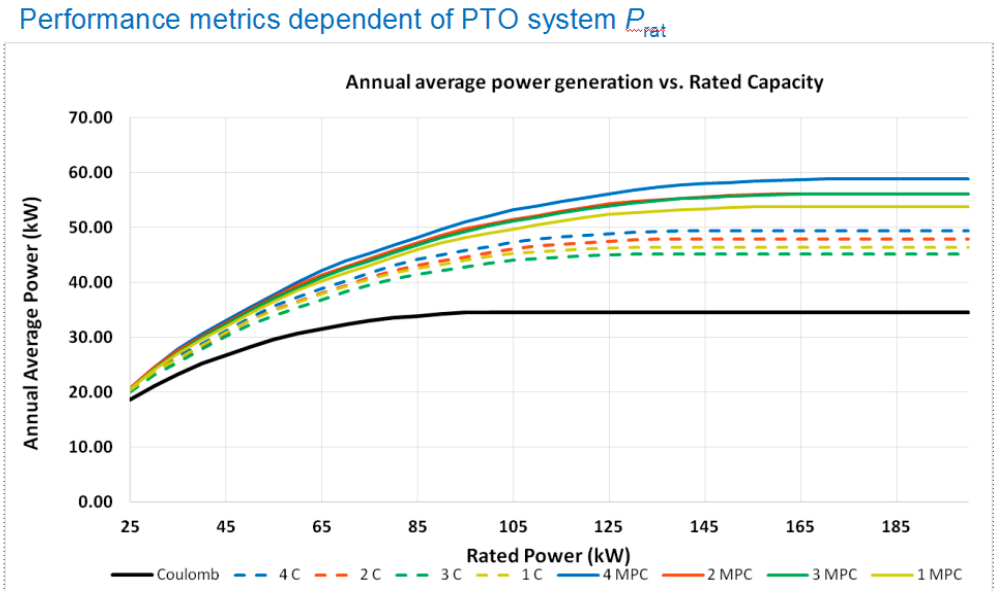

Figure 16 – Annual average electric power as a function of PTO rating

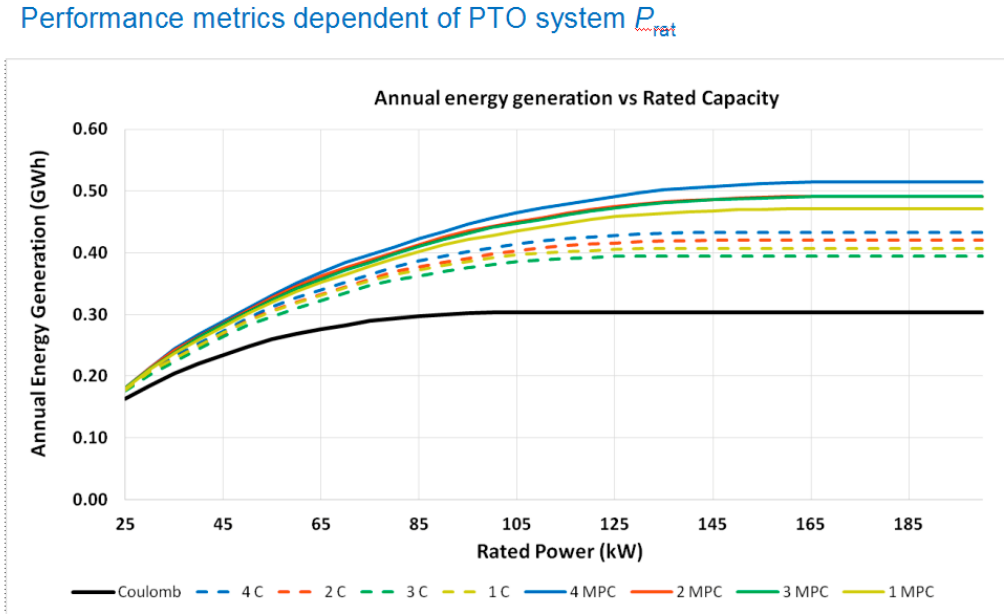

Figure 17 – Annual average electrical energy production as a function of PTO rating

RESULTS AND DISCUSSION - continued

Plant capacity factor as a function of PTO power rating

Figure 18 shows the decline of capacity factor with increasing PTO rating for each control system considered

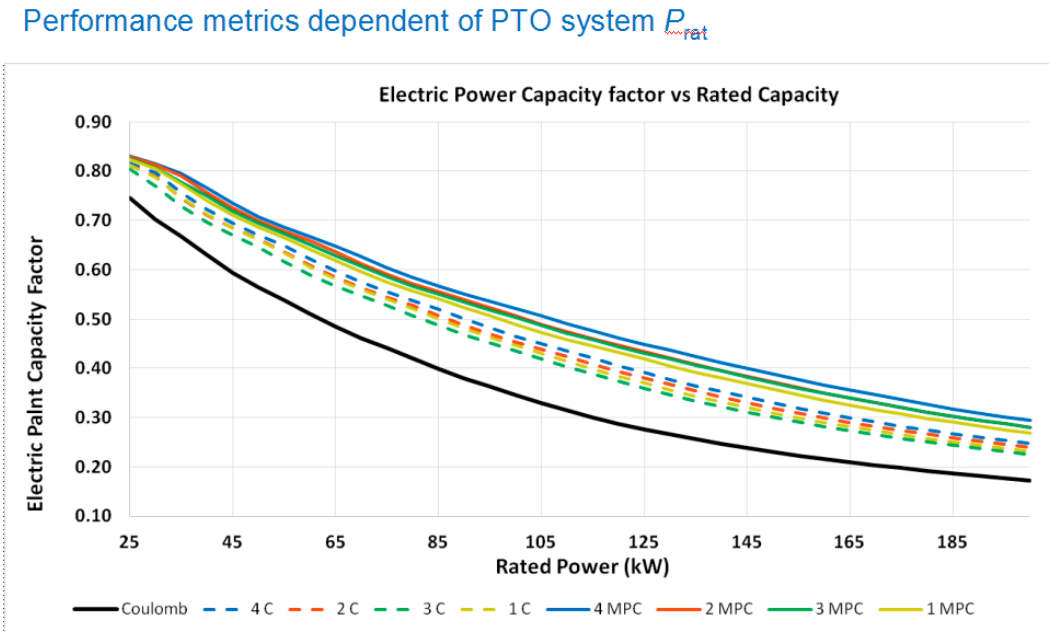

Figure 18 – Capacity factor as a function of PTO power rating

[REMAINDER OF PAGE PURPOSELY LEFT BLANK]

RESULTS AND DISCUSSION - continued

Illustrative power trajectories of causal systems at rated conditions Hs = 2.5m, Tp = 9s

Figure 19 depicts case of uni-directional power flow and tri-state flap load torque control. Figure 20 reports case of uni-directional power flow with continuous flap load torque control.

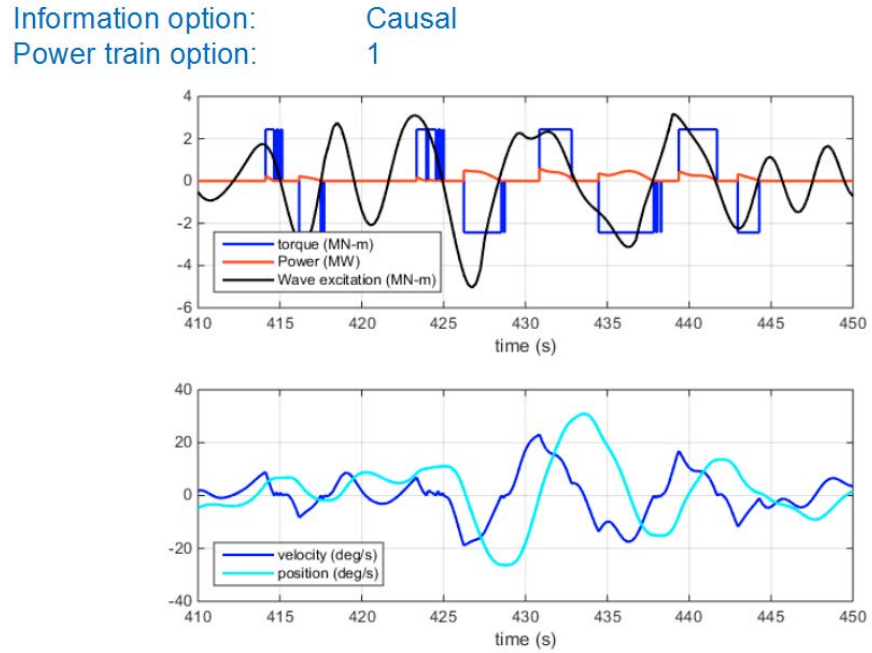

Figure 19 – Uni-directional power flow with tri-state flap load torque control - Causal

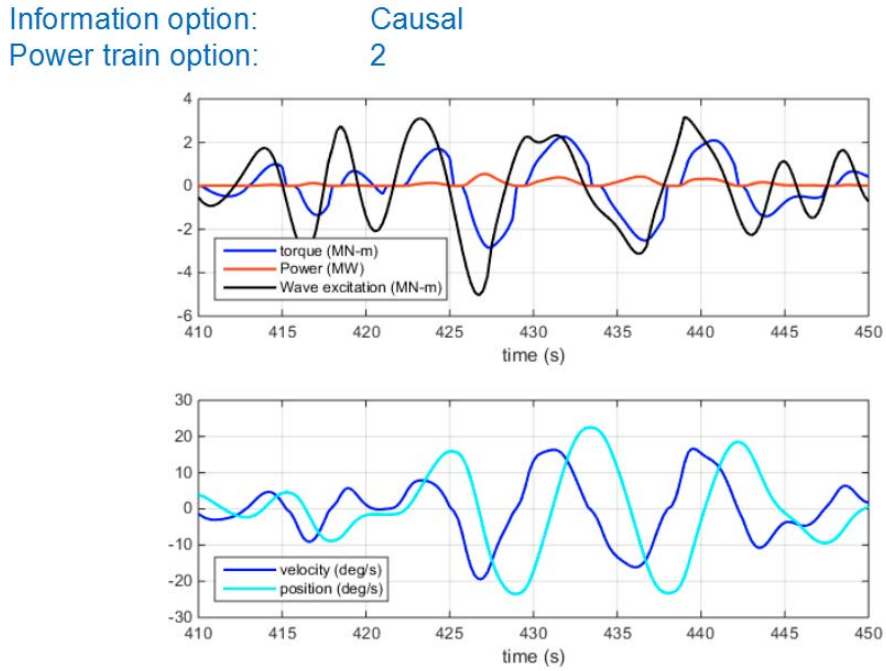

Figure 20 – Uni-directional power flow with continuous flap load torque control – Causal

RESULTS AND DISCUSSION - continued

Illustrative power trajectories of causal systems at rated conditions Hs = 2.5m, Tp = 9s

Figure 21 depicts case of bi-directional power flow and tri-state flap load torque control. Figure 22 reports case of bi-directional power flow with continuous flap load torque control.

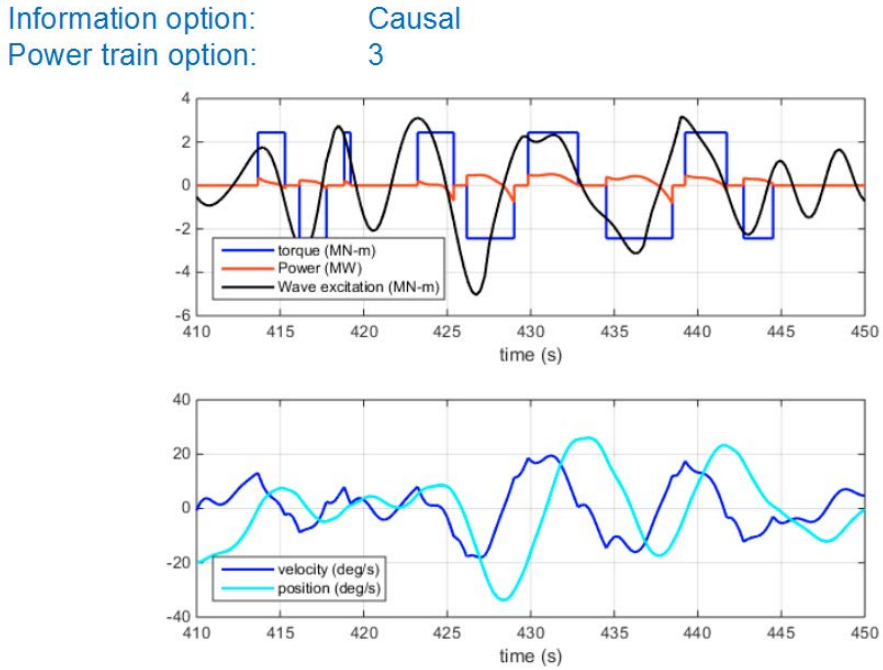

Figure 21 – Bi-directional power flow with tri-state flap load torque control - Causal

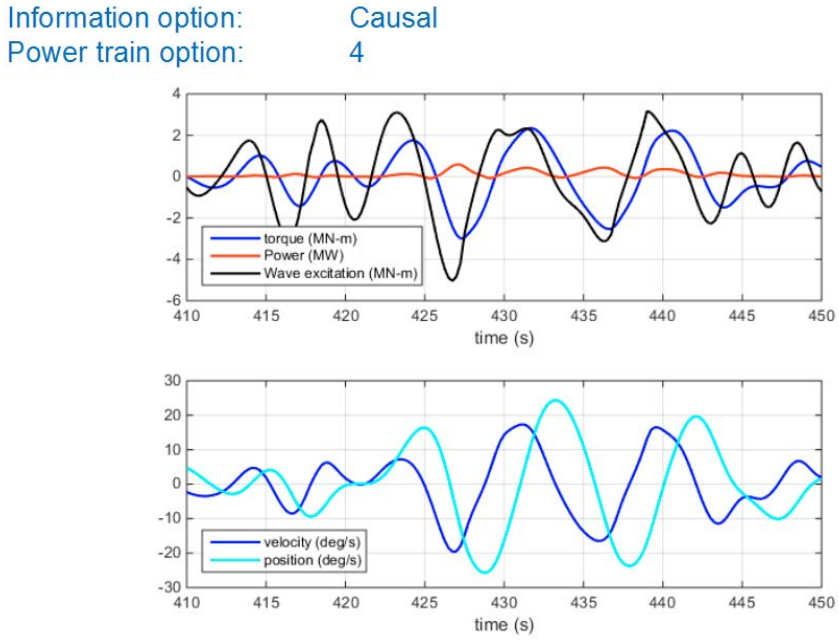

Figure 22 – Bi-directional power flow with continuous flap load torque control – Causal

RESULTS AND DISCUSSION - continued

Illustrative power trajectories of <u>non-causal</u> systems at rated conditions Hs = 2.5m, Tp = 9s

Figure 23 depicts case of uni-directional power flow and tri-state flap load torque control. Figure 24 reports case of uni-directional power flow with continuous flap load torque control.

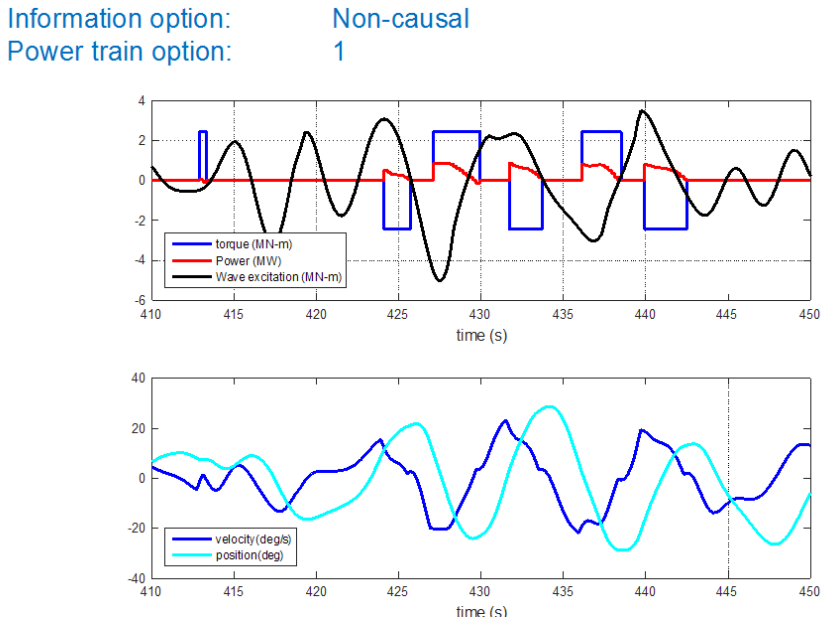

Figure 23 – Uni-directional power flow with tri-state flap load torque control – Non-causal

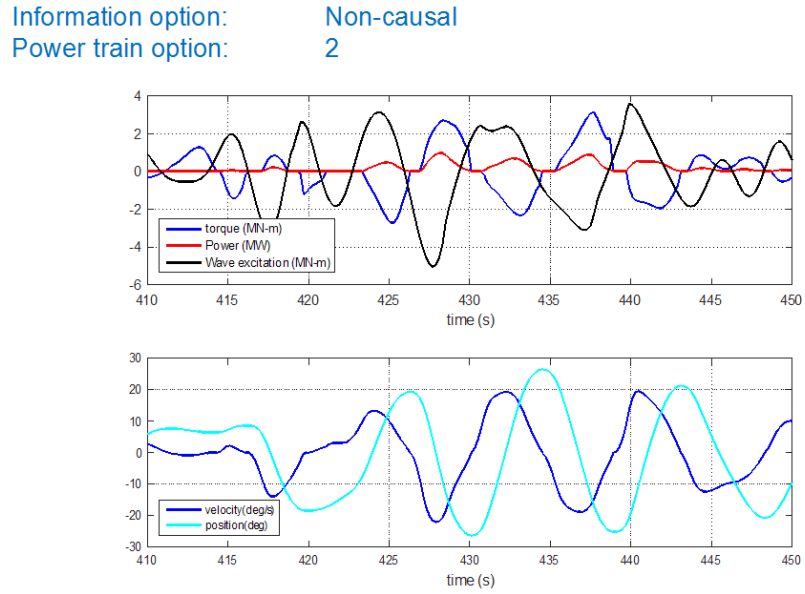

Figure 24 – Uni-directional power flow with continuous flap load torque control – Non-causal

RESULTS AND DISCUSSION - continued

Illustrative power trajectories of <u>non-causal</u> systems at rated conditions Hs = 2.5m, Tp = 9s

Figure 25 depicts case of bi-directional power flow and tri-state flap load torque control. Figure 26 reports case of bi-directional power flow with continuous flap load torque control.

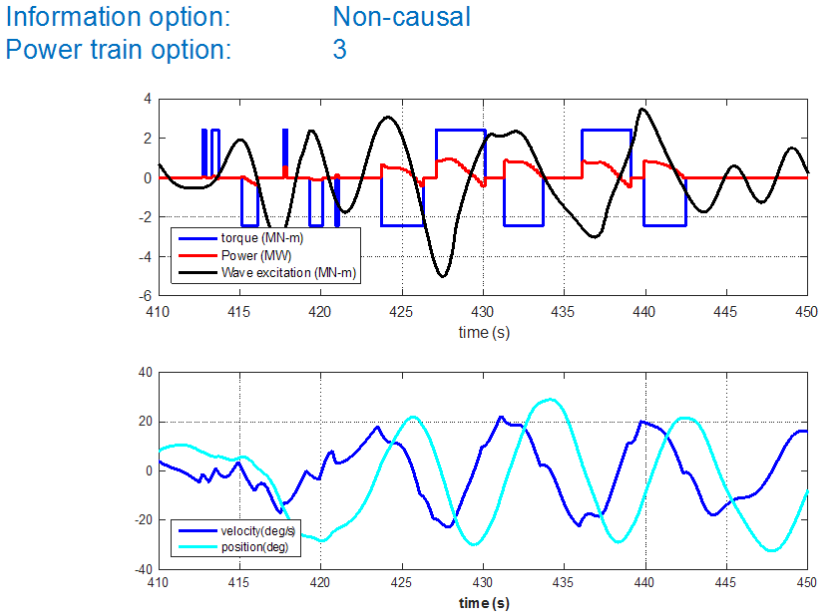

Figure 25 – Bi-directional power flow with tri-state flap load torque control – Non-causal

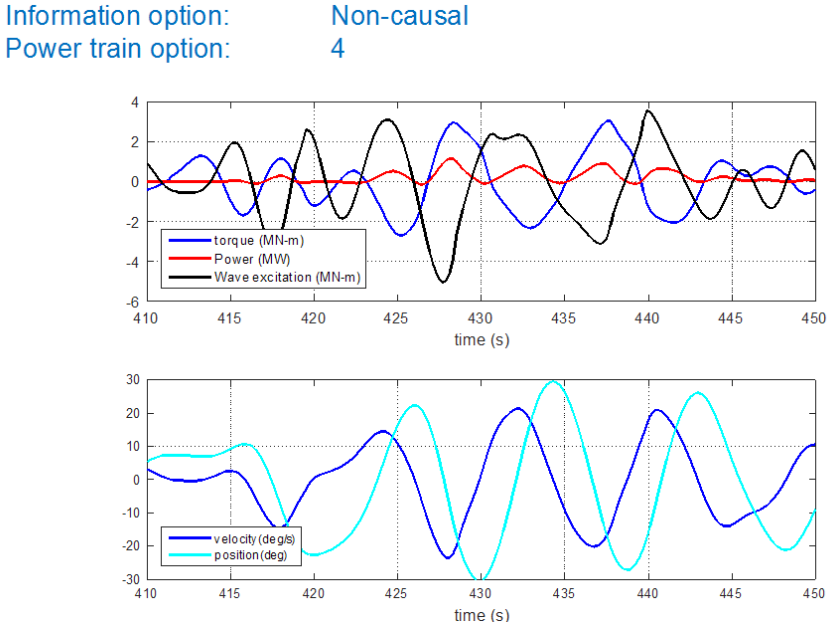

Figure 26 – Bi-directional power flow with continuous flap load torque control – Non-causal

RESULTS AND DISCUSSION - continued

Illustrative power trajectories of <u>non-causal</u> systems at rated conditions Hs = 2.5m, Tp = 9s

Figure 27 compares flap load torque control for non-causal options 1 – 4.

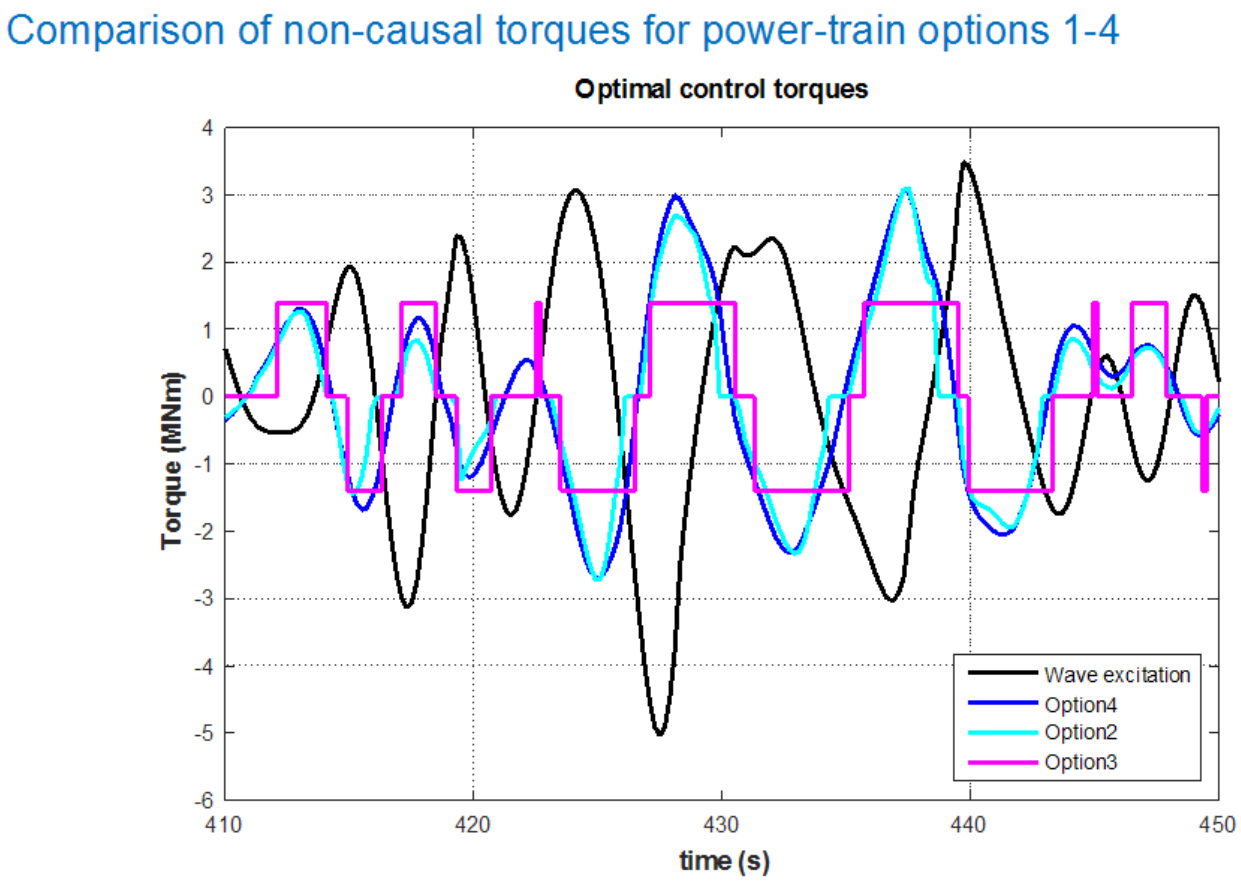

Figure 27 – Comparison of flap load torque for non-causal control options 1 – 4

[REMAINDER OF PAGE PURPOSELY LEFT BLANK]

RESULTS AND DISCUSSION – continued

Commentary on robustness

As explained in Figure 28 implementation of bi-directional power flow causal control using tri-state flap torque control revealed a robustness challenge. The sacrifice in optimum performance negated the modest advantage of bi-directional power flow (causal option 3).

Control architecture

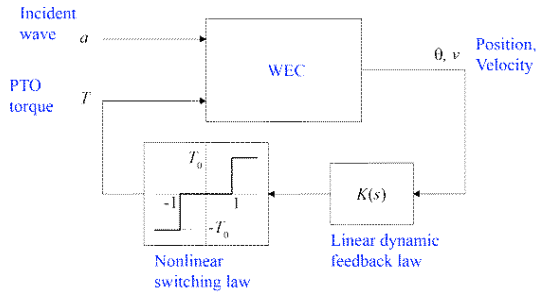

Development history

- Preliminary results obtained in first budget period, but deemed unsatisfactory
- Finalized results required significant development:
  - New analytical approximation model for stochastic power generation
  - New optimization techniques to optimize *K*(*s*)
  - Transient simulation code augmented to handle discrete-event switching
  - Implementation of hysteretic switching techniques & minimum switching times

Stability robustness was a challenge

- Theoretically-optimal causal controllers operate very close to the stability boundary – very small stability margins
- Model uncertainty leads to instabilities
- Example
  (Tp = 7s, Hs = 3.75m)

- Loop-transfer-recovery (LTR) techniques used to enhance stability margins
- Theoretical performance had to be sacrificed considerably to achieve robustness

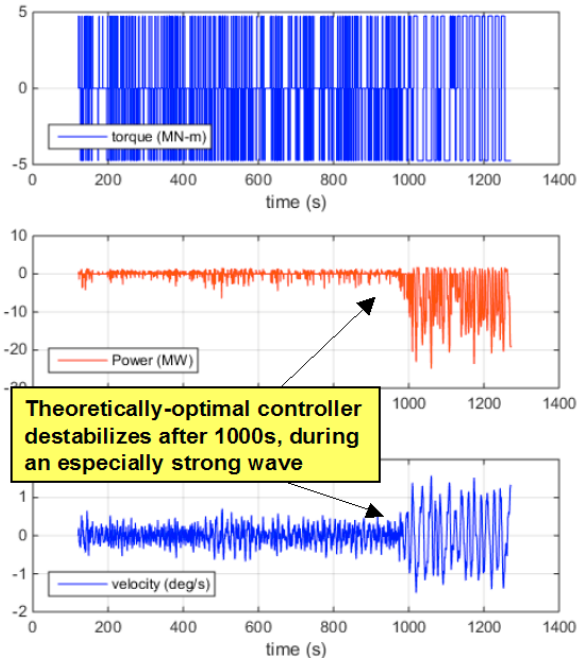

Figure 28 – Robustness observations for causal control option 3 – bi-directional power flow and tri-state flap load control.

RESULTS AND DISCUSSION – continued

Design considerations for non-causal control wave forecasting sensor array

Figure 29 summarizes the considerations taken by Re-Vision to determine the spatial density of seaward wave forecasting sensors required for effective non-causal control

Issue:
• Non-causal control requires accurate forecasts for incident wave torque

Question:
• How many sensors are required, and where should they be placed, to achieve acceptable accuracy?

Status:
• Investigation completed by Re-Vision, concluding that 6 sensors provide adequate predictive capability for this application

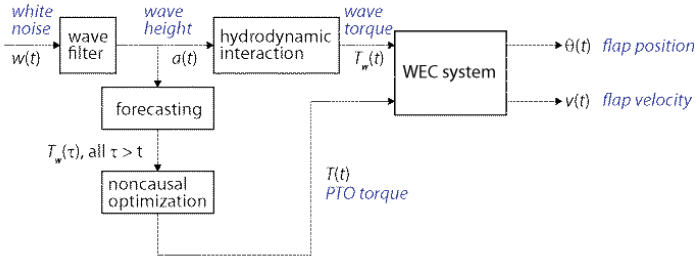

Wave Prediction: The model components

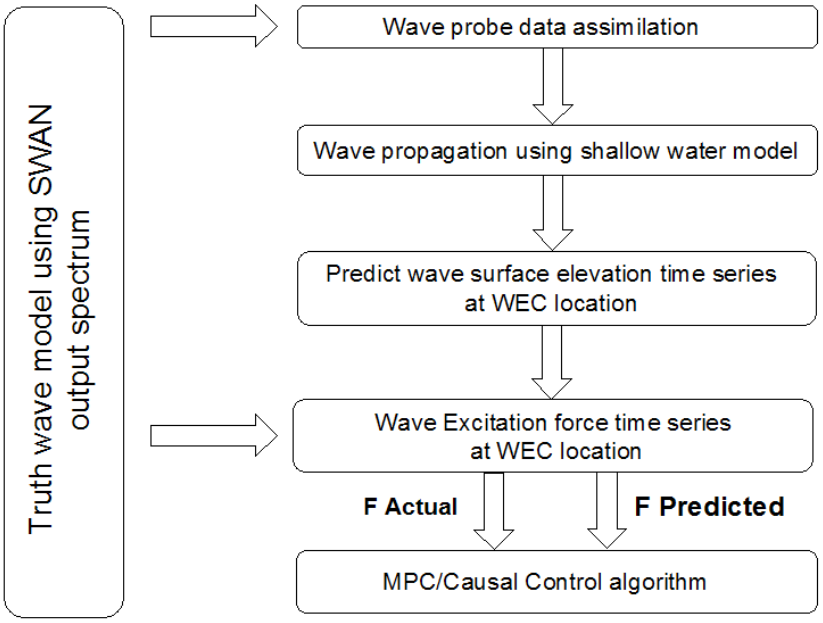

Figure 29 – Determining the spatial density of wave forecasting sensors

RESULTS AND DISCUSSION – continued

Analysis methodology for estimating the spatial density of wave sensors required for a non-causal control wave forecasting sensor array

The methodology employed by Re-Vision to determine the spatial density of wave forecasting sensors is summarized in Figure 30.

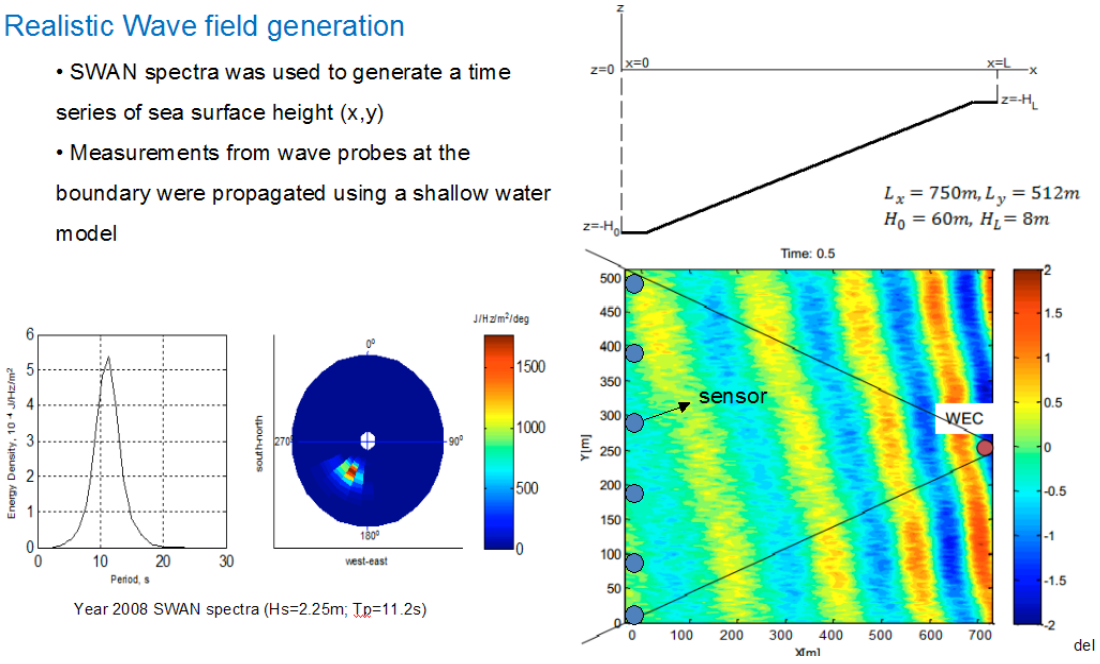

- Amplitude and phase errors for an input wave of Tp = 11s shown in table
- With 8 sensors the normalized performance of MPC is at 97.8%

Number of measurements	Amplitude error (%)	Phase error (%)
512	0.00	0.00
256	0.19	0.62
128	0.42	1.52
64	0.39	2.82
32	0.34	3.01
16	4.47	9.50
8	19.41	59.57
4	47.55	30.60

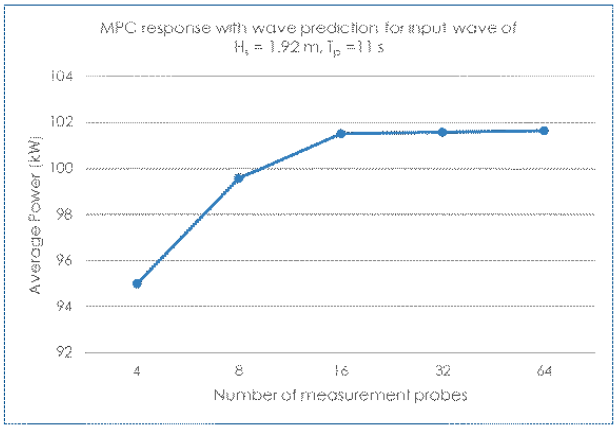

Figure 30 – Determination of spatial density of wave forecasting sensors

RESULTS AND DISCUSSION – continued

Continuous torque control bandwidth and shunt valve switching rate

The continuous torque control spectrum was examined to determine the shunt valve PWM switching rate required for reasonably faithful implementation of the torque command for options 2 and 4. The methodology and conclusions are summarized in Figure 31.

Issue:

- Options 2 and 4 (both causal and non-causal) can exhibit high-frequency torque content
- May be expensive (or impossible) to implement with practical hydraulics

Question:

- What bandwidth does the hydraulic torque control system need to have, to come close to tracking the desired trajectories?

Status:

- Spectral analyses completed for Option 2 (both causal and non-causal).
- Analyses used by RME to develop specifications for switch-mode hydraulic means to control the effective displacement of flap pumps under investigation by Prof. James Van de Ven at the University of Minnesota

Spectral analysis for option 2

- Evaluate empirical PSD of PTO torque command
- Determine band of ideal low pass filter to preserve desired percentage of original torque command signal

Conclusions:

- PTO torque control system needs ~ 0.2 - 0.3Hz bandwidth to attain 90 - 95% of the signal power of the optimal control
- Assessed at rated conditions: H_s = 2.75m, T_p = 9s
- About the same for causal & non-causal
- May require PWM switching at >= 2 - 3Hz

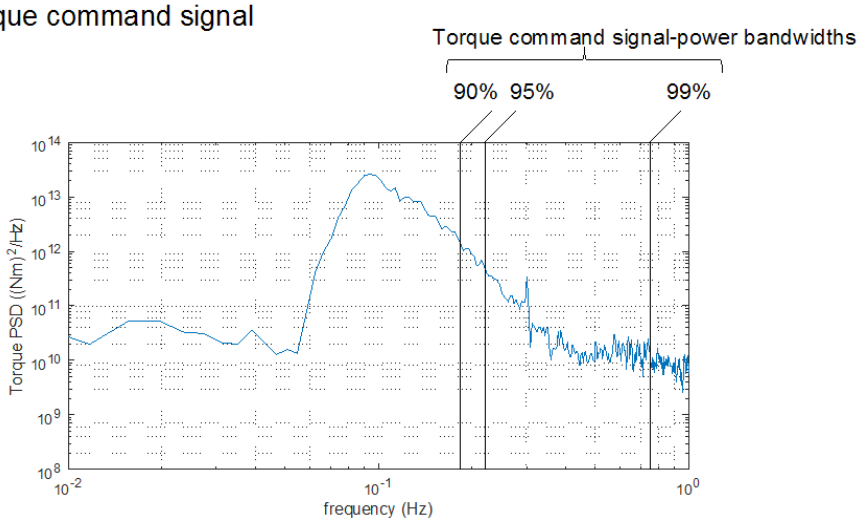

Figure 31 – Analysis of continuous control torque spectrum and estimate of required shunt valve PWM switching rate

RESULTS AND DISCUSSION – continued

Required flap pump reaction torque magnitude for tri-state (aka bi-polar) control

Tri-state (aka bi-polar) control would be simpler to implement than continuous control of effective flap pump displacement and reaction torque by shunt valve PWM. However, concern was raised and investigated regarding the required tri-state torque magnitude for effective control. The issue and preliminary findings are reported below in Figure 32.

Issue:

- It was found that for bi-polar torque options (i.e., Options 1 and 3), performance could depend heavily on torque magnitude U_0
- The optimal U_0 is generally larger than the optimal Coulomb damping torque of the baseline system
- Operating pressure is constrained to ~ 1,000 psi (6.8MPa) by the available sea water compatible hydraulic motor
- Hence implementation of higher U_0 requires higher flap pump displacement and cost
- *Example:*

Causal Option 3,
Hs = 2.75m

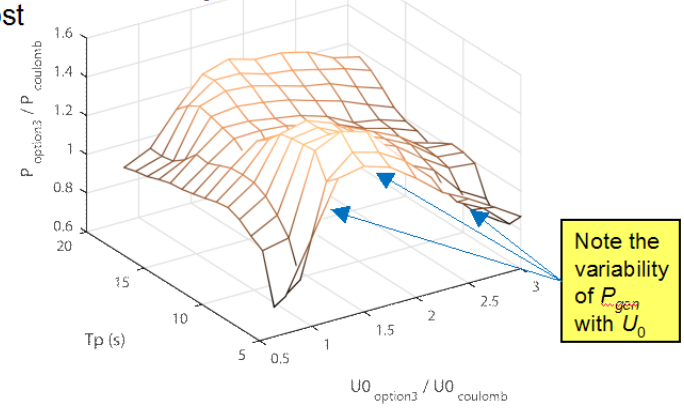

Question:

- What is the cost / benefit tradeoff of U_0 level, vs. performance
- In particular, what is the performance of U_0 values relative to the optimal Coulomb damping torque at rated conditions?

Status:

- Tradeoff analysis conducted for Option 3, both causal and non-causal, at rated conditions
- Appears that significant flap performance enhancement might be achieved without increasing flap pump displacement

Figure 32 – Assessment of tri-state control torque magnitude requirement

RESULTS AND DISCUSSION – continued

Required flap pump reaction torque magnitude for tri-state (aka bi-polar) control

Analysis of non-causal and causal option 3 cases (bi-directional power flow with tri-state control) found that most of the flap capture efficiency advantage can be achieved without increasing the displacement and cost of the baseline flap pumps. The results are reported in Figure 33.

Flap performance enhancement at rated conditions for non-causal case

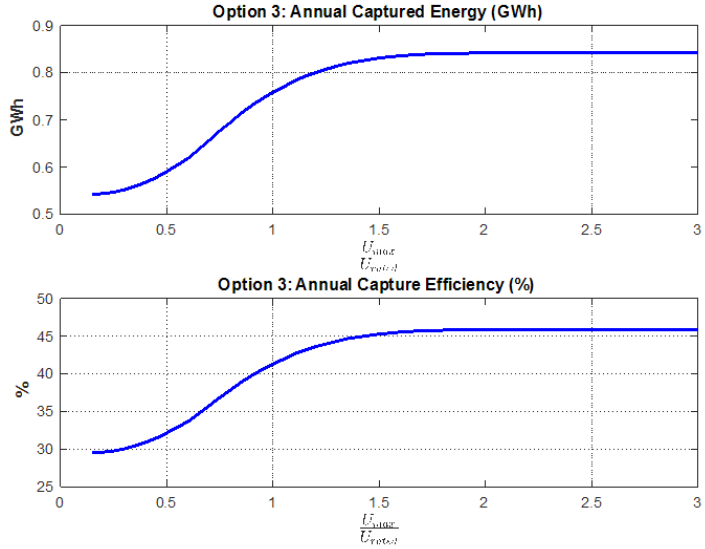

Flap performance enhancement at rated conditions for the causal case

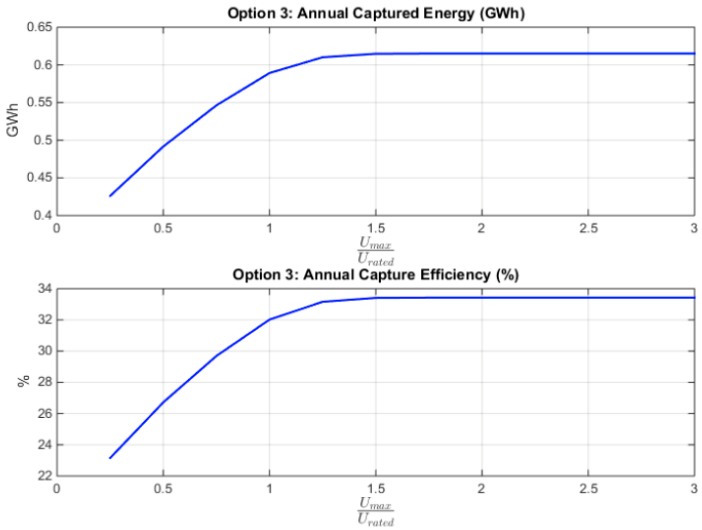

Figure 33 – Option 3 performance vs flap pump displacement relative to baseline pump displacement

RESULTS AND DISCUSSION – continued

Shunt valve switching rate for tri-state (bi-polar) control

It was expected that tri-state control of effective flap pump displacement and hence reaction torque would require less frequent shunt valve operations than required for continuous control via PWM valve operation. Figure 34 summarizes the results of an investigation by Re-Vision for the case of non-causal option 3 control. The median switching rate was found to be 0.7Hz approximately 1/3rd to 1/4th that required for PWM operation. In consequence it is anticipated that valve response time requirements would thus be eased and service life significantly increased—both having a favorable impact on LCOE.

Issue:

- Feasibility of efficient and cost-effective ON/OFF modulation of flap pump effective displacement by switch mode control of a shunt valve--or manifolded bank of valves--depends on the required switching rate and flow to be accommodated with acceptable pressure drop

Questions:

- What is the range of switching event intervals and frequencies?
- What is the range of flows to be accommodated by the valve(s)

Status:

- Analysis of switching events for the case of non-causal Option 3 was performed by Re-Vision as a function of maximum torque/Coulomb damping torque $\alpha = U_{max}/U_{Coulomb}$
- For case of a = 1
    - Median switching interval and frequency ~ 1.4s and ~ 0.7Hz
    - Open to close flow ~ 4.5x mean for Coulomb damping
    - Close to open flow ~ 3.1x mean for Coulomb damping

Figure 34 – Analysis of tri-state control valve switching frequency

[REMAINDER OF PAGE PURPOSELY LEFT BLANK]

RESULTS AND DISCUSSION – continued

Implementation of real-time flap load control

Methods considered for physically implementing real-time flap load control and the rationale for a solution based on advanced switch-mode hydraulic means are summarized below in Figure 35.

Issue:

- Realization of advanced real-time flap load control policies--continuous or tri-state (aka bi-polar) to enhance capture efficiency presents a challenging PTO implementation problem

- Concepts considered
  1) Modulate load on the pumps by the hydraulic motor-generator set
  2) Modulate the effective flap pump displacement

1) requires elimination of accumulator power pulsation and fluctuation suppression and a motor-generator set capable of handling a peak/average power >= 5x. High capacity electrical energy storage would be required to suppress power pulsations and fluctuations due to wave grouping

2) requires only fast-acting, low loss shunt valves and avoids significant oversizing and inefficient operation of the motor-generator. Accumulator suppression of power pulsations and fluctuations is retained and electrical energy storage capacity to suppress power ramp rate would be smaller

Questions:

Do commercial valves exist that can meet switching rate and flow requirements?

- Would these valves provide a reasonable service-life … e.g., 20+ million operations over a 5 year period?
- What losses would be encountered? What efficiency could be attained?
- How much would these valves and associated components cost?
- If commercial solutions are not suitable could a purpose-designed valve meet our requirements? What would it cost to develop and manufacture?

Approach:

- RME engaged switch-mode hydraulics expert Prof. James Van de Ven of the University of Minnesota, Mechanical Engineering Department, Center for Compact and Efficient Fluid Power (CCEFP)
- RME provided Prof. Van de Ven with preliminary requirements based on the preceding findings and a feasibility investigation is under way

Figure 35 – Approach to real-time control of flap load control

RESULTS AND DISCUSSION – continued

Analysis of PWM switch-mode flap pump displacement modulator

The model adopted by Prof. James Van de Ven and design considerations are summarized in Figure 36

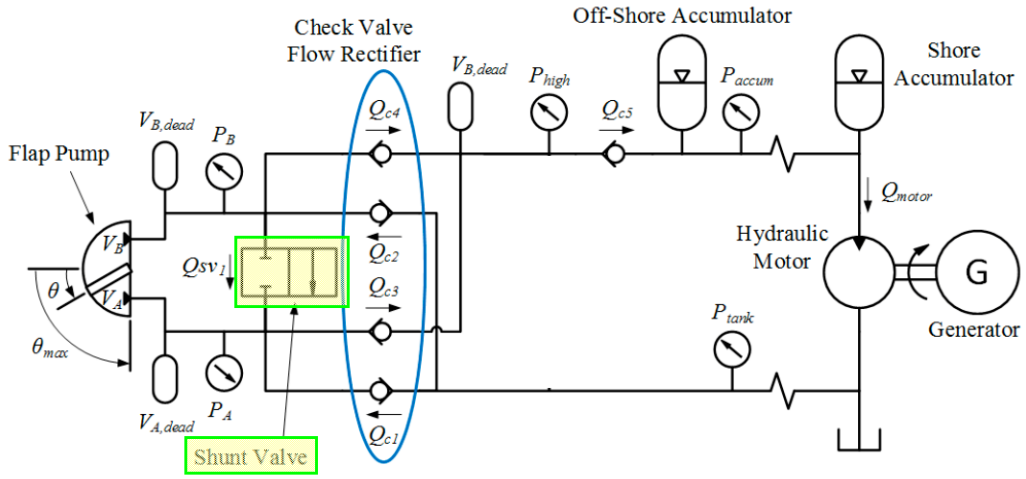

- When shunt is open pump ports are bypassed and effective displacement = 0
- Alternatively can view shunt as a pump pressure modulator
- Pump reaction torque = pressure x displacement -- so either controls flap load

- The shunt valve will only reduce effective pump displacement and flap load
- Flap capture efficiency gain is due to avoiding instances of Coulomb damping overloading -- especially for sea conditions below rated
- For continuous load control methods (Options 2 and 4) valve state is pulse width modulated (PWM)
    - Low duty cycle = reduced shunting and flap unloading
    - High duty cycle = increased shunting and flap unloading

- Tri-state (aka bi-polar) control methods (Options 1 and 3) would require less frequent valve operation and extend valve service life
- Control methods which allow reverse power flow to improve flap tuning (Options 4 and 3) would require active control of the 4 flow rectifier valves-- each as costly as the shunt valve
- Since a flap of modest size (e.g., 8 to 10m width) is intrinsically well-tuned bi-directional power flow (Options 2 and 4) add little capture efficiency benefit

Figure 36 – PWM switch-mode flap pump displacement modulator model

RESULTS AND DISCUSSION – continued

Numerical analysis of PWM switch-mode flap pump displacement modulator

An initial analysis of the system implemented with MathWorks SimHydraulics presented uncertainties regarding the validity of its component models. Prof. Van de Ven subsequently constructed a numerical model de novo and solved its governing equations via MatLab. Originally it was envisioned that the shunt valve would be placed across the output of the flow rectifier but Prof. Van de Ven discovered better performance could be obtained by directly shunting the pump ports—easily accomplished in the hydraulic realm since the shunt valve, unlike a typical power electronic switch, is naturally bi-directional. The model and governing equations are presented below in Figure 37.

- Lumped parameter model constructed in Matlab
- Sinusoidal flap pump input -12s period & peak flow ~ 4x rated average

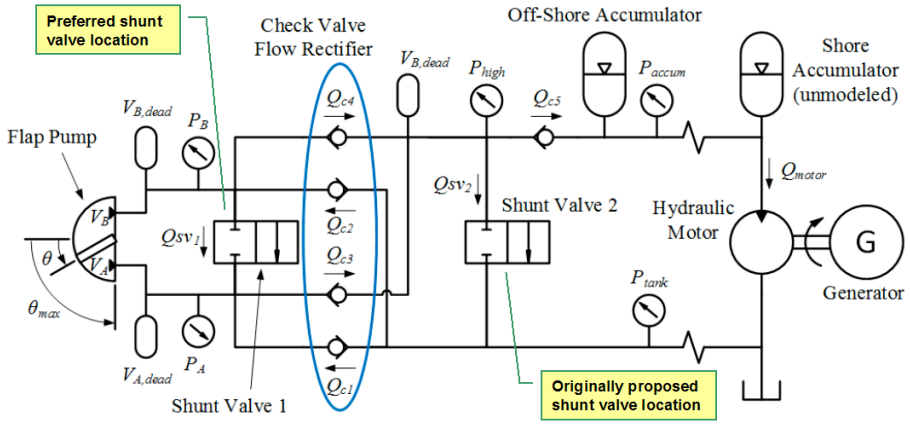

Pump chamber Volumes:

$$V_A(t) = \frac{\theta_{max} - \theta(t)}{2\theta_{max}} V_{pump} + V_{A,dead}$$

$$V_B(t) = \frac{\theta_{max} + \theta(t)}{2\theta_{max}} V_{pump} + V_{B,dead}$$

Lumped Pressures:

$$\frac{dP_A}{dt} = \frac{\beta_{eff}(P)}{V_A}\left(Q_{c1} - Q_{c3} + Q_{sv1} + \frac{dV_A}{dt}\right)$$

$$\frac{dP_B}{dt} = \frac{\beta_{eff}(P)}{V_B}\left(Q_{c2} - Q_{c4} - Q_{sv1} + \frac{dV_B}{dt}\right)$$

$$\frac{dP_{high}}{dt} = \frac{\beta_{eff}(P)}{V_{high}}\left(Q_{c3} + Q_{c4} - Q_{sv2} - Q_{c5}\right)$$

Accumulator:

$$P_{accum} = P_{charge}\left(\frac{V_{charge}}{V_{gas}}\right)^{\gamma}$$

$$\frac{dV_{gas}}{dt} = Q_{motor} - Q_{c5}$$

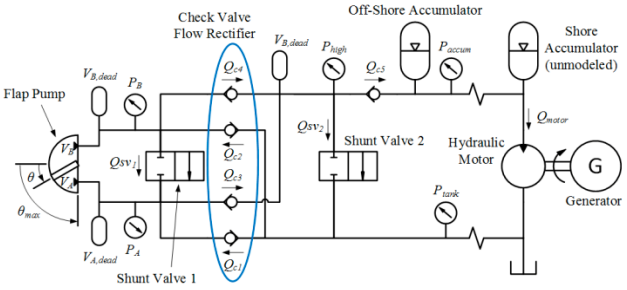

Figure 37 – Switch-mode flap pump displacement modulator model and governing equations

RESULTS AND DISCUSSION – continued

Numerical analysis of PWM switch-mode flap pump displacement modulator - continued

Figure 38 defines additional governing equations and table 5 reports key parameter values. Note this preliminary analysis was conducted assuming a 1Hz PWM switching rate although Figure 31 suggests a rate of 2 to 3Hz might be required. Further analysis beyond the scope of this program would implement the leading continuous control mode controller with a PWM implementation of the flap pump reaction torque to better assess the impact of switching rate on flap capture efficiency improvement.

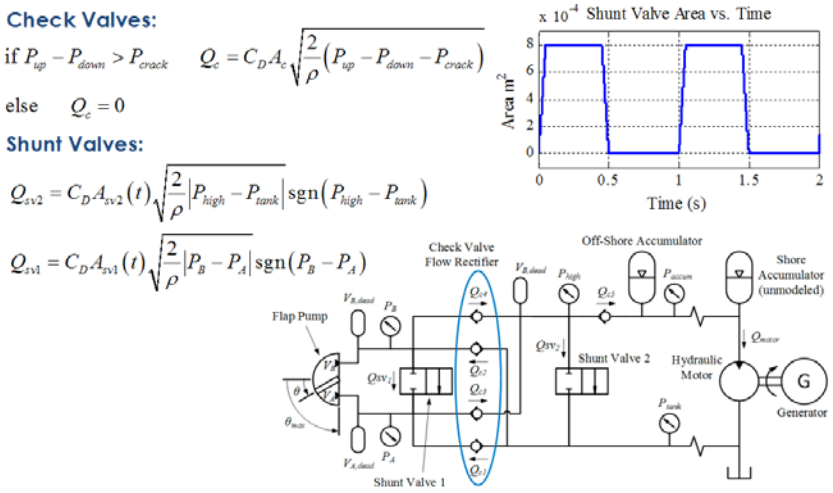

Figure 38 - Switch-mode flap pump displacement modulator model and governing equations--continued

Property	Symbol	Value	Units
Seawater density (40g salt/liter, 20°C)	ρ	1028.8	kg/m^3
Seawater bulk modulus	β	2.2	GPa
Entrained air fraction by volume at atm pressure	R	0.005	Fraction
Ratio of specific heats for air	γ	1.4	Unitless
Pump displacement	D_{pump}	$18*10^{-3}$	m^3/**radian**
Pump rotation from center	θ_{max}	1.22	rad
Dead volume of pump, A side	$V_{A,dead}$	$1*10^{-3}$	m^3
Dead volume of pump, B side	$V_{B,dead}$	$1*10^{-3}$	m^3
Motor displacement (Danfoss APP 26/1500)	D_{motor}	$308*10^{-6}$	m^3/**rev**
Volume in high pressure rail	V_{high}	$1*10^{-3}$	m^3
Accumulator precharge pressure	P_{charge}	$4*10^{6}$	Pa
Accumulator volume	V_{charge}	$50*10^{-3}$	m^3
Tank Pressure	P_{tank}	$404*10^{3}$	Pa
Shunt valve fully open area	$A_{sv,max}$	$8*10^{-4}$	m^2
Check Valve Cracking Pressure	P_{crack}	$101*10^{3}$	Pa
Check Valve Open Area – High Pressure	$A_{check,h}$	$8*10^{-4}$	m^2
Check Valve Open Area – Low Pressure	$A_{check,l}$	$1.67*10^{-3}$	m^2
Valve discharge coefficient	C_D	0.6	Unitless
Switching frequency	f_{sw}	1	Hz
Duty cycle	$Duty$	0.5	Fraction
Transition fraction of switching period	f_{trans}	0.05	Fraction
Flap pump frequency	f_{pump}	0.083	Hz
Reference pressure	P_{ref}	6.9	MPa

Table 5 – Switch-mode pump displacement modulator parameters

RESULTS AND DISCUSSION – continued

Numerical analysis of PWM switch-mode flap pump displacement modulator - continued

Illustrative valve switching operations are depicted in Figure 39a with shunt valve across rectifier output and Figure 39b with shunt valve across pump ports.

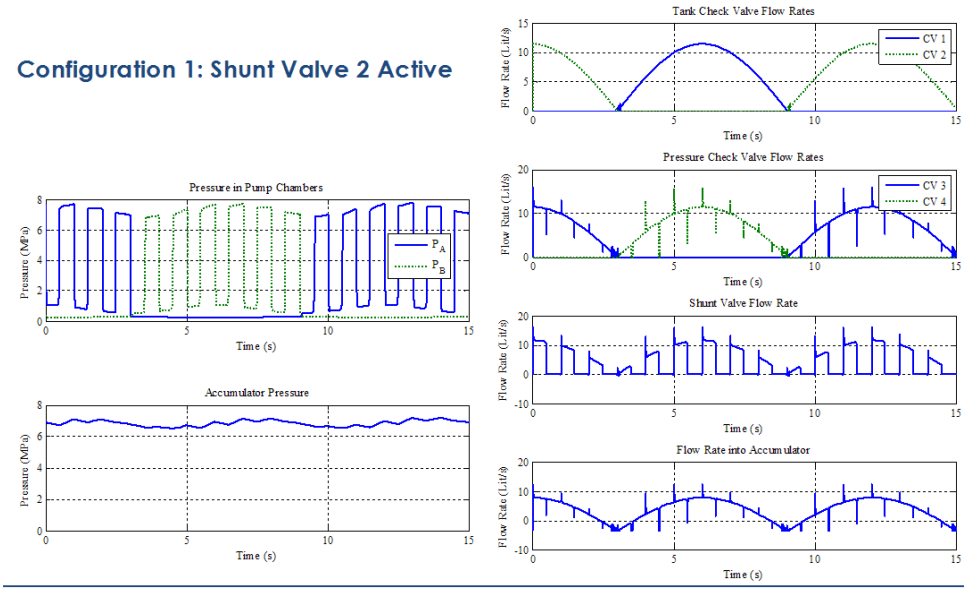

Figure 39a – Switching patterns with valve across flow rectifier output

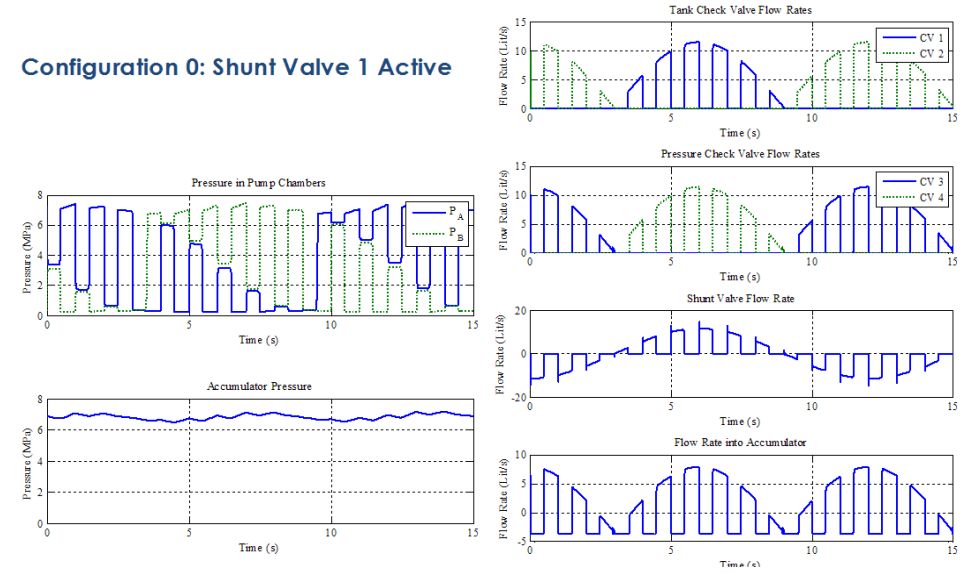

Figure 39b – Switching patterns with valve across pump ports

RESULTS AND DISCUSSION – continued

Numerical analysis of PWM switch-mode flap pump displacement modulator - continued

Figure 40 compares efficiency with shunt valve across the rectifier output (Configuration 1) vs directly across the pump ports (Configuration 0)

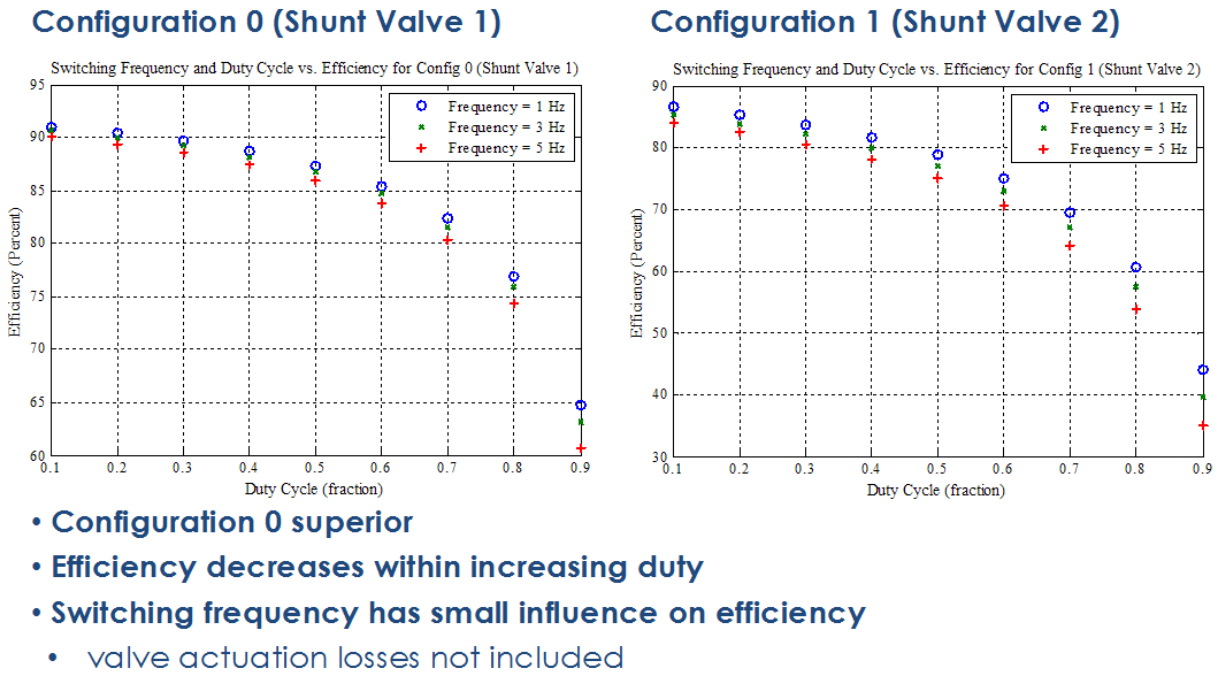

Figure 40 – Switch mode pump displacement modulator efficiency vs valve location

[REMAINDER OF PAGE PURPOSELY LEFT BLANK]

RESULTS AND DISCUSSION – continued

Numerical analysis of PWM switch-mode flap pump displacement modulator - continued

Figure 41a identifies influence of valve switching time on efficiency while Figure 41b shows how pump dead volume effects efficiency.

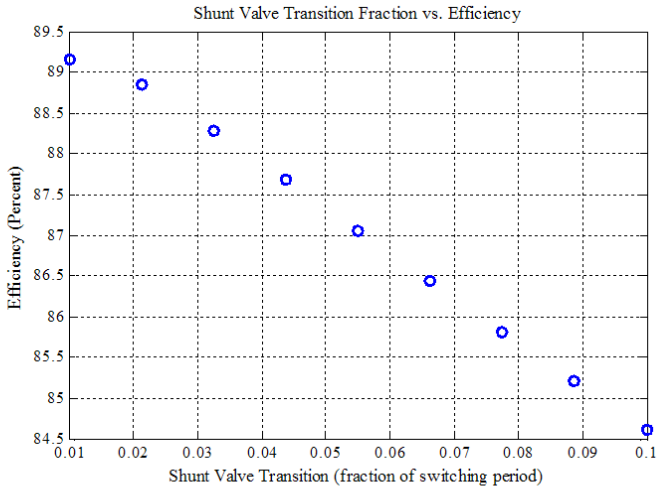

- Fast shunt valve important to efficiency

Figure 41a – Efficiency vs valve switching time

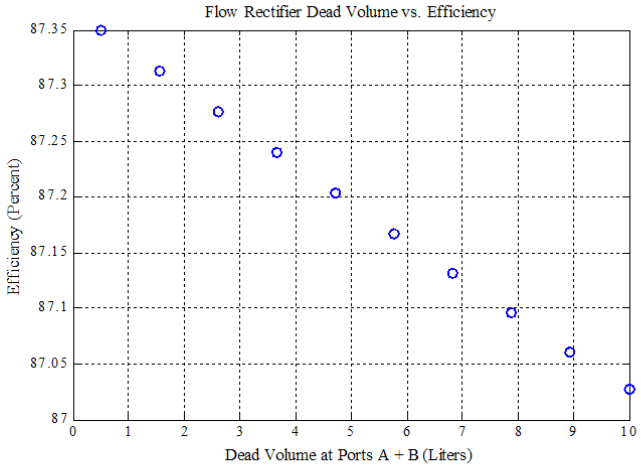

- Dead volume of flow rectifier plays an insignificant role due to large pump dead volume

Figure 41b – Efficiency vs pump dead volume

RESULTS AND DISCUSSION – continued

Numerical analysis of PWM switch-mode flap pump displacement modulator - continued

Figure 42 depicts results of analysis to determine size of off-shore high pressure accumulator to reduce pressure pipe line pressure ripple and concluding observations

$$Ripple = \frac{\max\left(P_{accum}\right) - \min\left(P_{accum}\right)}{\text{mean}\left(P_{accum}\right)}$$

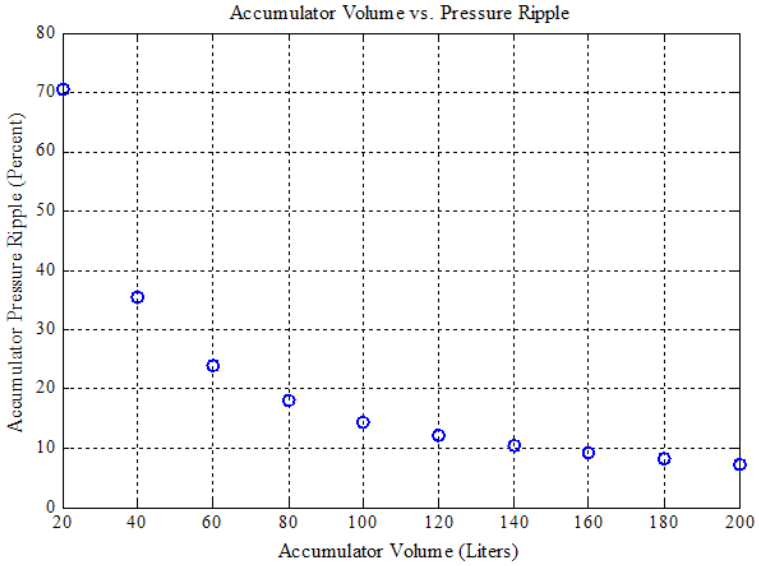

- **>140 liter off-shore accumulator required for <10% ripple**

- The shunt valve should be located across pump ports, not between high pressure rail and tank rail
- Increasing the area of the high pressure check valves and shunt valve above 8 cm^2 shows diminishing returns (peak flow rate of 11.5 L/min)
- Reducing valve transition time improves efficiency
- Flow rectifier dead volume not critical
- Off-shore accumulator should be ~140 liters (37 gal)

Figure 42 – Off-shore high pressure accumulator sizing and concluding observations

APPENDIX A – LCOE Analysis

We describe and justify herein the main assumptions used in our Levelized Cost Of Electricity (LCOE). We are using two DOE documents as references:

1) "Standardized Cost and Performance Reporting for Marine and Hydrokinetic Technologies" [1] for the methodology and main assumptions to be used in our LCOE estimates (e.g. Array losses; Wave energy resource in Humboldt Bay, CA)

2) "Cost and Performance Reporting Template" [2] provided by DOE to normalize competing claims of LCOE that requires that for wave energy technologies, the number of devices in the array should be selected so that the AEP is approximately 260,000 MWh/year

The "baseline" configuration corresponds to an 8 meter SurgeWEC flap using Coulomb damping flap load control. The improved configurations correspond to the different combinations of advanced control classes as described below:

	Control class	Flap load torque control option	Power flow direction control
Baseline	Causal	Coulomb damping	uni-directional
1	Causal	Tri-State (bi-polar)	uni-directional
2	Causal	Continuous	uni-directional
3	Causal	Tri-State (bi-polar)	bi-directional
4	Causal	Continuous	bi-directional
5	MPC	Tri-State (bi-polar)	uni-directional
6	MPC	Continuous	uni-directional
7	MPC	Tri-State (bi-polar)	bi-directional
8	MPC	Continuous	bi-directional

These systems are intended to be deployed in small arrays with an expected production capacity of 1-5 MW to address the near-term commercial opportunity identified by RME of off-grid applications in remote communities or islands.

For utility-scale applications as considered by DOE (i.e. EAP ~ 260,000 MWh/year), we believe SurgeWEC™ will need to be scaled up to a capacity rating ~400-600 kW/WEC, so that the number of devices per array remains within reasonable limits.

In this analysis, costs do not reflect any improvement in technology with respect to the configuration described in this report (e.g. improvement related to increase in WEC width). However, as per [1], we factored economies of scale in manufacturing, infrastructure, and operations and maintenance.

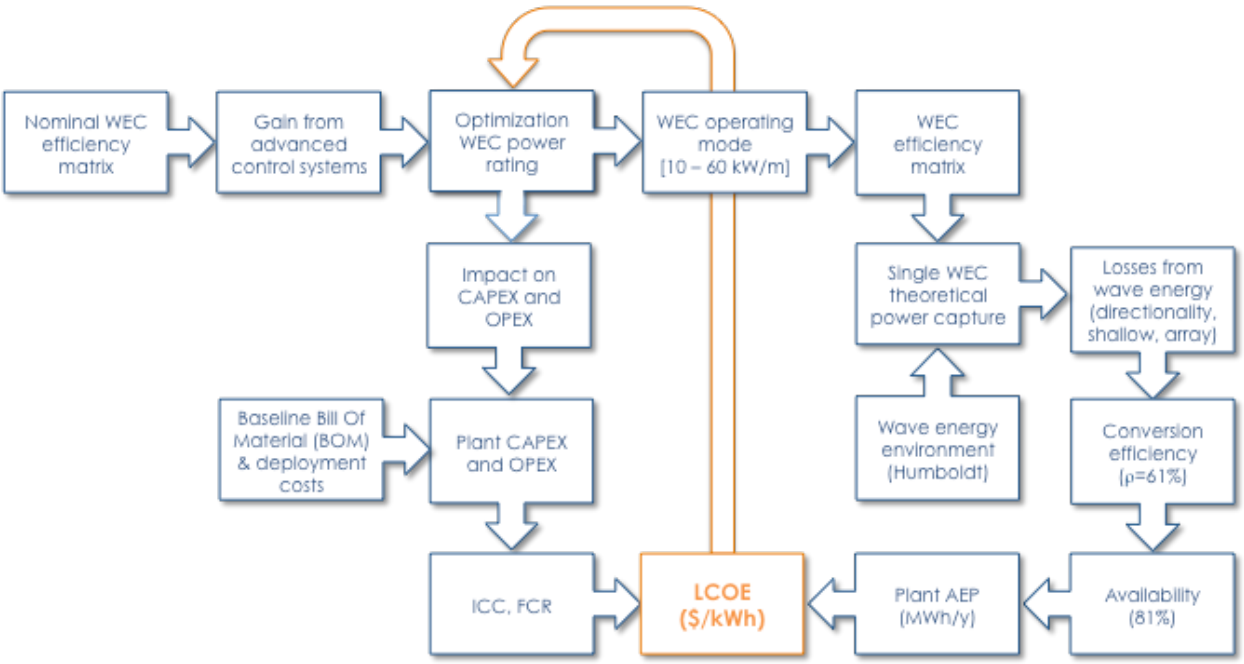

LCOE methodology and power rating optimization

To calculate LCOE provided by different solutions, we applied the methodology recommended by DOE referenced above. However, it is necessary to optimize the device power rating to capture the full benefits of improved performance. The DOE methodology and optimization process are described in the chart above. We used a linear interpolation ($/kW) to estimate the impact of improved power rating on the cost of all components from PTO to grid interface.

Our model also enables us to calculate other key parameters such as installed cost ($/kW) and power density (W/kg). Results of our LCOE analysis are presented below in Table 7.

Results of LCOE analysis for baseline and 8 advanced control systems

	Nominal	1	2	3	4	5	6	7	8
Number of device (#)	2,400	2,400	2,400	2,400	2,400	2,400	2,400	2,400	2,400
Device power rating (kW)	31	43	43	43	43	49	49	49	55
Array losses (%)	10%	10%	10%	10%	10%	10%	10%	10%	10%
Array rated capacity (MW)	73.20	102.48	102.48	102.48	102.48	117.12	117.12	117.12	131.76
Array AEP (GWh)	257.02	338.74	336.67	325.15	342.26	391.70	390.17	402.59	441.70
Array capacity factor (%)	40%	38%	37%	36%	38%	38%	38%	39%	38%
Capex - Equipment (M$)	438.47	555.12	555.12	569.03	569.03	616.93	616.93	632.77	687.81
Capex - Civil Engineering (M$)	218.63	218.63	218.63	218.63	218.63	218.63	218.63	218.63	218.63
Capex - Shipping and handling (M$)	22.45	24.78	24.78	25.06	25.06	26.02	26.02	26.34	27.44
Capex - Development (M$)	1.17	1.17	1.17	1.17	1.17	1.17	1.17	1.17	1.17
Capex - Other fixed assets (M$)	0.37	0.37	0.37	0.37	0.37	0.37	0.37	0.37	0.37
Capex - Financial costs (M$)	47.68	56.01	56.01	57.00	57.00	60.42	60.42	61.55	65.48
Capex - Total (M$)	728.76	856.08	856.08	871.26	871.26	923.54	923.54	940.83	1,000.90
OPEX (M$/y)	33.42	40.62	40.62	41.32	41.32	48.00	48.00	48.80	52.24
Installed cost ($/kW)	9.96	8.35	8.35	8.50	8.50	7.89	7.89	8.03	7.60
Plant weight (kt)	147.65	147.67	147.67	147.66	147.66	148.15	148.15	148.14	148.14
Power density (W/kg)	0.50	0.69	0.69	0.69	0.69	0.79	0.79	0.79	0.89
Availability (%)	0.81	0.81	0.81	0.81	0.81	0.81	0.81	0.81	0.81
LCOE ($/kWh)	0.44	0.39	0.40	0.42	0.40	0.38	0.38	0.37	0.36
CAPEX contribution	0.31	0.27	0.27	0.29	0.27	0.25	0.26	0.25	0.24
OPEX contribution	0.13	0.12	0.12	0.13	0.12	0.12	0.12	0.12	0.12
LCOE change vs. baseline		9.94%	9.39%	4.53%	9.30%	13.54%	13.20%	14.36%	16.79%

Observations

1. The maximum LCOE reduction of 16.79% is achieved with the most complex control solution #8—non-causal, continuous control, bi-directional power flow

2. 13.54% reduction is achieved with the simplest non-causal solution #5—tri-state (aka bi-polar) control and unidirectional power flow

3. The simplest causal solution #1—tri-state control and uni-directional power flow—achieves a 10% LCOE reduction, approximately half of that provided by the non-causal equivalent

The comprehensive Excel LCOE analysis document is submitted separately. However the Cost Breakdown Structure is provided in next page for all configurations.

Cost Breakdown Structure (All costs in $)

Item	CBS	Nominal	1	2	3	4	5	6	7	8
Capital Expenditures (CAPEX)	1									
Marine Energy Converter (MEC)	1.1									
Structural Assembly	1.1.1									
Primary Energy Capture	1.1.1.1	86,370,085	86,370,085	86,370,085	86,370,085	86,370,085	86,370,085	86,370,085	86,370,085	86,370,085
Additional Structural Components	1.1.1.2	31,413,636	31,413,636	31,413,636	31,413,636	31,413,636	31,413,636	31,413,636	31,413,636	31,413,636
Marine Systems	1.1.1.3	38,309,312	38,309,312	38,309,312	38,309,312	38,309,312	38,309,312	38,309,312	38,309,312	38,309,312
Control & Communication System (SCADA)	1.1.1.4	25,214,492	27,304,091	27,304,091	27,652,358	27,652,358	36,010,753	36,010,753	36,359,020	36,359,020
Power Conversion Chain (PCC)	1.1.2									
PCC Structural Assembly	1.1.2.1	5,223,997	7,313,596	7,313,596	7,313,596	7,313,596	8,358,395	8,358,395	8,358,395	9,403,195
Drivetrain (i.e., Prime Mover)	1.1.2.2	68,817,455	96,344,436	96,344,436	96,344,436	96,344,436	110,107,927	110,107,927	110,107,927	123,871,418
Hydraulic System	1.1.2.3	108,380,526	151,732,736	151,732,736	176,989,020	176,989,020	173,408,841	173,408,841	202,273,166	227,557,312
Electrical Assembly	1.1.2.4									
Frequency Converter	1.1.2.5									
Short-Tem Energy Storage	1.1.2.6	3,482,665	4,875,731	4,875,731	4,875,731	4,875,731	5,572,264	5,572,264	5,572,264	6,268,796
Power Electrical System	1.1.2.7	71,255,320	111,459,201	111,459,201	99,757,448	99,757,448	127,381,944	127,381,944	114,008,512	128,259,576
Balance of System	1.2									
Development	1.2.1									
Permitting & Leasing	1.2.1.1	20,000	20,000	20,000	20,000	20,000	20,000	20,000	20,000	20,000
Professional Advisory Services	1.2.1.2	250,000	250,000	250,000	250,000	250,000	250,000	250,000	250,000	250,000
Initial Engineering	1.2.1.3	60,000	60,000	60,000	60,000	60,000	60,000	60,000	60,000	60,000
Site Characterization	1.2.1.4	570,000	570,000	570,000	570,000	570,000	570,000	570,000	570,000	570,000
Interconnection & Power Marketing	1.2.1.5									
Project Management During Development	1.2.1.6									
Financing and Incentives	1.2.1.7	70,000	70,000	70,000	70,000	70,000	70,000	70,000	70,000	70,000
Engineering and Management	1.2.2									
Detailed Design and Construction Engineering	1.2.2.1	200,000	200,000	200,000	200,000	200,000	200,000	200,000	200,000	200,000
Procurement Management	1.2.2.2									
Construction Management	1.2.2.3									
Project Certification	1.2.2.4									
Health, Safety, & Environmental Monitoring	1.2.2.5									
Electrical Infrastructure	1.2.3									
Array Cable System	1.2.3.1									
Export Cable System	1.2.3.2									
Offshore Substation(s)	1.2.3.3									

Item	CBS	Nominal	1	2	3	4	5	6	7	8
Onshore Transmission Infrastructure	1.2.3.4									
Plant Commissioning	1.2.4	37,927,860	40,260,966	40,260,966	40,539,022	40,539,022	41,497,173	41,497,173	41,813,956	42,914,757
Site Access, Port & Staging	1.2.5									
Assembly & Installation	1.2.6									
Substructures & Foundations	1.2.6.1	38,696,275	38,696,275	38,696,275	38,696,275	38,696,275	38,696,275	38,696,275	38,696,275	38,696,275
Marine Energy Converter Device	1.2.6.2									
Electrical Infrastructure	1.2.6.3									
Other Infrastructure	1.2.7									
Offshore Accommodations Platform(s)	1.2.7.1									
Dedicated O&M Vessel(s)	1.2.7.2	300,000	300,000	300,000	300,000	300,000	300,000	300,000	300,000	300,000
Onshore O&M Facilities	1.2.7.3	67,000	67,000	67,000	67,000	67,000	67,000	67,000	67,000	67,000
O&M Equipment Purchases	1.2.7.4									
Other Infrastructure Transportation	1.2.7.5									
Substructure & Foundation	1.2.8									
Substructure	1.2.8.1	29,022,206	29,022,206	29,022,206	29,022,206	29,022,206	29,022,206	29,022,206	29,022,206	29,022,206
Foundation	1.2.8.2	61,914,039	61,914,039	61,914,039	61,914,039	61,914,039	61,914,039	61,914,039	61,914,039	61,914,039
Outfitting Steel	1.2.8.3									
Marine Systems	1.2.8.4									
Scour Protection	1.2.8.5	73,522,922	73,522,922	73,522,922	73,522,922	73,522,922	73,522,922	73,522,922	73,522,922	73,522,922
Substructure & Foundation Integration	1.2.8.6									
Substructure & Foundation Transportation	1.2.8.7									
Financial Costs	1.3									
Project Contingency Budget	1.3.1									
Insurance During Construction	1.3.2	35,757,109	42,004,002	42,004,002	42,748,497	42,748,497	45,313,945	45,313,945	46,162,132	49,109,526
Carrying Costs During Construction	1.3.3									
Reserve Accounts	1.3.4									
Maintenance Reserve Account	1.3.4.1									
Debt Service Reserve Account	1.3.4.2	11,919,036	14,001,334	14,001,334	14,249,499	14,249,499	15,104,648	15,104,648	15,387,377	16,369,842
Decommissioning Reserve Account	1.3.4.3									
Operational Expenditures (OPEX)	2									
Operations	2.1	160,500	160,500	160,500	160,500	160,500	160,500	160,500	160,500	160,500
Maintenance	2.2	33,254,899	40,464,015	40,464,015	41,159,155	41,159,155	47,842,706	47,842,706	48,634,664	52,074,840

APPENDIX A – LCOE Analysis - continued
LCOE Analysis cost data

Date: 1/25/2016, Revised 6/22/2016
To: Olivier Ceberio, Bill Staby
From: Allan Chertok
Re: Baseline BOM for W2E plant with 8m flap
File: Baseline_BOM_1.doc, Revised Baseline_BOM_2.doc

Scope

Cost estimates reported herein are provided to support development of LCOE analyses for RME Advanced Control DOE SPA1 programs. Provision of additional cost data for implementation of advanced control is pending results of a search for available shunt and check valve components by Jim Van de Ven. All costs are those estimated for a prototype system. Learning curve reductions will be applied in the LCOE model.

Plant configuration

For the baseline W2E configuration operated with Coulomb damping control only a single RME SurgeWEC unit with an 8m wide flap is considered. For the pending analysis case with advanced control—in particular using non-causal, model predictive control (MPC) methods—we will assume a configuration with 10 SurgeWEC units supported by a single array of seaward wave prediction sensors.

Electrical output power rating

Rated electrical power will be that attained at a rated sea conditions of Hs = 2.5m and Tp = 12s [5]. With a Coulomb damping load of ~ 0.3MNm [6] analysis by Darragh Clabby [7] finds the following at this sea state:

1. Average flap mechanical power = 50.5kW
2. Average flap angular velocity magnitude = 0.170 rad/s

The nominal PTO efficiency from flap mechanical power input to electrical power output is approximately 60% which leads to a rated electrical power of 30kW. A breakdown of PTO efficiency is developed below with possible adjustment of the approximate 60% value.

[5] Hs = 2.5m is a matrix row value at the upper row boundary. However, analysis is carried out for values of Hs at the center of the row boundaries—e.g., Hs = 2.25m. Tp, on the other hand is the center of a matrix column—e.g., for Tp = 12s the column boundaries are 11.5 and 12.5s.

[6] 0.3MNm is 70% (0.70pu) of that which develops maximum flap mechanical power. This reduced value is preferred as it significantly increases flap angular velocity thereby enabling a substantial reduction of flap pump displacement (m3/rad) and pump cost. The sacrifice of power is modest.

[7] e.g., file SW_B_0032_Matrices_D.xls

It is assumed that the plant will be allowed to operated in more energetic wave conditions up to Hs = 3.5m with output power limited to the rated value.[8] For more energetic sea conditions the flap would be unloaded and allowed to free wheel to minimize structural loads. [9]

Minimum electrical power rating

As wave energy diminishes a point will be reached where stable, continuous operation of the plant cannot be maintained and it will be shutdown.[10] This threshold is uncertain at this time but a review of the flap power matrix in Fig. 1 may provide some guidance:

Power Capture (POWER_MATRIX.Pc)

Pc [kW]	5	6	7	8	9	10	11	12	13	14	15	16	17	18	19	20	Tp [s]
0.5	0.97	1.07	1.18	1.28	1.36	1.44	1.41	1.39	1.24	1.09	0.95	0.81	0.72	0.62	0.54	0.47	
1	7.85	8.34	8.84	9.33	9.52	9.72	9.31	8.89	8.07	7.24	6.45	5.65	5.02	4.39	3.96	3.54	
1.5	21.32	21.91	22.50	23.09	22.98	22.87	21.65	20.44	18.58	16.73	15.02	13.31	11.90	10.50	9.53	8.57	
2	39.53	40.04	40.56	41.08	40.10	39.13	36.90	34.67	31.56	28.45	25.73	23.00	20.62	18.24	16.65	15.07	
2.5	59.92	60.24	60.56	60.88	58.85	56.81	53.68	50.55	46.16	41.77	37.87	33.97	30.67	27.36	25.08	22.80	
3	80.96	81.56	82.16	82.76	80.00	77.24	72.31	67.37	61.72	56.07	51.08	46.10	41.72	37.34	34.41	31.48	
3.5	104.72	105.87	107.02	108.17	102.13	96.09	90.19	84.30	77.50	70.71	64.77	58.83	53.46	48.08	44.48	40.87	

Hs [m]

Fig 1. Flap average mechanical power matrix [11]

For Tp = 12s we have flap mechanical power of approximately 9kW at Hs = 1m which is a likely cutout threshold corresponding to approximately 5kW electrical assuming a nominal PTO efficiency of 60%. However, this implies that the PTO has a 30/5 :1 or 6:1 turndown capability.

However, the Danfoss fixed displacement RO pump that we would use as a hydraulic motor to drive the generator has a speed range of only1,500 to 700 rpm—about 2:1. The low speed limit is that required to assume maintenance of a hydrodynamic lubricating film. Since the machine has a fixed displacement operation at its lowest allowable speed will result in a flow demand 3x greater than that the flap pumps can deliver at a 6:1 turndown condition.

Fortunately, this mismatch might be accommodated because at the low power condition the flap angular velocity—and hence pump flow—is only about half that at rated while the 70% of optimum flap torque—and hence HPA pressure—is about 3x lower. In other words, 1/6 rated power is achieved at 1/2 rated flow and 1/3 rated HPA pressure. We can easily drop the HPA

[8] Power limiting may be implemented by shunting High Pressure Accumulator (HPA) flow delivered to the Fixed Displacement Hydraulic Motor (FDM).

[9] Unloading would be achieved by continuously shunting flow delivered by the flap pumps … either at the pump ports or at the on-shore terminus of the high and low pressure pipe lines

[10] Shutdown under weak sea conditions will be accomplished as above by shunting flap pump flow.

[11] This power matrix is from file SW_B_0032_Matrices_D.xls

pressure by 3x and so the limited flow turndown capability of the Danfoss FDM may be OK. For example, see the flap load torque and angular velocity matrices in Figs 2 and 3 below.

Optimum Damping Torque (POWER_MATRIX.Tdamp)

Td [MNm]	5	6	7	8	9	10	11	12	13	14	15	16	17	18	19	20	Tp [s]
0.5	0.102	0.089	0.076	0.064	0.055	0.046	0.041	0.035	0.033	0.031	0.029	0.027	0.025	0.024	0.022	0.021	
1	0.230	0.208	0.186	0.165	0.146	0.127	0.115	0.104	0.097	0.090	0.085	0.080	0.076	0.071	0.070	0.069	
1.5	0.379	0.340	0.302	0.264	0.235	0.206	0.189	0.172	0.161	0.149	0.141	0.132	0.126	0.119	0.118	0.117	
2	0.505	0.456	0.407	0.358	0.319	0.279	0.259	0.240	0.224	0.208	0.197	0.186	0.175	0.165	0.165	0.165	
2.5	0.621	0.558	0.495	0.432	0.386	0.340	0.322	0.305	0.285	0.265	0.250	0.235	0.223	0.212	0.212	0.212	
3	0.710	0.643	0.577	0.510	0.466	0.421	0.394	0.368	0.344	0.321	0.302	0.284	0.270	0.256	0.257	0.258	
3.5	0.829	0.760	0.692	0.623	0.547	0.472	0.447	0.423	0.397	0.372	0.352	0.332	0.316	0.300	0.300	0.301	
Hs [m]																	

Fig 2. Flap load torque matrix (0.7 pu of optimum loads)

Note load torque at Hs = 1m and Tp = 12s = 0.104 MNm vs 0.305 MNm at Hs = 2.5m … a turndown of 0.104/0.305 ~ 1/3.

Average of absolute angular velocity (POWER_MATRIX.Velocity_avg)

Vavg [rad/s]	5	6	7	8	9	10	11	12	13	14	15	16	17	18	19	20	Tp [s]
0.5	0.018	0.020	0.023	0.026	0.031	0.036	0.039	0.043	0.041	0.039	0.037	0.034	0.032	0.029	0.028	0.026	
1	0.043	0.050	0.056	0.063	0.072	0.082	0.086	0.090	0.087	0.084	0.079	0.074	0.070	0.065	0.060	0.054	
1.5	0.066	0.075	0.084	0.094	0.105	0.116	0.119	0.123	0.119	0.116	0.110	0.104	0.098	0.092	0.084	0.077	
2	0.088	0.099	0.110	0.121	0.133	0.146	0.147	0.149	0.145	0.141	0.134	0.128	0.121	0.114	0.104	0.095	
2.5	0.107	0.121	0.134	0.148	0.160	0.172	0.171	0.170	0.166	0.161	0.155	0.149	0.140	0.132	0.122	0.111	
3	0.125	0.140	0.154	0.169	0.179	0.189	0.188	0.188	0.183	0.179	0.172	0.166	0.158	0.149	0.137	0.125	
3.5	0.137	0.152	0.166	0.181	0.195	0.209	0.207	0.204	0.199	0.194	0.188	0.181	0.172	0.164	0.151	0.139	
Hs [m]																	

Fig 3. Flap average angular velocity magnitude matrix

Note average |flap velocity| at Hs = 1m and Tp = 12s = 0.090 rad/s vs 0.170 rad/s at Hs = 2.5m … a turndown of 0.090/0.170 ~ 1/2.

This scheme for accommodating the limited speed and flow turndown range of the Danfoss FDM is not going work for an Integrated W2E-W2O system since optimum RO feed water pressure declines only modestly with available feed water hydraulic power. To overcome this barrier, we can employ switch-mode modulation to reduced the effective displacement of the W2E flap pump pumps.

Flap subsystem components

Flap - Capture factor performance and modular construction

The 8m wide flap is approximately 7m tall and 3.2m wide at its maximum cross-section. This design with bold rounding was developed by Darragh Clabby when he discovered that Matt Folley had assumed an optimistically low value of viscous damping coefficient Cd which resulted in overstating the capture factor of previous thinner, rectangular flap designs—e.g., the

10m wide flap proposed for Yakutat. With generous rounding of flap edges a more realistic value of Cd could be applied while maintaining a favorable capture factor—e.g., 0.29 pu at rated conditions of Hs = 2.5m and Tp = 12s. Capture factor at other sea states are shown in the matrix of Fig. 4. The broad cross-section of the new design shown in Fig. 5 also enabled an increase of restoring moment to better match the natural mode to that of the dominant wave frequency at sites of interest with Tp = 12s.

Capture Factor (POWER_MATRIX.Cf)

Cf	5	6	7	8	9	10	11	12	13	14	15	16	17	18	19	20	Tp [s]
0.5	0.77	0.75	0.72	0.70	0.70	0.70	0.67	0.63	0.56	0.48	0.41	0.35	0.30	0.26	0.23	0.19	
1	0.70	0.65	0.61	0.56	0.55	0.53	0.49	0.45	0.40	0.35	0.31	0.27	0.24	0.20	0.18	0.16	
1.5	0.68	0.62	0.56	0.50	0.47	0.45	0.41	0.37	0.33	0.29	0.26	0.23	0.20	0.18	0.16	0.14	
2	0.64	0.58	0.52	0.46	0.42	0.39	0.36	0.32	0.29	0.26	0.23	0.20	0.18	0.16	0.14	0.13	
2.5	0.59	0.53	0.47	0.41	0.38	0.34	0.31	0.29	0.26	0.23	0.20	0.18	0.16	0.14	0.13	0.12	
3	0.53	0.48	0.43	0.37	0.34	0.31	0.28	0.25	0.23	0.20	0.18	0.16	0.15	0.13	0.12	0.11	
3.5	0.49	0.45	0.40	0.35	0.31	0.28	0.25	0.23	0.21	0.18	0.17	0.15	0.13	0.12	0.11	0.10	

Hs [m]

Fig 4. Flap capture factor matrix

Note how capture factor increases significantly as Hs declines.

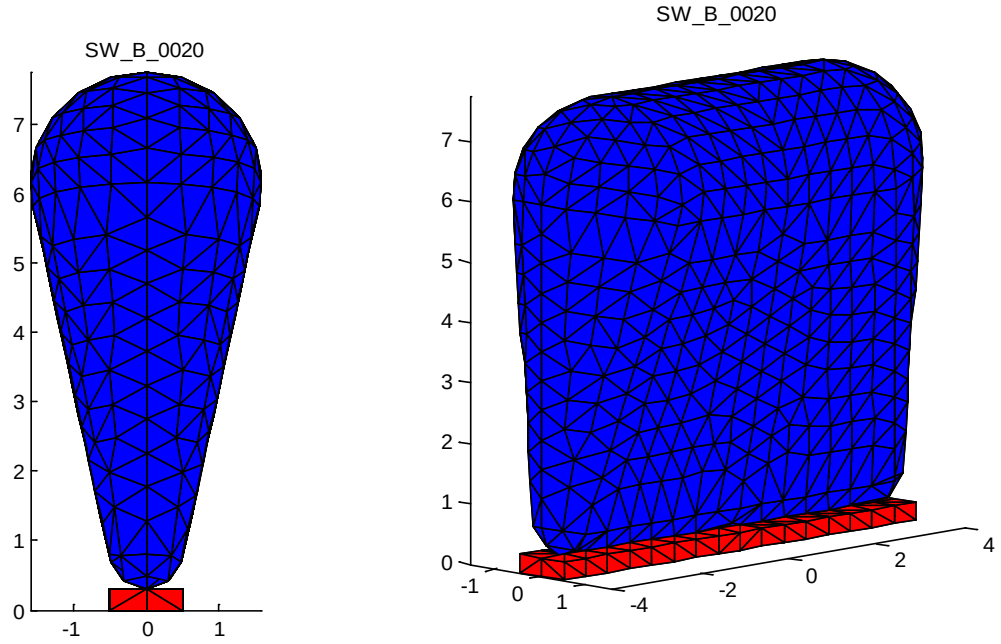

Fig 5. Rounded 8m flap design [1]

To enable shipment of the flap in standard Intermodal Containers it will be broken into modules with flanges enabling on-site assembly with bolted joints as depicted in Fig. 6. An alternative means of coupling the flap to the pumps is depicted by Fig. 7. [2]

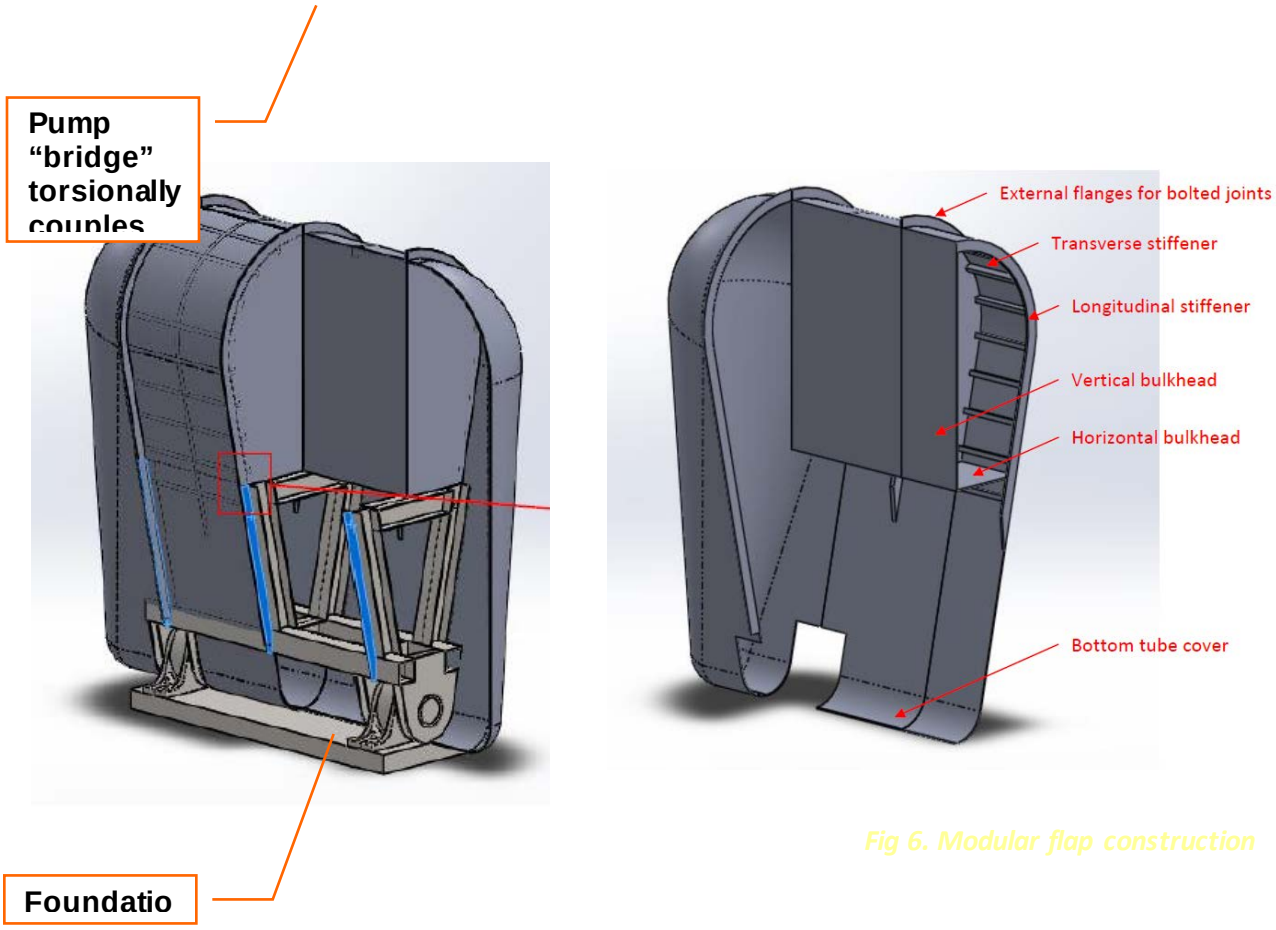

Fig 6. Modular flap construction

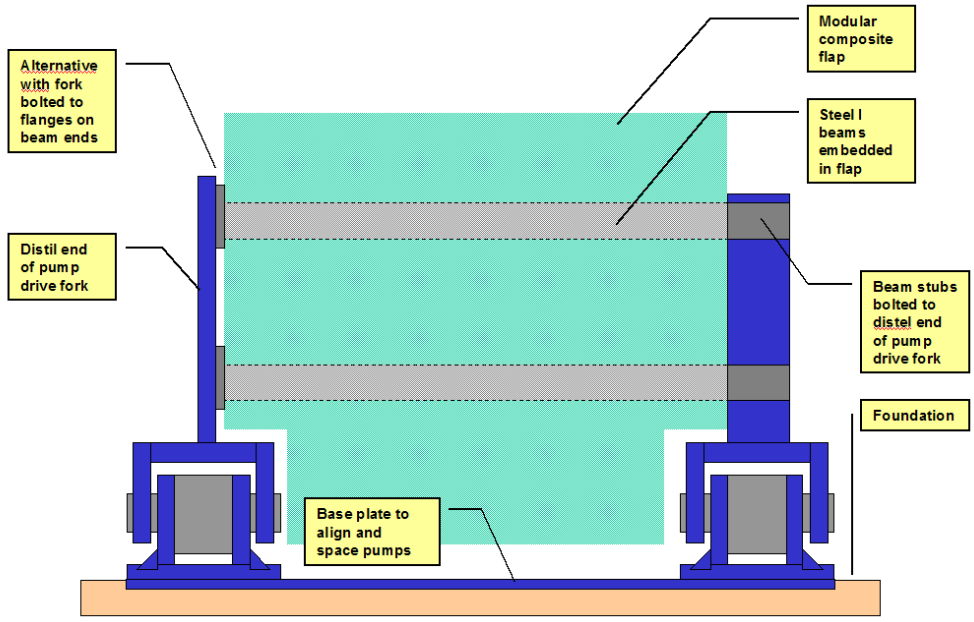

Fig 7. Alternative flap-pump connection similar to that used at Duck [3]

Flap - Mass and manufacturing cost

Darragh Clabby estimated the external surface area of the 8m flap [6] and the following factors are applied to arrive at a mass estimate and cost as follows:

1. Surface area = 153m^2
2. Nominal skin thickness = 0.0125m (~ 1/2")

3. Skin volume = 1.913m^3
4. Material volume to include internal ribs and stringers ("scantlings") = 1.3 x skin volume
5. Total composite volume = 2.50m^3
6. Nominal composite density = 1,800kg/m^3 [12]
7. Nominal composite weight = 4,500kg (~ 9,900lbm ~ 5T)
8. Prototyping unit cost = 25$/lbm [13]
9. Prototype flap cost = 248k$
10. Production unit cost = 12.5$/lbm [14]
11. Production flap cost = 124k$

Notes:

1. Skin thickness is a rough guess

2. Darragh followed up on a suggestion of relating the flap impact pressures to design pressures for boat hulls. He found that the impact pressures estimated based on tank tests are around the same as design pressures for high speed naval craft. But we have no idea of what the corresponding hull thickness would be for such vessels

3. The prototype and production $/lbm values above did not consider a modular construction and may not account for the additional complexity of bonding in steel flanges to enable bolted assembly of the flap modules and connecting the flap to the pump bridge. See detail produced by Eric Greene in Fig. 8 which suggests a skin thickness of 10mm—a bit less than 12.5mm assumed above. No detailed structural analysis has yet been performed to determine required thickness of skin and scantlings.

[REMAINDER OF PAGE PURPOSELY LEFT BLANK]

[12] Suggested by Dick D'Amato for wind turbine blades and other highly loaded structures - polyester or vinyl ester resin matrix

[13] Suggested by lead engineer at Tillotson Pierson during team visit 2014

[14] Suggested by lead engineer at Tillotson Pierson

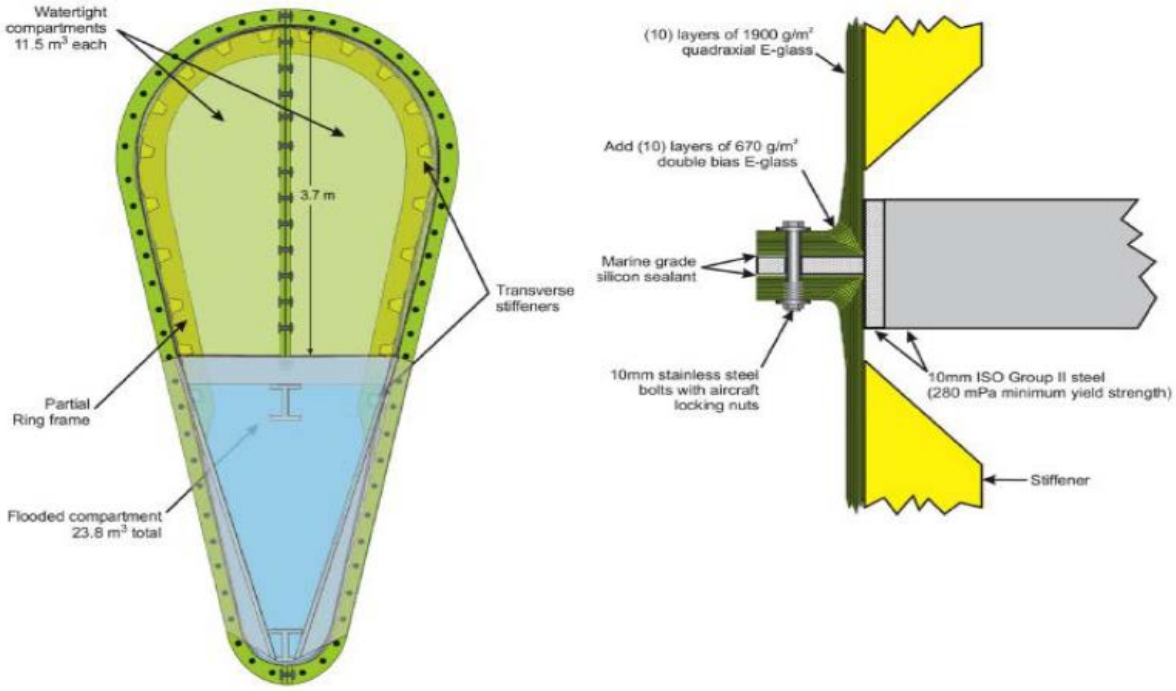

Fig 8. Flange connection detail for joining modules and flap to pump bridge [2

Flap-Pump Bridge - Mass and manufacturing cost

Darragh Clabby estimated the mass for the two welded steel flap-bridge structures depicted in Figs. 9a and 9b. [2] The masses of these two bridge designs are 6.5 metric tons for the reduced height bridge (Fig. 9a) and 8.2 metric tons for the full height design (Fig. 9b). **The design of Fig. 9b** may be preferred to better distribute the structural load on the flap. A **prototype cost of** $5/lbm including corrosion protection measures [15] may be reasonable in which case the design of Fig. 9b would cost 8.2mT * 2,200 lbm/mT * 5 $/lbm = **$90,200**. A production run of 10 units might bring the unit cost down to ~ $3/lbm or a finished cost of $54,120

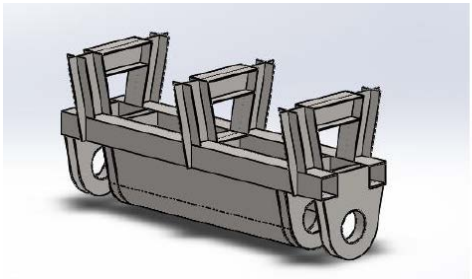

Fig 9a. Reduced height bridge [2]

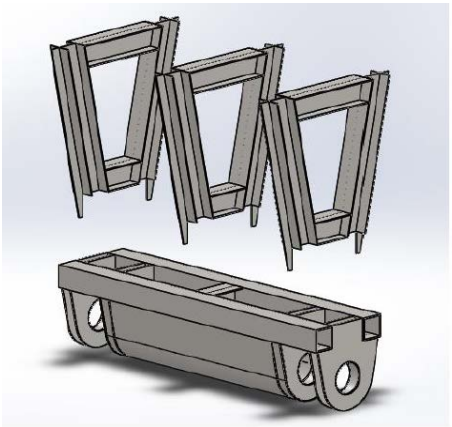

Fig 9b. Full height bridge with detachable upper portion to enable containerization [2]

[15] e.g., sandblasting, zinc loaded primer and epoxy paint

Foundation

Darragh Clabby developed a cost estimate for a beach launched gravity foundation consisting of 132 precast concrete ballast blocks resting on a steel frame and secured to it using ratchet straps as shown in Fig. 10. [7]

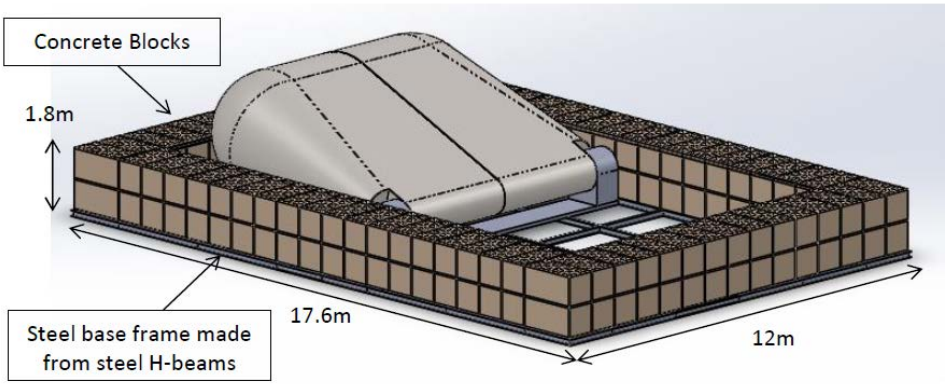

Fig. 10 – Gravity foundation [7]

Launching of the foundation would be achieved using rubber airbags. Such airbags are usually employed to move ships, as shown in Fig. 11 [7].

Fig. 11 – Ship launch using rubber airbags [7]

[REMAINDER OF PAGE PURPOSELY LEFT BLANK]

Foundation - continued

The cost of materials was $63,000 and buoyancy and launch airbags $47,000 for a total of **$110,000**.

Bob Bittner of Bittner-Shen Consulting Engineers provided an estimate for a sheet pile foundation to be jetted into a sandy bottom and anchored against uplift with toggle plates. [8]

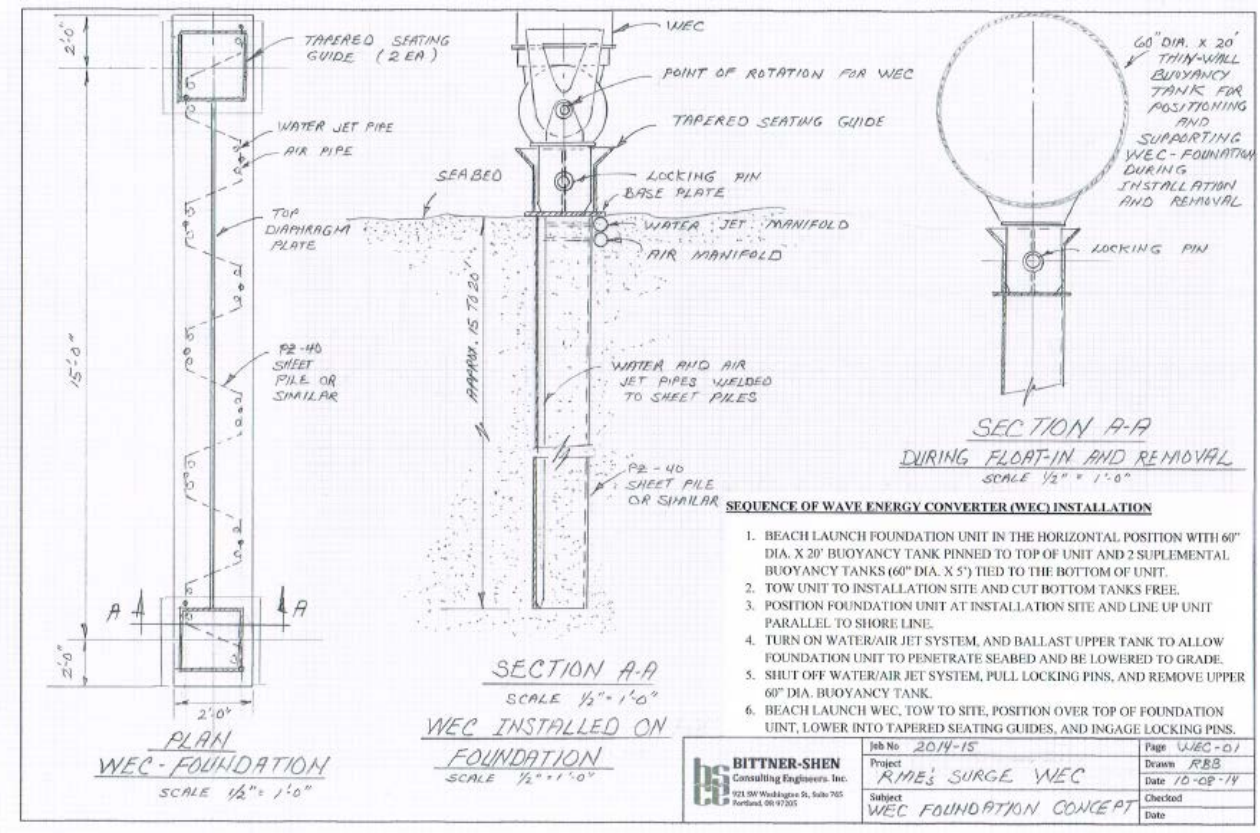

Fig. 12 – Bittner-Shen Sheet Pile Foundation Concept [8]

Estimated cost for a sheet pile foundation and deployment gear was approximately $100,000.

Both of the above estimates neglect vessel hire, diver time, and material transport costs. When these are included the gravity foundation's simpler installation process may result reveal a distinct cost advantage

All costs used in the gravity foundation's estimate were based on quotes obtained either from company websites or from contact with staff. On the other hand, the Bittner-Shen costs were calculated based on the application of a scale factor to the foundation and deployment equipment's total weights, so could be a bit more uncertain.

Another foundation option to investigate in future might be 'micro-piles'—e.g., see

http://www.rembco.com/micropiles_minipiles.html

http://www.ontonbolt.com/products/Micropiles-and-rock-drilling-rigs-2088730.html?gclid=CPm-srq3yMoCFQseHwodc9UKCg

http://www.haywardbaker.com/WhatWeDo/Techniques/StructuralSupport/Micropiles/default.aspx

The sheet pile foundation would not likely be suitable for the Camp Rilea Engineering Pilot test site which may have a sand bottom only a foot or so deep overlying a clay. A beach launched gravity foundation akin to that employed at Duck NC seems a more universal solution and it is suggested that its cost be used in LCOE analyses. A variation on above design might replace the concrete ballast blocks with pre-cast concrete slabs such as were used at the Duck NC site.

[REMAINDER OF PAGE PURPOSELY LEFT BLANK]

PTO subsystem components

Flap Pump – design, mass and cost

The unit cost for manufacturing flap pumps of our specific design machined from super duplex stainless steel castings was estimated by Yong Yang of Austin Power Engineering to be $12/lbm in single piece quantity. [4] This cost was estimated to decline to approximately $10/lbm for 10fin0 piece lots. Darragh Clabby conducted a pump sizing optimization and structural loads analysis and estimated the mass of a pump with displacement of 18L/rad (1,100 in3/rad) to be 3,885 lbm. [5]

I had previously suggested that a Micromatic 700in3/rad pump weight of 4,500 lbm would scale linearly with displacement rating and so we might expect an 1,100 in3/rad machine to come in at 11/7 * 4,500 = 7,070 lbm or roughly twice Darragh's estimate. The differences could be

1. Darragh assumed the shaft could be hollow vs the solid shaft of the Micromatic unit
2. The Micromatic unit may be designed to accommodate higher pressure—e.g., 3,000 psi vs ~ 1,200 psi in our application

It is suggested that we assume a prototype mass which is the average of these two estimates—i.e., (3,885+7,070)/2 ~ 5,500 lbm. Applying a unit cost of 12$/lbm finds a cost of ~ $66,000 for prototype units. However, this is the cost of fabricating the super duplex stainless steel components and does not include seals, bearings, assembly and testing. It is suggested that we allocate an additional $10,000 to cover the cost of these items at the prototype quantity level bringing the factory cost to $76,000.

To compare the cost of flap pumps with that of purchased flaps, piping, accumulators, hydraulic motors, generators and other components we should price the pumps as if they were being purchased from a manufacturer since it seems unlikely that we want to vertically integrate pump manufacture into RME's operations. Hence a gross margin of 30% which you had previously suggested will be assumed. With gross margin applied the **purchase cost of the pump in prototype quantity** would be 1.3 * $76,000 = **$98,800** or ~ 90 $ per in^3/rad. Compare this with a verbal quote of $167,000 provided by Micromatic for a 700 in3/rad pump or ~ $239 per in^3/rad—2.66x greater.

Pump manifold assemblies

Following the approach used for the Duck NC prototype the flap pump ports would be coupled to flow rectifier check valves and pressure sensors by means of a machined manifold block. The manifold blocks used at Duck were made of aluminum at a cost of $4,000 each. Stainless steel blocks were quoted at $18,000! The aluminum blocks, although anodized for protection showed signs of severe corrosion when retrieved from the Duck site. Manifolds blocks with their many internal passages and fine screw threaded ports for valves and sensors no doubt would have a much higher $/lbm than the $12/lbm Yong Yang estimated for pumps fabricated in super duplex stainless.

Pump manifold assemblies - continued

It will be assumed that a super-duplex stainless steel manifold block might have overall dimensions of 6 x 8 x 12 with a finished mass of ~ 150 lbm and a manufacturing cost of $50/lbm the piece cost would be $7,500.

Jim Van de Ven has estimated that check valves open area diameter would have to be 5cm but at the present time suitable commercial valves have not be identified. A placeholder cost of $1,000 will be assumed for each of 4 check valves per pump manifold assembly. Each manifold will be provided with a pressure relief valve and a placeholder cost of $1,000 will be allocated to this component. A cost of $1,000 will be assigned to each of four pressure sensors per manifold.

A summary of these component costs (per pump) follows:

1.	Manifold block	$7,500	
2.	4 check valves	$4,000	
3.	Relief valve	$1,000	
4.	4 pressure sensors		(reported in SCADA system)
5.	**TOTAL**	**$12,500**	

Low pressure accumulator assemblies

A submerged low pressure accumulator (LPA) will be required local to each flap pump to assure maintenance of a minimum net positive suction head (MNPSH) at the flap pump ports to avoid cavitation erosion damage. Analysis of required LPA volume is pending but it is believed that something on the order of 40-50 gallons may suffice for each pump. The largest commodity accumulator bottles have a capacity of 15 gallons so we might assume 3 units would suffice for each pump. Conventional 15 gallon bottles cost approximately $2,000 each but it can be expected that units suitable for continuous submersion in sea water may cost more. A placeholder cost of $3,000 will be assumed. An additional $1,000 will be allocated to packaging 3 bottles in a frame that can be mounted to the flap foundation adjacent to each pump and piping connections to the pump manifold. Hence a cost of **$10,000** is estimated for each of two LPA assemblies

Manifold to pipe line transition

The pressure and suction ports of each of two manifolds will need to be connected to the large diameter Fiberspar pipes. A placeholder cost of **$2,000 per manifold** will be assigned for commercial piping hardware and fitting labor to accomplish this interface.

Pressure and suction pipe lines

A nominal pipe line length of 1,000m (3,280') from WEC to shore will be assumed. [16] Some preliminary analyses suggest a required pipe ID of 5" to achieve a loop loss under 10% at rated flow conditions. Pipe material is assumed to be that provide by Fiberspar. [9] 5" ID (6" OD) pipe with a 1,500 psi working pressure rating would be suitable for the pressure line and a quote from December 2014 suggests a cost of $90/m at the factory dock. [10, 11] A 750 psi rated product was quoted at slightly lower cost ($87/m) which might be used for the suction line but as the cost saving is modest it will be assumed that the same 1,500 psi rated material would be used for both pressure and suction lines. Also up to 1,200' of the 1,500 psi pipe can put up on a 16' OD reel whereas only 610' of the 750 psi material can be accommodated. Hence use of the high pressure material for the suction line will require fewer reels, couplings and less installation labor.

In addition, Fiberspar connectors will be required to join pipe segments and terminate the ends. 1,200' of the 6" OD (5"ID) pipe can be spooled on a 16' OD reel. With a run length of 3,280' there will be 3 sections to join requiring 2 couplings plus terminations at each end. **Couplings** and terminations were quoted to cost ~ **$1,900** each.

Shore pipe line terminations

Some cost should be assigned to the termination of the Fiberspar pipes on shore in addition to interface the large diameter pipe lines to smaller diameter pipes to the containerized "back-end" of the PTO system. A placeholder of **$2,000** will be allocated for materials and labor.

PTO back-end container

A 20' Intermodal container fitted out with access doors, electrical service panel, inside and outside power outlets/inlets, lighting, filtered ventilation and other supporting features will be estimated to cost $15,000.

High pressure accumulator (HPA)

The high pressure accumulator volume is sized to adequately suppress power fluctuations due to pulsating flap pump flow and episodic fluctuations of wave power—e.g., tendency for waves to arrive in groups. Spice model analysis of the PTO back-end supplied with a flap pump flow derived from simulated flap angular velocity [1] was performed to assess the required HPA volume. Fig. 13 depicts analysis results with a 150 gallon HPA (5x that of the Duck system) while Fig. 14 depicts the result with a 300 gallon HPA.

Power output (3rd chart) with the smaller HPA (Fig. 13) has significant twice wave frequency ripple that may stress the flywheel energy storage unit in its attempt to smooth the power flow.

[16] This may be less than required for the Camp Rilea pilot site. Pat Rezza had estimated 750m but Westy Ford believes a run of 1,500m may be required.

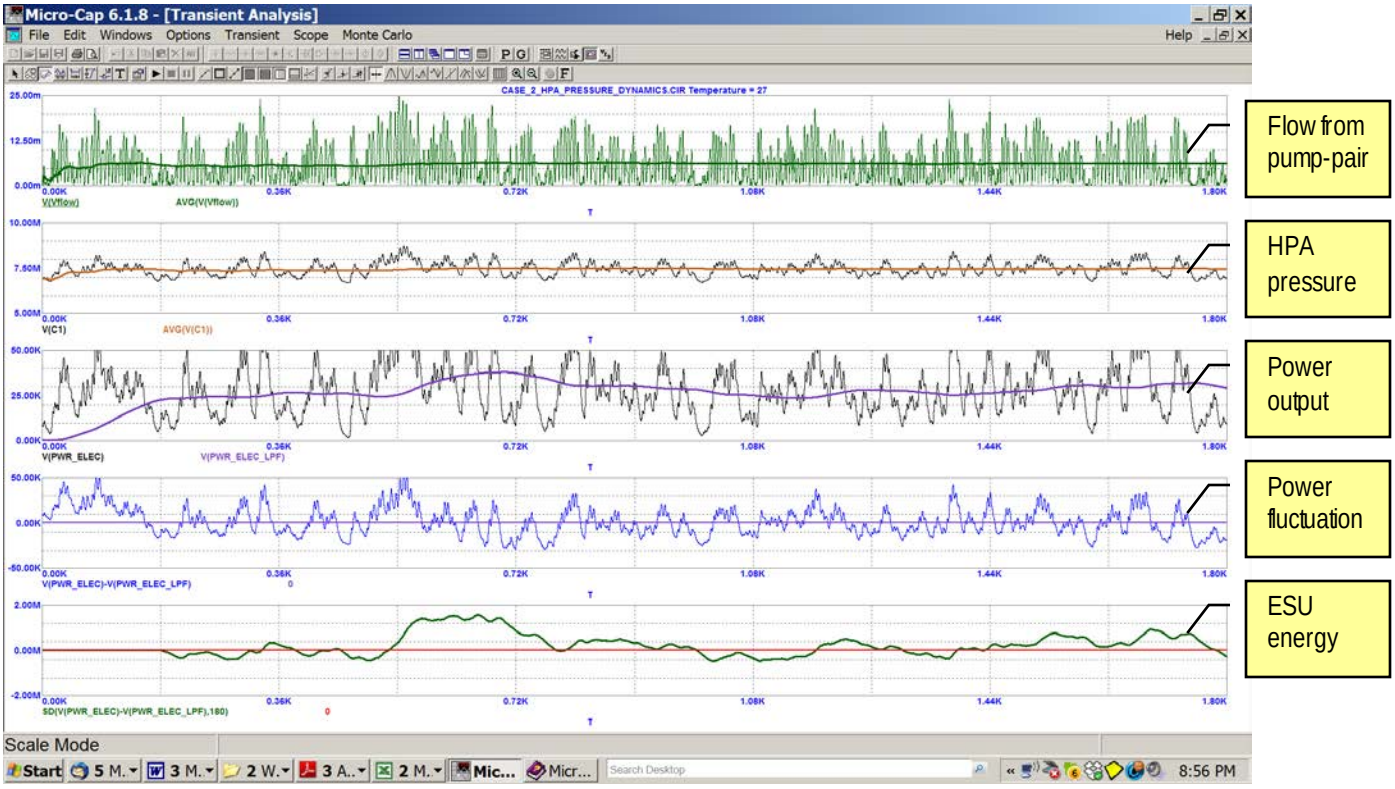

Fig. 13 – Back-end PTO performance with 150 gallon HPA

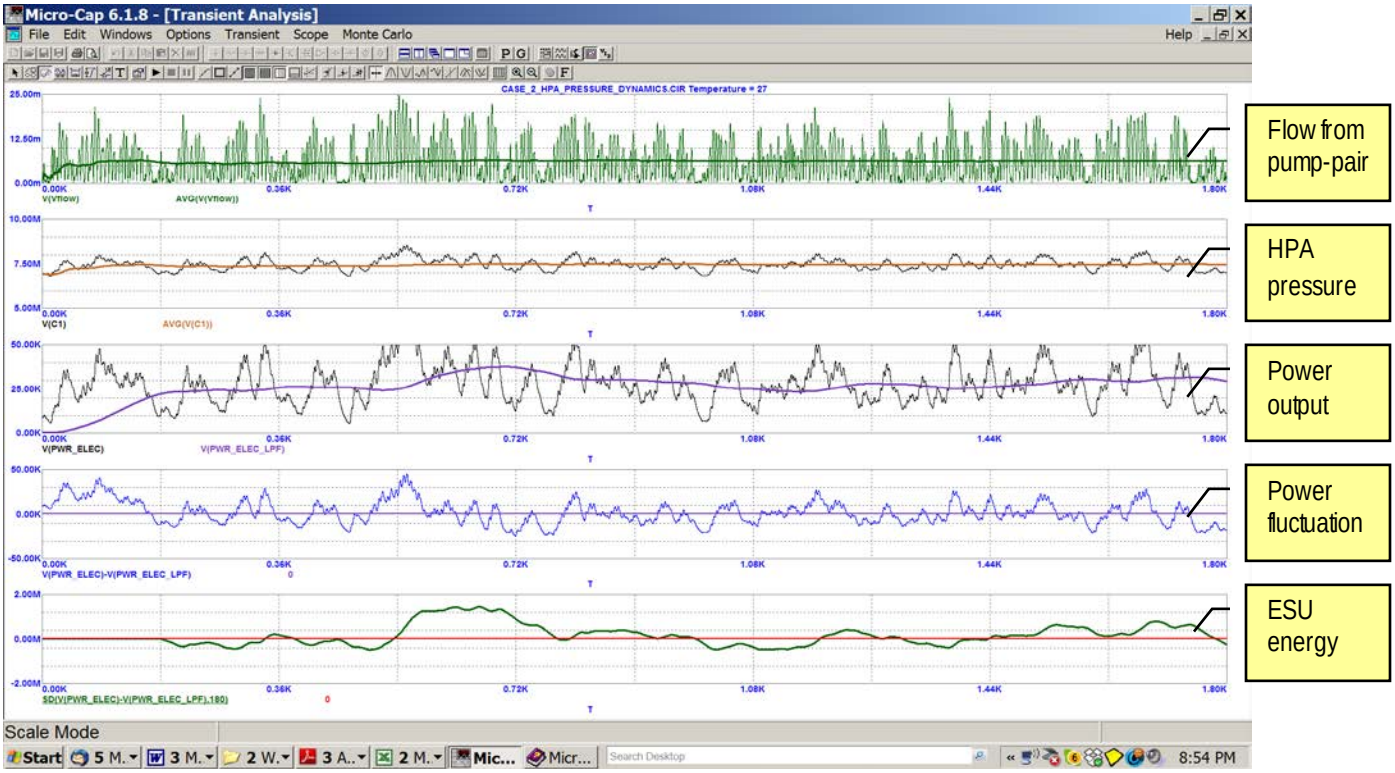

Fig. 14 – Back-end PTO performance with 300 gallon HPA

A further reduction of HPA capacity—e.g., to 90 gallons—further amplifies the fluctuation of power. In all cases increasing HPA volume reduces HPA pressure fluctuation (2nd chart). For a W2E system the fluctuations of pressure and power with a 150 gallon HPA may be acceptable. However, this may not be the case for the Integrated W2E-W2O system where pressure fluctuations may have a negative impact on RO membrane life.

The 4th chart reports the difference between the fluctuating electrical power output from the generator power converter shown in the black trace of the 3rd chart and a low pass filtered version of the converter power output plotted in blue on the 3rd chart. The filtered version is what we aim to deliver to the grid and the energy storage unit (ESU) will absorb or deliver the difference to achieve this end. The green trace in the 5th chart is the running integral of the difference between the unfiltered and filtered power and represents the stored energy state of the ESU. This trace reports a positive peak magnitude of approximately 1.6MWs (MJ) = 1,600kWs = 0.44kWh. The negative peak magnitude is approximately 0.5MWs. The flywheel ESU energy rating would be on the order of 3MWs so that it can swing between these states with some headroom with modest depth of discharge to assure a long fatigue life.

Returning to the matter of HPA cost the following allocations will be made for a 150-gallon unit. Conventional accumulators of 15-gallon capacity sell for approximately $2,000. This cost will be augmented to allow for internal corrosion protection for operation with sea water.

1.	10, 15 gallon accumulators at $2,500 ea	$25,000
2.	Packaging—framing and piping	5,000
3.	**TOTAL**	**$30,000**

Reservoir and charge pump

A reservoir of filtered sea water will be pressurized by a charge pump to maintain a modest pressure in the suction pipe line. Likely we could use a relatively small Danfoss RO axial piston pump. The maximum pressure might be 200 psi and relieved by a safety valve so a simply constructed steel tank with anti-corrosive liner might serve for the reservoir. Absent any analysis a **conservative "guesstimate"** for this package would be **approximately $10,000**.

Shunt and pressure relief valves

1.	Shunt valve across input to back-end to enable shutdown	$1,000
2.	Modulating shunt valve across HPA output to bypass large peak flows	$2,000
3.	Pressure relief valve across HPA	$1,000
4.	**TOTAL**	**$4,000**

Fixed displacement hydraulic motor

The selected Danfoss AP26/1500 axial piston pump to be operated as a motor was priced by Alex Chen of Parker Hannifin circa 2014 at $52,200. For optimum motor-mode operation the valve plate would be replaced with a modified version. The additional cost is unknown but might bring the price up to a **nominal $53,000**.

Induction generator with shaft encoder

The selected unit is a 6 pole, 75HP (56kW) inverter-duty Marathon Electric induction motor model Y588 fitted with an optical shaft encoder. The generator price was estimated from The Galco website (www.galco.com/buy/Marathon-Electric/Y588) and an additional $1,500 was added for the shaft encoder based on experience with the Duck project. The total estimated cost is **$16,600.**

Power converter

The power converter will allow the generator and FDM to operate at variable speed so that the FDM flow drawn from the HPA can be controlled to regulate HPA pressure. The preferred converter is a fully line-regenerative motor drive from Yaskowa Electric. It will enable control of generator reaction torque presented to the FDM to enable control of system speed. The drive employs a matrix converter architecture which eliminates need for electrolytic DC link capacitors which tend to be the weak link in such systems and may require replacement from time to time. A quote was received circa 2014 for approximately **$10,000**.

Flywheel energy storage unit (ESU)

We have been in communication with Vycon Energy, a leading supplier of flywheel energy storage units for back up power and energy recovery applications such as ours. A variety of configurations have been discussed starting with those for the originally envisioned Yakutat project. Vycon ESUs typically interface with a DC bus so a separate inverter will be required to couple to the AC grid. More recently, circa June 2015, John Jeter provided budgetary cost of $355,500 for 3 of their model R125 ESUs with a 100kW inverter by Socomec. [12]. This package would provide 6,000 kWs of energy storage vs the 3,000 kWs requirement noted above. Hence for budgetary purposes half of the $355,500 ~ **$178,000** will be assumed.

There may be a better balance of HPA and ESU energy capacities to achieve a power flow to the grid with acceptable maximum ramp rate at minimum equipment cost. However, the utilization of HPA capacity for power fluctuation smoothing is constrained by the desire to control its pressure for optimum flap energy capture whereas the energy capacity of the flywheel can be better utilized by allowing its speed to fluctuate. This is the subject for a future investigation.

Electrical power interfaces

Electrical power interfaces include wiring and protection features between

1. Generator and the power converter
2. Power converter and grid
3. ESU and grid

A cost of **$10,000** for materials, including cabinets, contactors, relays and wiring is allocated.

Supervision Control and Data Acquisition (SCADA) system

The following costs are estimated for this system

1.	Allen Bradley ControlLogix PLC hardware/software platform	$10,000
2.	Back-end pressure and flow sensors	10,000
3.	Front-end pressure sensors (8 @ $800 ea)	6,400
4.	Back-end electrical sensors (voltage, current, power, etc.)	5,000
5.	Wave pressure sensors + mountings (2 @ 1,500)	3,000
6.	Wave pressure analyzer	3,000
7.	Remote terminal unit (RTU) for front-end sensor multiplexing	5,000
8.	Submarine cable and installation labor from RTU to back-end	10,000
9.	Back-end cabling and assembly	10,000
10.	**TOTAL**	**$62,400**

Costs not included

1. Site engineering
2. Site permitting
3. Foundation deployment (with pumps and pump bridge) – vessels, labor
4. Flap module transportation from fabricator to site
5. Flap assembly
6. Flap deployment
7. Fiberspar pipe transportation from factory to site
8. Installation of Fiberspar pipe lines and connections to front and back end systems
9. Foundation and grid interface for back-end container
10. Back end PTO system container assembly and shop testing
11. Back end PTO system container shipping from assembler to site
12. System commissioning tests

[REMAINDER OF PAGE PURPOSELY LEFT BLANK]

COST ROLL UP

Subsystem	Component	Qty	Unit cost	Extended cost	Subsystem subtotal
Flap	Flap	1	248000	248000	
	Pump bridge	1	90200	90200	
	Foundation	1	110000	110000	
					448200
PTO	Flap pump	2	98800	197600	
	Pump manifold	2	12500	25000	
	LPA	2	10000	20000	
	Pipe transition	2	2000	4000	
	Fiberspar pipe	2000	90	180000	
	Pipe couplings	10	1900	19000	
	Shore termination	1	2000	2000	
	Container	1	15000	15000	
	HPA	1	30000	30000	
	Reservoir & charge pump	1	10000	10000	
	Shunt and relief valve set	1	4000	4000	
	Fixed displacement motor	1	53000	53000	
	Generator	1	16600	16600	
	Power converter	1	10000	10000	
	Flywheel ESU	1	178000	178000	
	Electrical power interfaces	1	10000	10000	
	SCADA system	1	62400	62400	
					836600
					1284800

[REMAINDER OF PAGE PURPOSELY LEFT BLANK]

LCOE cost data references

Originals or copies in my folder ***c:\AAPS\Magnecon\RME\LCOE_W2E_Analysis***

[1] SW_B_0032_Matrices_D.xls

[2] DC-RME-150917-B Status of Work on Structural Design of SurgeWEC.pdf

[3] Pump_connection_4.ppt

[4] PumpHeadCosting_austinpower.pdf

[5] DC-RME-150424-A Pump Parametric Analysis-2.pdf

[6] SW_B_0020-07_Hydrostatics-B .xlsx

[7] DC-RME-150204-A Cost Estimate for a Gravity Foundation.pdf

[8] WEC Foundation Concept by BSCE 9-08-14.pdf

[9] Fiberspar (NOV) [17]
http://www.nov.com/Segments/Completion_and_Production_Solutions/Fiber_Glass_Systems/Oil_and_Gas/Spoolable/Spoolable.aspx

[10] Fiberspar_D9C1004570-MKT-001.pdf

[11] Fiberspar pipe – budgetary pricing data.eml [18]

[12] Vycon flywheel system requirements for RME wave energy system.eml

[REMAINDER OF PAGE PURPOSELY LEFT BLANK]

[17] Fiberspar is now part of the NOV organization that provides products and services to the oil industry
[18] Quote cited a 6-1/2" (OD) size. This is a typo … should have been labeled 6"

APPENDIX A – LCOE Analysis - continued
Additional or revised LCOE Analysis cost data

Baseline cost adjustments

Baseline costs are those reported above with the following adjustments:

1 On page 61 we estimated the cost of 4 rectifier check valves per pump to be $4,000. Jim Van de Ven has since reported an estimate he received from Oilgear Inc. of $1,500 - $1,900 per valve in prototype quantities. Using the $1,900 estimate would increase the original $4,000 value to $7,600. Note that this is a ***cost per pump*** so it is doubled in the final roll up.

2. On page 61 add two submerged High Pressure Accumulators (HPA)---***one per pump***---of similar capacity to the low pressure units at an additional cost of $10,000 ***for the pair***. These HPAs would be of smaller capacity than the on-shore unit and would suppress the twice-wave frequency pulsations and thus reduce pipe line loss. They are also necessary for the advanced control configurations.

Added costs to implement *causal* control options w/o reverse power flow - Options 1 and 2

1. Shunt valve ***per pump*** ~ $7,600 based on an estimate received by Jim Van de Ven from Oilgear Inc. for first prototypes
2. Piping and fittings ~ $2,000 ***per pump***
3. On page 66 SCADA costs, add item 1a "Hardware/Software Control Platform to implement real-time causal control" ~ $5,000 ***per flap***
4. On page 17 of first attachment increase SCADA system item 7 (remote terminal unit) from $5,000 to $6,000 for shunt valve control capability ***per flap***
5. License fee to University of Michigan for use of Jeff's solutions?

Added costs to implement *causal* control options with reverse power flow - Options 3 and 4

1. On page 61 of first attachment replace "4 check valves" with "4 ***controllable*** valves" ~ $40,000 per pump = $80,000 for pump-pair
2. Piping and fittings ~ $2,000 per pump
3. On page 66 SCADA costs, add item 1a "Hardware/Software Control Platform to implement real-time causal control" ~ $5,000 ***per flap***
4. On page 66 increase SCADA system item 7 (remote terminal unit) from $5,000 to $6,000 for shunt valve control capability ***per flap***
5. License fee to University of Michigan for use of Dr. Scruggs' solutions?

Note that these controllable valves would eliminate the need for the shunt valve required for the case without reverse power flow.

CAPEX costs would apply to either continuous or ON/OFF control options. However, OPEX would be higher by a factor TBD for the continuous case due to more frequent valve operation.

Added costs re: *non-causal* control options w/o reverse power flow - Options 1 and 2

1. Shunt valve ***per pump*** ≈$7,600 based on an estimate received by Jim Van de Venfrom Oilgear Inc. for first prototypes
2. Piping and fittings ~ $2,000 ***per pump***
3. On page 66 SCADA costs, add item 1a "Hardware/Software Control Platform to implement real-time causal control" ~ $5,000 ***per flap***
4. On page 66 increase SCADA system item 7 (remote terminal unit) from $5,000 to $6,000 for shunt valve control capability ***per flap***
5. License fee to Re-Vision for use of their MPC solutions?
6. Wave forecasting sensors based on following input
    a. Re Vision stimate that 8 sensors might cover a SurgeWEC array extending over 300m
    b. Assuming 8m wide units would be spaced no less than 50m apart to provide minimal space between units (42m = 138') for service vessels
    c. Then 8 sensors would service 7 SurgeWEC units
    d. Then 3 arrays required for 18 SurgeWEC units
    e. Re Vision estimate of $100,000 for 8 sensors + $50,000 for installation and commissioning for its SPA2 program -- hence $450,000 ***for 3 sensor arrays***
    f. Re Vision estimating maintenance check every 6 months with day rate for boat and crew of $4,500 or $9,000 annually. Triple this to ***$27,000/y for 3 arrays***
7. On-shore sensor signal processing -- assume this is covered by the Hardware/Software Control Platform cost of $5,000/flap

Added costs re: *non-causal* control options w/ reverse power flow - Options 3 and 4

1. On page 61 replace "4 check valves" with "4 ***controllable*** valves" ~ $40,000 per pump = $80,000 for ***pump-pair***
2. Piping and fittings ~ $2,000 per pump
3. On page 66 SCADA costs, add item 1a "Hardware/Software Control Platform to implement real-time causal control" ~ $5,000 ***per flap***
4. On page 66 increase SCADA system item 7 (remote terminal unit) from $5,000 to $6,000 for shunt valve control capability ***per flap***
5. License fee to Re-Vision for use of their MPC solutions?

[REMAINDER OF PAGE PURPOSELY LEFT BLANK]

APPENDIX B – Power/Weight Analysis

Table 6 reports power/weight findings for the 8m flap configuration

Estimated costs and weights for a single 8m flap W2E unit rated ~30kW at Hs = 2.5m and Tp = 9s at Yakutat site

MATERIAL DESCRIPTION	Unit cost	Qty	Ext cost	Ext cost	Illustrative supplier	Unit weight	Unit	Ext weight	Notes
	($)		($)	(% of total)		(kg)	($/kg)		
Composite flap	364000	1	364000	23.3	Tiltotson Pierson	6600	55.15	6600	1
Gravity foundation concrete	16000	1	16000	1.0	TBD	294000	0.05	294000	2
Flap and pump mounting base	10000	1	10000	0.6	TBD	2000	5.00	2000	3
Flap pump	310000	2	620000	39.7	TBD	3800	81.58	7600	5
Recifier valve manifold assembly	25000	2	50000	3.2	TBD	30	833.33	60	6
Rectifier manifold to pipe transition	2000	2	4000	0.3	TBD	10	200.00	20	7
5"ID, 1,500 psi rated pipe - cost = ($/m)*m	90	1000	90000	5.8	Fiberspar	20830	4.32	20830	8
5"ID, 750 psi rated pipe - cost = ($/m)*m	87	1000	87000	5.6	Fiberspar	16530	5.26	16530	9
Pipe connectors	1900	11	20900	1.3	Fiberspar	20	1045.00	220	10
High pressure accumulator (HPA)	33000	1	33000	2.1	TBD	2222	14.85	2222	11
Low pressure accumulator (LPA)	33000	1	33000	2.1	TBD	2222	14.85	2222	11
Hydraulic motor	52200	1	52200	3.3	Danfoss	105	497.14	105	12
Induction generator + encoder	16600	1	16600	1.1	Marathon	567	29.28	567	13
Generator supervision, protection	10000	1	10000	0.6	TBD	50	200.00	50	14
Hydraulic system sensors	10000	1	10000	0.6	TBD	10	1000.00	10	15
PLC controller	10000	1	10000	0.6	Allen-Bradley	10	1000.00	10	16
PTO ISO container	15000	1	15000	1.0	TBD	2200	6.82	2200	17
RRL FW (shared by 2 35kW W2E)	35000	1	35000	2.2	Vycon	250	140.00	250	18
NON-MATERIAL COSTS									
Foundation installation	15000	1	15000	1.0	TBD				4
Pipe line installation	10000	1	10000	0.6	TBD				22
Share of multiple unit civil engineering costs	10000	1	10000	0.6	TBD				22
Share of multiple unit permitting costs	10000	1	10000	0.6	TBD				22
Flap deployment	10000	1	10000	0.6	TBD				22
Assembly of backend PTO ISO container	20000	1	20000	1.3	TBD				22
Share of multiple unit grid interface costs	10000	1	10000	0.6	TBD				22
				100.0					
SALIENT RESULTS									
Flap & foundation cost ($)			390000						
Total cost ($)			1561700						20
Total cost ($/kW)			44620						
Cost effected by adv ctrl ($)			1171700						
Cost effected by adv ctrl (%)			75.0						
Total weight for ~30kW W2E (kg)								355496	
Total "active" weight wo foundation (kg)								61496	
Average power (W)	17807								19
Capacity factor (%)	50.9								
SPA#1 Average power/total weight (W/kg)	0.050								
SPA#1 Average power/active weight (W/kg)	0.290								

Table 8 – Power/Weight analysis

APPENDIX C – BENEFIT OF SEAWATER PTO VS. HYDRAULIC FLUIC PTO

One of Wave2E's main innovations is that its hydraulic pumping system uses sea water as the working fluid. We believe such a system will have a positive impact upon a number of marine renewable energy applications (including power generation and sea water desalination) and, as importantly, will reduce the environmental impact of any marine renewable energy technology that utilizes hydraulic power take-off (PTO) systems for energy production by eliminating the use of oil- or glycol-based hydraulic fluids.

The main reasons for using an innovative hydraulic WEC PTO system that utilizes sea water as the fluid power medium are as follows:

- compared to direct drive PTO systems (rotary and linear generators), hydraulic PTO systems are well suited to convert the low-speed and high torque mechanical power of WEC devices into electricity due to their known ability to reliably handle extreme and transient loads;
- to date, no low speed, high displacement sea water pumps are available for use in WEC-driven desalination and/or electric power generation plants. However, the existence of high speed, motor-driven low displacement sea water pumps widely employed in RO plants provides confidence that a low speed, WEC-driven high displacement sea water pump is attainable. RME has thoroughly investigated linear hydraulic cylinders for this pumping function and has found a rotary vane device would be a simpler and more affordable solution. To fill this gap, RME has conceived a rotary vane pump design employing novel high endurance labyrinth seals and has recruited TBE to assist with the detail design and manufacture of prototypes for the proposed HIL test program;
- marine renewable energy technologies are beginning to emerge as contributors to a low-carbon future and it is highly likely that WEC systems, in particular those employing sea water hydraulic PTOs, will see widespread adoption if proved feasible and cost effective;
- wave energy capture of WEC devices can be significantly enhanced by advanced real-time load control methods now being investigated by RME and its research partners under a research program funded by the DOE Water Power Program. To achieve this performance gain WEC load could be modulated in real-time by application of state-of-the-art switch-mode hydraulic techniques given the availability of switching valves of adequate flow capacity, speed and endurance. RME has recruited Dr. James van de Ven and his team at the University of Minnesota CCEFP to assist in the development and testing of these special-purpose valves.
- direct pressurization of sea water by WEC pumps for RO desalinization (another targeted market for RME) is considerably more efficient than using WEC-generated electricity to power motor-driven pumps;
- using seawater as working fluid will prevent the use of hydraulic fluid such as glycol which represent additional environment risk and significant additional cost that we estimate at approximately $200,000 per WEC. The table and the chart below provide a comparison of our baseline configuration as calculated for our LCOE analysis using either a seawater driven hydraulic system or a glycol-based

Installation cost ($/kW) - Comparison between Wave2E (Seawater) vs. SurgeWEC (Hydraulic fluid)

Cost Breakdown Structure ($/kW)	Wave2E (Seawater)	SurgeWEC (Hydraulic fluid)	Difference
Structural Assembly			
Primary Energy Capture	1,180	1,180	0%
Additional Structural Components	429	429	0%
Marine Systems	523	523	0%
SCADA	344	344	0%
Power Conversion Chain			
Structural Assembly	71	71	0%
Drivetrain (i.e., Prime Mover)	940	750	-20%
Hydraulic System	1,481	2,432	64%
Short-term storage	48	48	0%
Power Electrical System	973	973	0%
Development	13	13	0%
Engineering and Management	3	3	0%
Plant Commissioning	518	533	3%
Assembly & Installation	529	529	0%
Other Infrastructure	5	5	0%
Substructure & Foundation	2,247	2,247	0%
Financial Costs	651	706	8%
Total ($/kW)	**9,956**	**10,787**	**8%**

Note:

- Wave2E: Installation cost calculated for a "baseline" configuration without advanced control system using the same assumptions as LCOE calculation (e.g. Humboldt sea power rating 31 kW/meter of wave front)
- SurgeWEC: Cost of component and hydraulic fluid calculated based on a projection of a SurgeWEC of same power rating as Wave2E. PTO costs are reduced to reflect decrease in material costs but the cost of the hydraulic system is increased to reflect the cost of hydraulic fluid (est. $200,000 per WEC)

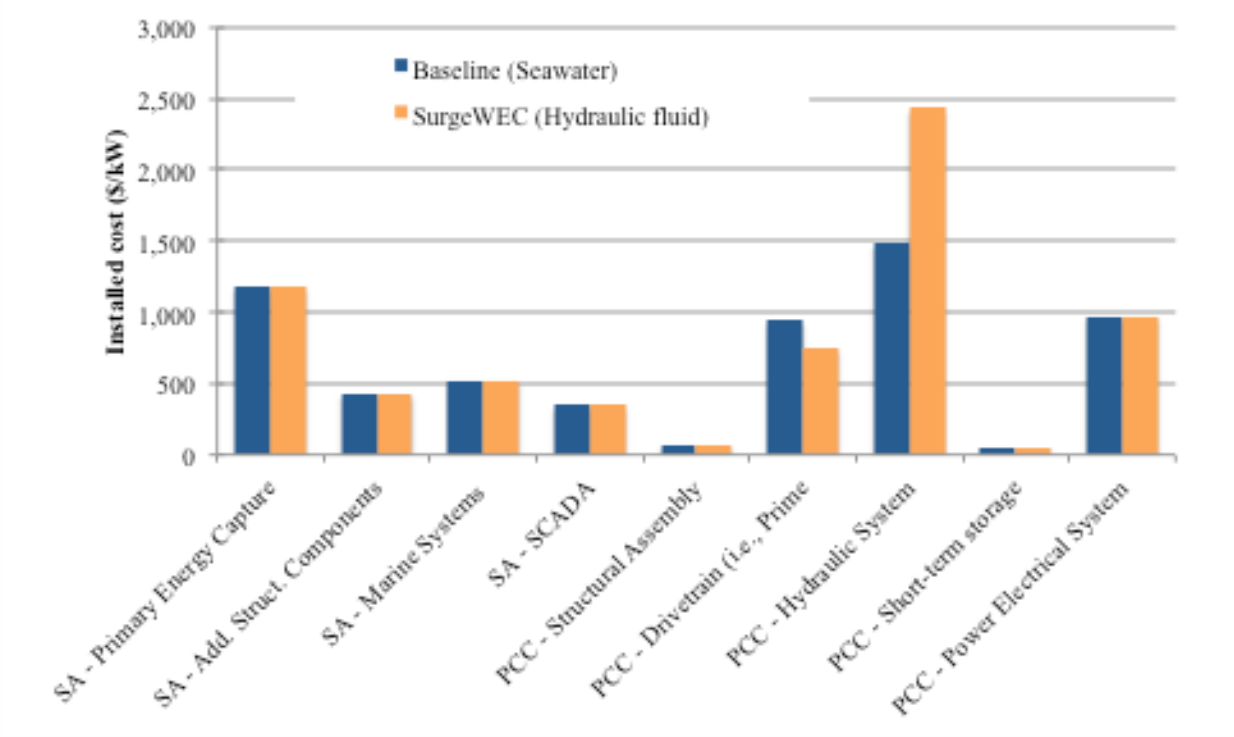

PROJECT MANAGEMENT AND REPORTING

1. **Project Management Plan (PMP)** - A PMP was provided detailing how the project will be managed. The PMP provides detailed project information including project objectives, deliverables, schedules and Gantt charts, technical risk mitigation table, risk management procedures, funding and costing profiles, work breakdown schedules, and project organization and structure.
2. **Component Design Report** – This report includes any tradeoff studies, numerical predictions, design drawings and schematics.
3. **Intellectual Property (IP) Management Plan** - A final IP Management Plan was submitted within six weeks of the effective date of the EERE funding agreement. (M2)
4. **System Integration Plan** - A systems-integration plan was developed, fully identifying and specifying all the system-level interfaces and sensor integration aspects. The plan addressed implementation of the advanced controls as applied to the Yakutat Project.
5. **Impact Analysis** - An impact analysis was developed that included a study detailing impacts of the component technology development to the targeted MHK system's performance as it relates to the SPA Goals, and quantifying the reduction in LCOE resulting from the improvements realized under this proposal.
6. **Final HIL Test Report (where applicable)** The HIL test program was not funded and hence not undertaken.
7. **Periodic Progress Reports/Presentations, quarterly reports, and annual peer review presentations** were provided as required.
8. **Final Technical Report** – A final technical report will provide a detailed summary of the completed project is in progress

TAKE OUTS FROM BP2

Parameter	P1 SOPO Baseline	P1 SOPO Advanced	P1 SOPO Benefits	P2 SOPO Baseline	P2 SOPO Advanced	P2 SOPO Benefits	Notes
Rated plant power (kW)	720	1,123	56%	315	405	29%	1, 2, 3
Average flap capture eff (%)	35	57	63%	26	36	38%	4
Plant capacity factor (%)	26	28	8%	42	54	29%	4
SPA#1: Power density (W/kg)	0.37	0.62	67%	0.29	0.37	29%	5
SPA#2: Availability (%)	61	70	15%				6, 7
LCOE ($/kWh)	0.44	0.26	41%	TBD	TBD	TBD	8

[1] Plant power at rated sea Yakutat Cannon Beach conditions Hs = 2.5m, Tp=9s
[2] Reduced baseline rated power from 80 to 35kW for each of 9 units
[3] Estimated increase of unit rating from 35 to 45kW enabled by greater flap capture efficiency and optimum size for least LCOE
[4] More realistic findings of substantially improved analysis tools since time of proposal and P1 SOPO
[5] Revised weight does not include dominant and site-dependent foundation mass. Advanced control will add little mass.
[6] In P1 SOPO inadvertently reported % time waves sufficient to operate plant vs % time ready to operate
[7] Availability analysis underway and self-funded by RME but deleted from P2 scope
[8] LCOE at 100% availabililty